UNIVERSITY OF TRENTO

PhD Program in Biomolecular Sciences

Department of Cellular, Computational and Integrative Biology – CIBIO

38th Cycle

"OptoTrkB activation for *in-vivo* translation of optogenetic memory engram consolidation"

Tutor

Prof. Marco CANOSSA

CIBIO – University of Trento

Advisor

Prof. Beatrice VIGNOLI

CNR – Neuroscience Institute in Padua

Ph.D. Thesis of

Paolo BRUNELLI

CIBIO – University of Trento

Laboratory of Synaptic Plasticity

Academic Year 2024-2025

Declaration of Authorship

I Paolo Brunelli, confirm that this is my own work and the use of all material from other sources has been properly and fully acknowledged.

INDEX

List of figures and tables

Abbreviations

4-OHT: 4-Hydrotamoxifen

AAV: Adeno-Associated Virus

Arc: Activity-regulated cytoskeleton-associated protein

BDNF: Brain-Derived Neurotrophic Factor

BL-OG: Bioluminescent-Optogenetic

C/EBP: CCAAT/Enhancer Binding Protein

CNO: Clozapine-N-oxide

CREB: cAMP Response Element-Binding protein

Cry2PHR: Cryptochrome 2 Photolyase Homology Region

CTZ: Coelenterazine

DI: Discrimination Index

DLP: Digital Light Processor

DREADD: Designer Receptors Exclusively Activated by Designer Drugs

E-LTP: Early-phase Long-Term Potentiation

ERK1/2: Extracellular Signal-Regulated Kinases 1/2

fEPSP: Field Excitatory Postsynaptic Potential

hcNOR: home-cage Novel Object Recognition

hM3Dq: human M3 muscarinic DREADD (Gq-coupled)

IEGs: Immediate Early Genes

L-LTP: Late-phase Long-Term Potentiation

LTM: Long-Term Memory

MAPK: Mitogen-Activated Protein Kinases

mBDNF: mature Brain-Derived Neurotrophic Factor

NOL: Novel Object Location

NOR: Novel Object Recognition

$p75^{NTR}$: p75 Neurotrophin Receptor

pCREB: phosphorylated CREB

pERK1/2: phosphorylated ERK1/2

PRC: Perirhinal Cortex

STM: Short-Term Memory

TBS: Theta Burst Stimulation

TRAP: Targeted Recombination in Active Populations

TrkB: Tropomyosin receptor kinase B

VAMP2: Vesicle-associated membrane protein 2 (Synaptobrevin-2)

ABSTRACT

The consolidation of memory engrams relies fundamentally on robust synaptic plasticity, specifically Late-phase Long-Term Potentiation (L-LTP), which is governed by the Brain-Derived Neurotrophic Factor (BDNF) and its high-affinity receptor, TrkB. While neuronal BDNF synthesis is critical, recent evidence suggests that astrocytes play an equally pivotal role in maintaining the pool of bioactive neurotrophins through a $p75^{NTR}$-dependent recycling mechanism. This doctoral thesis investigates the physiological necessity of astrocytic BDNF recycling for long-term memory (LTM) consolidation and establishes a novel, non-invasive optogenetic strategy to rescue cognitive deficits associated with the disruption of this pathway.

Utilizing a conditional $p75^{NTR}$-flox mouse model, we first demonstrated that impaired astrocytic BDNF recycling selectively abolishes LTM in a context-minimized home-cage Novel Object Recognition (hcNOR) paradigm, while sparing short-term memory. Electrophysiological assessments confirmed that these behavioural deficits correlate with a failure to sustain L-LTP. To bypass the limitations of traditional, invasive optogenetic stimulation, we employed OptoTrkB, a light-sensitive chimeric receptor, to directly modulate TrkB signaling. We validated the functionality of OptoTrkB in cortical neuronal cultures and demonstrated its efficacy in restoring L-LTP in p75-deficient *ex vivo* preparations. To translate these findings *in vivo*, we implemented a Bioluminescent-Optogenetic (BL-OG) system. This approach utilizes a luciferase released by astrocytes to activate TrkB signaling non-invasively via the systemic administration of a luciferin substrate. Our results indicate that non-invasive BL-OG activation of OptoTrkB successfully rescues LTM deficits in p75-deficient mice. Furthermore, we established that this rescue is dependent on astrocytic vesicular release mechanisms.

Crucially, to dissect the specific contribution of the memory trace, we utilized a custom-designed external LED cage lid system rather than invasive optical fibers. By delivering light during a defined critical time window in the consolidation phase, we achieved a complete, engram-specific rescue of

LTM. This pivotal finding demonstrates that temporally precise boosting of TrkB signaling exclusively within the memory trace is sufficient to compensate for the lack of astrocytic support.

Collectively, this work elucidates the critical contribution of astrocytic BDNF recycling to support memory engram consolidation. It further validates OptoTrkB-BL-OG as a powerful, non-invasive tool for the precise temporal manipulation of neurotrophic signaling, offering a promising translational avenue for treating cognitive disorders characterized by synaptic dysregulation.

INTRODUCTION

1.1 - The concept of memory

1.1.1 – Definition

The understanding of memory has evolved over centuries, leading to a functional fragmentation of the concept to systematically account for the diverse ways information is acquired, stored, and retrieved. A fundamental partition in modern neuroscience and psychology is the long-term memory dichotomy between implicit (or non-declarative) and explicit (or declarative) systems. These two functionally distinct memory classes rely on separate neural substrates. Implicit memory, often referred to as procedural memory or skill memory, facilitates the acquisition and execution of tasks and motor patterns that are recalled unconsciously, as in riding a bicycle. This system is critically modulated by phenomena like priming, where a prior exposure to a stimulus influences a subsequent response without conscious awareness. Within the domain of implicit memory, perceptual learning is particularly relevant as it refines sensory processing, providing a foundational mechanism that enables the distinction between similar stimuli and enhances the efficiency of higher-order cognitive processes. In contrast, explicit memory is the collection of factual information and events that can be consciously recalled. It is further subdivided into semantic memory, which constitutes an individual's organized knowledge of the world independent of temporal context (e.g., historical facts or general concepts), and episodic memory. Episodic memory is the capacity to encode, store, and retrieve specific personal events and discrete past experiences, intrinsically linking the 'what,' 'where,' and 'when' of an event. This unique ability to mentally "time travel" into the past serves the crucial, adaptive purpose of informing, influencing, and planning future actions.

Recognition memory is a form of declarative memory classically defined by two dissociable components: the familiarity of a stimulus or item and the recollection of its context (spatial and/or temporal) within an event[1]. This distinction is conceptually modelled by an individual’s interaction

with a room and its contents. For instance, after becoming familiar with the environment, the spontaneous detection of a familiar object being substituted by a novel one, and thus the recognition of the object, is assessed by the Novel Object Recognition (NOR) memory test. Alternatively, if the same familiar object is simply relocated, the ability to spontaneously notice the change and thus recognize the novelty of the location, is assessed by the Novel Object Location (NOL) memory test[2,3]. These distinct components of recognition memory are thought to engage separate, but interconnected, neural circuits within the medial temporal lobe[4]. Specifically, the perirhinal, prefrontal and insular cortices are consistently implicated in processing the familiarity component of stimuli, while the hippocampus is considered critical for the recollection of rich contextual information[4,5,1,6,7]. The NOR and NOL paradigms serve as powerful, non-aversive behavioural assays for studying the neurobiological mechanisms underlying long term memory (LTM) formation in animal models[8]. Memory performance is quantified by calculating discrimination indices based on the animal's preferential exploration time of the novel item (in NOR) or the displaced item (in NOL). As represented in Figure 1, the manipulation of the retention interval between the acquisition and test phases allows for the selective evaluation of different temporal memory phases, such as short-term versus long-term memory (STM vs LTM). The search for the enduring physical substrate underlying these long-term traces is a central quest in neuroscience, leading to the modern concept of the engram.

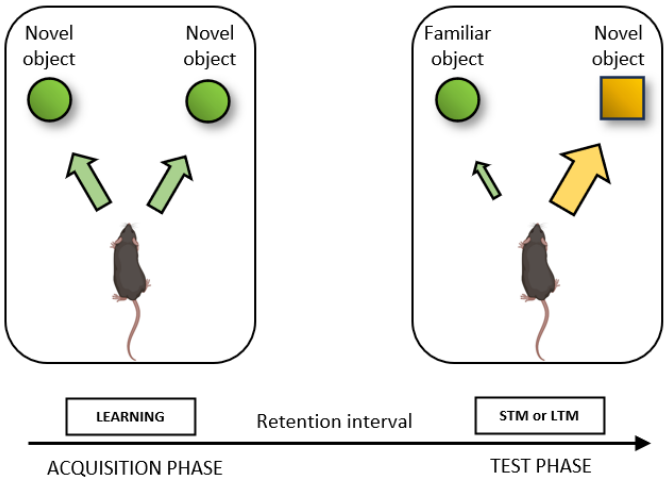

Figure 1. The Novel Object Recognition (NOR) test paradigm

The task consists of two main phases. During the Acquisition or Sample phase (learning), a mouse freely explores an arena containing two identical familiar objects (green circles). After a retention interval (which determines if short-term or long-term memory is assessed), the rodent enters the Test phase. Here, one familiar object is replaced by a novel object (orange square). Memory is measured as the time the rodent spends exploring the novel object compared to the familiar one. Successful recognition memory is indicated by preferential exploration of the novel object (indicated by the thicker yellow arrow). Arrow thickness indicates the mouse's predisposition and time spent exploring the objects.

1.1.2 – The engram

The physical nature of memory has been elusive for a long period of time. In 1904, Richard Semon attempted to formalize the biological identity of these internal representations, introducing the term "engram", which he defined as "the enduring though primarily latent modifications in the irritable substance produced by a stimulus"[9]. For Semon, the engram represented the lasting chemical and physical alterations in brain state and structure that occur in response to an experience. Although he did not propose a precise biological storage model, Semon posited that engrams are stored via

physiochemical processes, becoming "dormant" once formed, yet susceptible to reactivation by a presentation of partial or similar cues. This conceptualization emphasized that the memory trace exists as a stable entity independent of the active processes required for its formation and recovery.

Another important contribution to the engram hypothesis came from Donald Hebb (1949), who developed a “cell assembly” theory. This theory proposed that when reciprocally interconnected neurons are simultaneously active during an experience, sufficient co-activity induces growth or metabolic changes that strengthen the connections between them. Hebb famously summarized this principle with the phrase: “neurons that fire together wire together”[10]. This enduring increase in synaptic strength, known as Hebbian plasticity, increases the probability that the specific spatiotemporal pattern of neural activity initiated during memory encoding will be faithfully recreated during later retrieval.

Semon’s and Hebb’s theories are corroborated by contemporary advances in engram investigation. Research now defines the engram as neuronal assemblies (or engram cells/neurons) which are sparse populations of co-active neurons carrying out a specific neural computation during a behavioural events[11,12,13]. Learning is viewed as the result of persistent physical/chemical changes in the selected neurons and their synaptic connections, thereby mediating the expression and storage of the encoded memory. The specific synaptic and cellular changes within these assemblies collectively reflect the engram itself. The converging evidence from diverse memory studies suggest that complex information is not represented by single cells; instead the engram is the basic unit of computation that stores information in the brain[14,15]. Furthermore, neurons belonging to a single assembly are not confined to one brain area but are distributed across several interconnected regions depending on the specific cognitive computation required[16].

Nonetheless, the fundamental building blocks of the engram can be studied at the level of single brain regions. Engrams are fundamentally dynamic structures: they are rapidly allocated and formed, subsequently undergo modification, and can eventually dissolve. Following encoding, consolidation

processes alter the engram's physical and chemical organization, enhancing its strength and quality. Moreover, memory retrieval may transiently destabilize a previously consolidated engram, initiating a new reconsolidation cycle that can lead to its further modification. Although the engram represents a highly dynamic and temporally evolving structure, this characteristic has proven not to preclude its tractability and success in being captured and studied at any given moment in time.

This tractability is historically rooted in the use of Immediate Early Genes (IEGs) as a classical method for identifying and tracking these neural assemblies. Since IEGs are rapidly transcribed in response to neuronal activity, their expression serves as a molecular signature for neurons that were selectively engaged during the encoding of a specific memory (e.g., c-Fos or Arc). IEGs are essential for synaptic plasticity induction and memory formation, with their transcription occurring independently of new protein synthesis. They function both as transcription factors regulating late-response genes, and as effector proteins directly modulating synaptic structure and strength[17]. Genes such as Arc, Egr1 (Zif268), and c-Fos are highly susceptible to DNA methylation and are expressed in the cortex, hippocampus and amygdala during learning and memory formation.

IEGs are an important tool for experimental access to the engram and the different phases of memory; for instance, c-Fos expression has been widely used to map the functional circuits underlying various complex behaviours, including neuroendocrine, autonomic, and behavioural responses to stress, nociception, sleep, and addiction[18]. These molecular activity markers initially provided the foundation for non-causal anatomical mapping of engrams, but their true power was unlocked through integration with advanced technologies. The combination of IEGs with techniques such as optogenetics, chemogenetics, single-cell transcriptomics, and combined tracing methods has dramatically enhanced the resolution and specificity of the system. For instance, transgenic reporter mice that express fluorescent proteins under IEG promoters (e.g., c-Fos or Arc) now enable repeated measurements of cortical activity over long time scales and facilitate the high-resolution, three-dimensional spatial mapping of behaviourally relevant circuits[19]. Most critically, these reporter lines

have been integrated with inducible technologies, such as the Targeted Recombination in Active Populations (TRAP) method. TRAP utilizes gene-targeted mice expressing tamoxifen-dependent Cre recombinase under IEG promoters to provide a revolutionary system that allows researchers to selectively manipulate and analyse activated neuronal ensembles at defined temporal windows, moving the field beyond observation to direct causal manipulation of memory[20,21]. Overall, this powerful set of genes and the correlated tools are constantly upgrading, giving the possibility to address questions about the molecular and cellular mechanisms associated with learning to help us understand memory function and neurobiological correlates of memory.

1.1.3 – The different phases of memory

Memory is generally conceptualized as a multi-staged process that includes distinct temporal phases: encoding, consolidation, retrieval, and eventually forgetting[22]. Historically, Semon suggested that an engram has four defining characteristics that govern its existence and functionality[23]. First, an engram is a persistent change in the brain resulting from a specific experience or event. This formation process, known as encoding, is conceptually represented by a subject's engagement with a novel environment or stimulus (as seen, for instance, by a mouse exploring new objects in the NOR test). Second, an engram has the potential for ecphory, the process through which it is expressed behaviourally via interaction with appropriate retrieval cues (which can be sensory input, ongoing behaviour, or voluntary goals). Third, the content of an engram reflects what was encoded and accurately predicts what can be recovered during subsequent retrieval. Fourth, and critically for modern research, an engram may exist in a dormant state between the two active processes of encoding and retrieval. This final characteristic emphasizes that the physical memory trace exists and persists beyond the direct operations required to form and actively recover it. These characteristics underpin the modern experimental framework used to study engram formation and manipulation, which is visually summarized in the conceptual model of engram dynamics (Figure 2). Specifically,

encoding marks the initial allocation and activity of a sparse neural ensemble; consolidation is the period where synaptic connectivity within the ensemble is structurally and functionally strengthened; retrieval is the cued reactivation of this established, persistent network; and finally, forgetting represents the loss of behavioural expression which follows the physiological decay of certain memories.

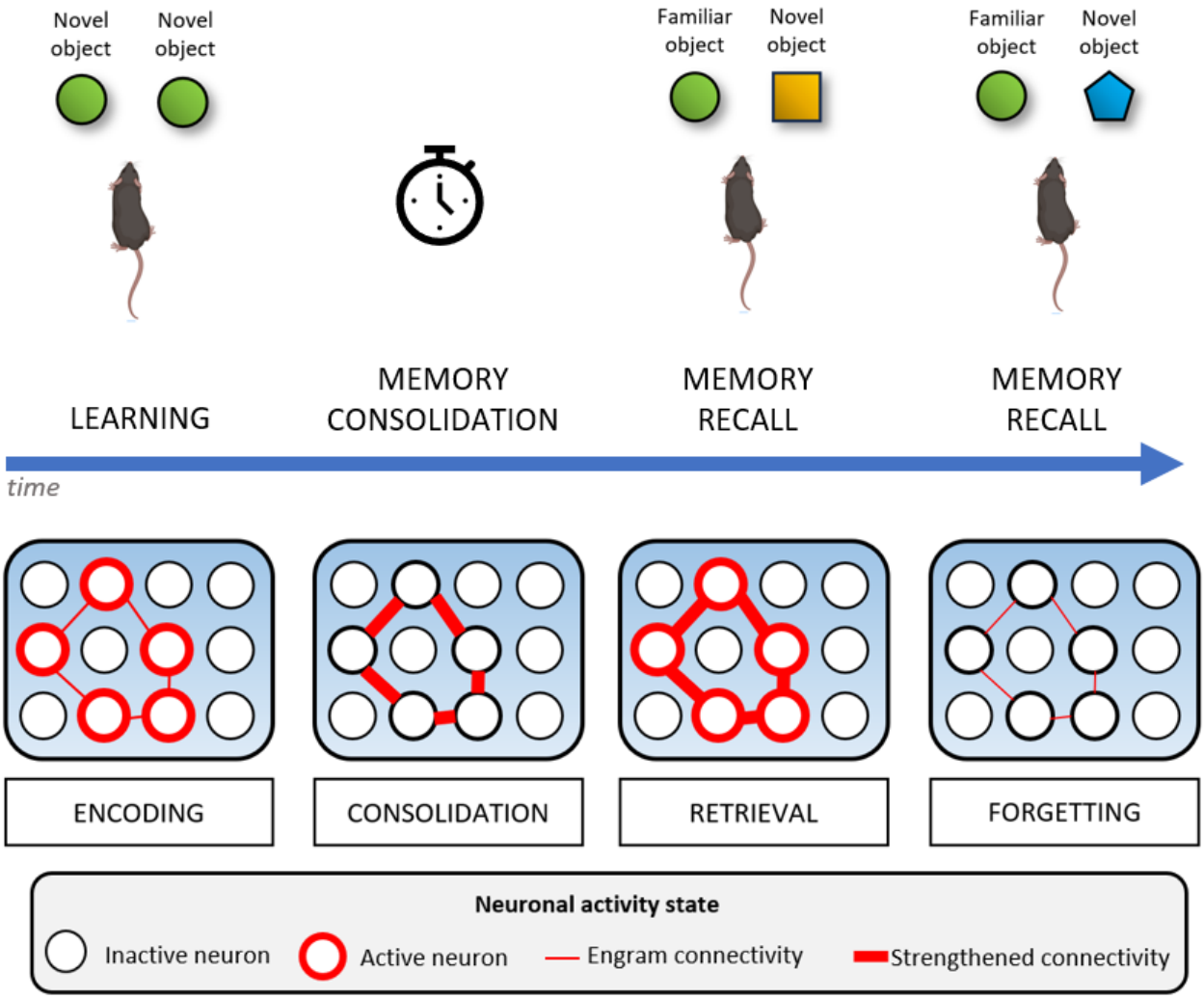

Figure 2. The behavioural and cellular temporal phases of memory

Behavioural Timeline (top panel)*: the mouse undergoes a four-step process, assessed using the NOR test: 1. Learning (acquisition/encoding) - the mouse explores two identical objects, forming a memory of the objects and the context. 2. Memory Consolidation - a time-dependent process (often assessed via a retention interval) where the initial, labile memory trace is stabilized into a LTM. 3. Memory*

Recall (Retrieval) - during the testing phase, the mouse is re-exposed to a novel object (orange square or blue pentagon) and shows preferential exploration, indicating successful retrieval of the familiar object's identity, until memory for the familiar object is eventually forgotten.

Cellular and Network States (Bottom Panel): *the diagram illustrates the memory engram across four theoretical states. Encoding: the specific subset of neurons that register the new information becomes Active (red thick circles), and the connections between them form the engram connectivity (thin red lines). Consolidation: the connections within the engram are strengthened (thick red lines), stabilizing the memory, while the neurons return to a "dormant" state (inactive neurons). Retrieval: the re-activation of the engram neurons, indicated by the strengthened connectivity, results in successful memory recall. Forgetting: the loss of the memory trace is characterized by the fading of the engram connectivity, with the neurons reverting to an inactive state (white circles) or maintaining only weak, ineffective connections.*

Learning is defined as the behavioural and cognitive process through which new information is acquired, culminating in the establishment of a memory trace. The initial encoding of information for a particular experience is rapid, typically occurring within a critical temporal window of seconds to minutes[24]. This process fundamentally relies on rapid, activity-dependent modifications to the efficacy of synaptic connections, a phenomenon broadly termed synaptic plasticity. Specifically, the persistent allocation of mnemonic information to a distinct neuronal ensemble - the engram - is physically mediated by changes in synaptic strength and connectivity. This underlying mechanism adheres to the principles that Hebb postulated: neurons that are functionally active at the same time adapt their synapses to become linked forming an ensemble, thereby establishing and reinforcing the connectivity within the memory-encoding circuit. The critical link between these cellular processes and behavioural learning was pioneered by Kandel and Tauc[25]. Their seminal work, utilizing the simple nervous system of *Aplysia*, unequivocally demonstrated that learning directly influenced

synaptic efficacy. They showed that short-term synaptic changes, such as facilitation and depression, underpinned the neural basis of non-associative learning, specifically habituation and sensitization, within the gill-withdrawal reflex. This shift from transient to persistent synaptic change was experimentally bridged by the discovery of Long-Term Potentiation (LTP). Building upon the principles of activity-dependent plasticity, Bliss and Lømo described a robust, long-lasting modification in synaptic strength induced by high-frequency electrical stimulation of afferent fibers in the hippocampus[26]. This effect provided the first compelling cellular mechanism for how a neuronal circuit could maintain enhanced connectivity over extended periods, making it the leading candidate for the synaptic basis of learning and memory storage. Subsequently, the inverse phenomenon, Long-Term Depression (LTD), was also described[27]. Collectively, LTP and LTD represent the bidirectional spectrum of long-term synaptic plasticity and are the principal cellular mechanisms underlying the enduring formation and modification of the memory engram.

The initial, transient phase of synaptic strengthening, termed Early-LTP (E-LTP), is critical for rapid encoding and short-term memory. E-LTP relies primarily on post-translational modifications, such as the phosphorylation of resident synaptic proteins, and is independent of *de novo* protein synthesis. This early phase is what initiates the allocation of information to the engram. The phase of E-LTP typically persists from seconds up to a few hours and relies solely on covalent modifications of pre-existing synaptic proteins[28]. Mechanistically, E-LTP is triggered upon high-frequency presynaptic firing, which leads to the release of glutamate into the synaptic cleft. Glutamate primarily activates the α-amino-3-hydroxy-5-methylisoxazole-4-propionic acid receptors (AMPARs) on the postsynaptic membrane, mediating the rapid influx of Na^+ and efflux of K^+. Simultaneously, the N-methyl-d-aspartate receptors (NMDARs), another class of ionotropic glutamate receptor, function as crucial coincidence detectors. Being sensitive to the depolarization state of the postsynaptic element (which relieves the Mg^{2+} block), NMDARs open to permit a significant Ca^{2+} influx into the postsynaptic terminal. This localized and rapid elevation of intracellular Ca^{2+} triggers a complex

cascade of intracellular signaling events. Among these is the activation of the Ca^{2+}/CaM-dependent protein kinase II (CaMKII)[29,30]. CaMKII acts as a central regulator of plasticity that rapidly enhances postsynaptic responsiveness through two key mechanisms: (1) Phosphorylation of the GluA1 subunit of AMPARs, which increases their single-channel conductance[31,32]; and (2) facilitating the insertion of additional AMPARs into the postsynaptic density (PSD) from an intracellular pool[33]. This rapid increase in the number and efficacy of surface AMPARs is the primary expression mechanism of E-LTP, facilitating enhanced impulse transmission. In parallel, the immediate increase in intracellular Ca^{2+} also orchestrates cytoskeletal modifications that are independent of new protein synthesis[34]. These signaling events, mediated by enzymes such as tyrosine kinases and Src family kinases, activate small GTPases (e.g., Rho and Ras GTPases)[35,36]. These signaling pathways are rapidly regulating Actin polymerization, and the spine structure is quickly modified, in a phenomenon known as structural plasticity[37,38,39]. This acute structural change physically reinforces the newly potentiated connection. However, the stabilization achieved during E-LTP is intrinsically transient, depending on the phosphorylation state of existing proteins. For the mnemonic information encoded by this initial synaptic strengthening to endure and be considered a long-lasting memory, the nascent engram must undergo a critical phase known as consolidation. This process requires a more robust and permanent physical stabilization, which is dependent on gene transcription and the synthesis of new proteins to maintain the synaptic and structural changes initiated during the early phase.

Learning induces changes in a population of neurons that respond to an experience; those neurons are selected through specific mechanisms. The initial process of engram encoding is governed by a competition-based rule, a mechanism wherein highly excitable neurons out-compete their less excitable counterparts for recruitment into the specific memory traces[40]. Generally, neurons with higher intrinsic excitability – the propensity of a neuron to activate and fire an action potential – are involved in the process of memory encoding[41,42,43]. In this context, the transcription factor cAMP Response Element-Binding protein (CREB) has been extensively studied. In many cortical and

subcortical regions, the protein CREB directly regulates neuronal activity during neuronal allocation in a specific engram[44,45,46,47]. Several works demonstrated that is possible to include or exclude specific group of neurons in the encoding phase by increasing or decreasing their levels of CREB[48,49]. Intrinsic neuronal excitability has been also described as an important mechanism of memory allocation. Neuronal excitability fluctuations occur naturally in the brain, determining which neurons are selectively encoding a memory, even in a CREB-independent manner[50]. Different evidences suggest other key players in the encoding phase, form epigenetic priming to other neuronal-intrinsic molecular properties and synaptic connectivity patterns, which are engaged during learning and bias neurons toward the encoding phase of memory[51,52].

As mentioned before, once the memory trace is successfully formed and allocated within specific neuronal ensembles, its persistence depends on its conversion into either a STM or a LTM. For an experience to persist as LTM, the activated neurons must undergo the process of synaptic consolidation, in which gene expression and de novo protein synthesis transform the initial, labile memory into a stable, persistent trace. This process is fundamentally characterized by an increased synaptic coupling and structural modification among the neurons co-active at the time of learning. The molecular underpinnings of synaptic consolidation have been extensively studied through pharmacological and genetic manipulation, including the suppression of CREB activity and the inhibition of general protein synthesis. These experimental approaches confirm that this time-limited molecular cascade is the critical point of divergence where a memory is either stabilized for long-term storage or is lost[53,54,55].

Once an engram has been consolidated and stored, it can be activated to induce memory retrieval[56]. Memory recall may be successful to the extent that the brain recapitulates the same neuronal activity present during the encoding phase[57]. The association between retrieval and the reactivation of the same neurons involved during learning has been consistently demonstrated using diverse engram tagging methods, across multiple memory paradigms and various neural regions[13]. Selectively

silencing engram neurons disrupts the corresponding memory retrieval[58], and on the other hand, activating these neurons promotes memory retrieval. Optogenetic or chemogenetic approaches aim at reactivating memory-encoding engram neurons inducing retrieval of the corresponding memory, even in the absence of proper environmental retrieval cues[59,60,61,62]. Despite the inherently non-physiological nature of these stimulation paradigms, experimental evidence indicates that activation of as few as two engram neurons within the visual cortex can suffice to induce pattern completion across the associated neuronal ensemble[63], thereby facilitating retrieval of the encoded mnemonic representation. Moreover, such protocols exert widespread neuronal effects, capable of reinstating endogenous-like spatiotemporal activity patterns in downstream neural circuits beyond the primary site of stimulation. This suggests a clear correlation between the engram formed during encoding and consolidated and its reactivation during memory retrieval.

An additional memory phase is forgetting. Forgetting can occur if the memory is no longer available because of complete engram degradation or a storage deficit, or because it is not currently accessible as a consequence of a retrieval deficit. Prevailing theoretical frameworks posit that neural systems are intrinsically predisposed toward information decay rather than indefinite retention[64]. Despite its traditionally negative connotation, forgetting constitutes an evolutionarily adaptive mechanism that facilitates efficient memory updating, optimizes decision-making processes, supports affective regulation, and contributes to overall cognitive and psychological homeostasis[65]. Synaptic remodelling occurs from different mechanisms, from depotentiation and pruning of existing synapses to elimination by non-neuronal cells like microglia and astrocytes[66,67]. By disrupting the properties of engram synapses, strengthened during early memory stages, circuit remodelling can decrease the probability of engram reactivation promoting forgetting of specific memories.

1.1.4 - Optogenetic breakthrough and critical limitations

Due to the intrinsic dynamic nature of the engram, major efforts have focused on specifically marking the neurons that are active during encoding. This field of research underwent a fundamental transformation in 2012 with a breakthrough study that moved beyond mere observation to direct manipulation. Transgenic mice were generated in which neurons that are active during a memory-encoding event are captured and tagged. Utilizing IEG promoters to drive the expression of the light-sensitive protein Channelrhodopsin-2 (ChR2), researchers could specifically tag and, crucially, optogenetically reactivate the exact neuronal ensemble formed during a learning event[59]. This revolutionary approach provided the first causal evidence that a defined group of neurons is both necessary and sufficient for the storage and retrieval of a specific memory, fundamentally validating Semon's century-old hypothesis and establishing the modern era of engram research.

With this strategy, direct stimulation of the tagged engram neurons leads to involuntary memory expression, addressing Semon's ecphory criterion. Moreover, memories can be evoked at time points remote from encoding, even when downstream synaptic strengthening is blocked, thus directly addressing the persistence and dormancy criteria. However, this powerful methodology presents several critical limitations that must be considered to advance and refine the study of engrams.

First, this technique achieves memory retrieval by forcing the simultaneous activity of the engram neurons through non-physiological light stimulation. This forced, synchronous activation is unlikely to recapitulate the precise spatiotemporal activity pattern that accompanied encoding. The loss of this fidelity may occur in the spatial, temporal, or both domains, leading to less effective reinstatement and a subsequently weaker behavioural expression than the naturally reinstated response evoked by an external sensory cue[62 68]. At the psychological level, natural memory retrieval is thought to be most successful when environmental and internal cues available at encoding are also present at retrieval[69], aligning with the principle of encoding specificity[70]. Second, the methodology fundamentally bypasses the normal timeline of memory. Memory is a constructive process, where

engrams are dynamically reconstructed in a use-dependent manner that is influenced by available details and current goals[71,72]. This reconstruction can lead to changes in the corresponding engram (i.e., the engram may be updated), including the formation of new associations. However, the artificial re-expression strategy reactivates the engram in its "tagged" state, which means during encoding, thereby completely bypassing the physiological and fundamental role of the consolidation phase in refining and stabilizing the memory trace. Third, these artificial expression studies have so far been limited to fear- and reward-conditioning paradigms. In these simpler paradigms, the behavioural readout is limited in complexity, making it challenging to fully address the engram's content criterion. One promising avenue for future studies is to use more complex tasks where the details of the encoding experience can be probed more extensively.

Finally, from a practical and translational point of view, the main limitation is the necessity of an external light source (for opsins) or drug (for DREADDs) whenever the memory needs to be re-activated. This represents a critical departure from classical memory formation and reactivation, where the consolidation phase plays a major role in stabilizing the memory trace, allowing subsequent neuronal reactivation simply by presenting the encoding cue or stimulus. Therefore, the limitations inherent in these artificial re-expression strategies underscore a critical shift in focus: understanding and modulating the consolidation phase represents the most compelling therapeutic and scientific avenue for achieving robust, persistent, and physiologically accurate recall of the memory engram.

1.2 - Molecular and cellular mechanism of engram consolidation

Having established that the consolidation phase is the critical determinant of an engram's persistence and physiological retrievability, this chapter now explores the cellular and molecular mechanisms responsible for stabilizing the newly encoded memory trace. Engram consolidation is the active, time-

limited process by which an initially labile memory is transformed into a stable, durable memory. At its core, this process involves the selective structural and functional remodelling of the sparse neuronal ensemble that comprises the engram. This remodelling is characterized by two distinct, yet interacting, forms of plasticity: local synaptic consolidation and distributed systems consolidation[73]. Systems consolidation involves the gradual, long-term reorganization and functional shift of the memory engram from a temporary storage site (the hippocampus) to more permanent circuits within the neocortex[22]. Synaptic consolidation relies on the synthesis of new proteins and the subsequent long-lasting reinforcement of connectivity within the engram circuit which can endure from hours to weeks[74]. This is achieved through the transition from E-LTP to Late-LTP (L-LTP), which establishes a physical scaffolding to stabilize the early synaptic changes. During this phase, both *de novo* mRNA transcription and translation of pre-existing mRNA take place[53,75,76]. Intracellular Ca^{2+} increase driven by E-LTP activates different signaling cascades mediated by PKA, PKC and mitogen-activated protein kinases (MAPKs), which in turn activate transcription factors such as CREB and C/EBP[77,44]. Their activation regulate the transcription of a repertoire of IEGs such as c-Fos, Arc, Homer, Zif268 and kinases such as CaMKIIa and cytoskeletal proteins[78]. Notably, the precise transcriptomic response is heterogeneous, varying significantly depending on the specific brain region and cell type involved. In the dendritic spines, protein synthesis occurs locally by ribosomes translating mRNAs in a localized manner, a process described as "synaptic tagging"[79].

During later consolidation into LTM, the transcriptomic profiles of engram cells undergo further, cell-type-specific changes, involving genes critical for transcriptional and translational regulation, vesicle exocytosis, transmembrane transport, and the organization of the dendritic spine and long-range intracellular transport[80]. Furthermore, gene expression during consolidation is also modulated by noncoding RNAs. Localized at the synapses, these RNAs provide a layer of molecular fine-tuning, adjusting gene expression to meet dynamic neuronal activity requirements. They function through multiple mechanisms, including modifying mRNA stability and translation, regulating transcription,

and triggering epigenetic modifications[81,82]. The cytoskeleton dynamics are equally critical to the consolidation mechanism. Beyond its role as a structural component, Actin directly modulates postsynaptic proteins within the PSD in response to activation, anchoring receptors via interaction with scaffolding proteins[83]. The stable polymerization of Actin and its associated scaffolding apparatus provides the long-lasting physical infrastructure necessary to maintain the enlarged spine structure and the enhanced number of surface receptors characteristic of the consolidated synapse[84].

While the molecular and structural changes described above are localized to the synapse, the precise boundaries of the memory trace remain a subject of intense research. Specifically, a persistent debate on the cellular versus synaptic engram continues to be a hot topic in the field. The crucial question is whether the fundamental unit of information storage is the collection of potentiated synapses (the "synaptic engram") or the entire activated neuron itself, encompassing all its global transcriptional and physiological states (the "cellular engram").

While decades of research have centered on the intrinsic properties of the neuronal engram circuit, an additional and increasingly recognized layer of complexity is introduced by the crucial role of non-neuronal cell types in memory processing and plasticity. Among the key non-neuronal regulators are microglial cells, the resident immune cells of the central nervous system parenchyma[85]. Microglia rapidly activate and proliferate in response to injury and pathology, and their homeostatic function is frequently impaired in various neurological disorders[86,87]. Critically, in development and adulthood, microglia actively participate in synaptic remodelling through processes such as pruning, thus regulating connectivity between neurons[88]. Studies involving the ablation of microglial cells have described their significant role in regulating the rate of forgetting, suggesting their continuous involvement in maintaining or clearing specific engram connections[89]. Similarly, oligodendrocytes, the glial cells responsible for axon myelination, are now understood to be responsive to neural activity[90]. Studies using mutant mice with deficits in oligodendrogenesis have demonstrated impaired remote memory consolidation, a deficit hypothesized to arise from improper synchronization or

efficiency during engram reactivation[91]. This suggests that structural white matter integrity, actively controlled by oligodendrocytes, is integral to the long-range integration required for stable memory storage.

Although microglia and oligodendrocytes contribute to engram dynamics through structural maintenance and circuit refinement, a deeper understanding of the immediate metabolic, homeostatic, and direct modulatory signaling within the local synaptic environment is essential. This critical function is primarily attributed to astrocytes[92]. As they functionally interact with the tripartite synapse, astrocytes represent a unique and integral component of the engram's structural and chemical regulation. Therefore, the subsequent chapter will focus on elucidating the diverse mechanisms by which astrocytes contribute to the synaptic consolidation of the memory engram.

1.2.1 - Astrocytes and memory consolidation

Astrocytes play multiple roles in the CNS, where they provide support and guidance for migrating neurons, and are involved in the physical structuring of the brain. They regulate cerebral blood flow and act as energy reserves, provide neurons with nutrients such as lactate, store glycogen and are capable of glycogenesis. Thus, astrocytes can fuel neurons with glucose during periods of high rate of glucose consumption and glucose shortage in CNS.

The astrocyte end-feet surrounding endothelial cells play a critical role in the development, maintenance and regulation of the blood–brain barrier. At the synaptic level, astrocytes express surface transporters for several neurotransmitters, helping in their uptake and inactivation and regulating neurotransmission. Also, astrocytes take part in regulation of ion concentration in the extracellular space; indeed, they express high levels of potassium channels that rapidly clear the excessive accumulation of these ions in the extracellular space[93,94,95,96,97]. In addition, astrocytes have been shown to improve neural survival and control neural differentiation and growth by releasing different neurotrophic factors, such as Neurotrofin-3 (NT3) and Brain Derived Neurotrophic Factor

(BDNF)[98,99]. In the last decade, many important breakthroughs have been obtained in the study of astrocytes and their involvement in memory formation and stabilization: from structural synaptic plasticity modulation to neuromodulation.

Astrocytes, traditionally viewed as passive support cells due to their lack of electrical excitability and inability to generate action potentials, are now recognized as active participants in brain information processing. Their unique form of excitability is manifested as dynamic elevations in cytosolic Ca^{2+} concentration, primarily through the mobilization of Ca^{2+} stored within the endoplasmic reticulum[100,101]. This signaling capability is mediated by the expression of a wide variety of functional neurotransmitter receptors, many of which are G-protein coupled receptors (GPCRs). Stimulation of these GPCRs by neuronal activity evokes diverse glial cell responses, with the intracellular Ca^{2+} elevation being the most extensively characterized[102,103]. Furthermore, multiple studies have demonstrated that astrocytes can release neuroactive molecules, collectively termed gliotransmitters, such as glutamate, adenosine triphosphate (ATP), and D-serine, in a Ca^{2+}-dependent manner. By binding to both presynaptic and/or postsynaptic receptors, these gliotransmitters effectively regulate neuronal excitability and synaptic transmission, thereby directly contributing to the mechanisms underlying memory formation[104,105,106]. The direct involvement of astrocytes is evidenced by several specific cellular and molecular mechanisms critical for engram consolidation. For instance, the inhibition of connexin hemichannels during memory consolidation has been shown to impair LTM[107], suggesting that glial-neuronal or glia-glia communication via these channels is essential. Conversely, targeted manipulations that disrupt normal astrocytic function also impair plasticity; the overexpression of the astrocytic protein S100β in transgenic mice, for example, results in impaired hippocampal LTP and deficits in spatial learning[108]. Beyond specific signaling molecules, astrocytes provide essential metabolic support critical for the high energetic demands of memory formation. Several studies have established that astrocytic metabolic functions are essential to sustaining the neural activity required for synaptic plasticity and consolidation[109,110,111,112]. Furthermore, astrocytic involvement extends to morphological plasticity. The dynamic retraction of astrocytic processes

suggests that the coverage of synapses is not random but precisely controlled, a mechanism believed to permit the enlargement of active synapses following learning[113]. This evidence highlights their role as active structural modulators of the synapse. Consistent with their fundamental role, a significant body of work in neurodegenerative diseases, particularly Alzheimer's disease, directly links memory impairment to abnormal astrocytic functioning, underscoring their critical and protective role in maintaining cognitive health[114,115,116]. Finally, the critical role of astrocytic signaling is starkly illuminated by studies targeting their capacity for vesicular release. Multiple lines of investigation demonstrate that the impairment of astrocytic vesicular release is an essential contributor to deficits in memory formation and consolidation[117,118,119]. These findings reinforce the necessity of gliotransmission for normal synaptic plasticity. To fully understand the mechanisms through which astrocytes regulate long-term plasticity, an increasingly crucial area focuses on their interaction with BDNF. BDNF is the most abundantly expressed and extensively studied neurotrophin in the brain, well-established for its indispensable role in memory and synaptic scaling. While the effects of BDNF on neuronal function are detailed, the intricacies of its physiology within astroglia have only recently begun to emerge. Over the last years, compelling new findings have demonstrated that astrocytes take an active and critical part in BDNF physiology, suggesting they are key players not just in the synthesis or release of BDNF, but also in its trafficking and recycling within the tripartite synapse. This astrocytic function provides a powerful, specialized mechanism through which they could regulate the availability of BDNF and, consequently, the persistence of memory traces. This mechanism forms the central focus of the following chapter, specifically examining the BDNF-TrkB signaling axis and the novel evidence for BDNF recycling and maintenance actuated by astrocytes.

1.3 - The BDNF-TrkB pathway

1.3.1 – Description

Brain-derived neurotrophic factor (BDNF) is a member of the neurotrophin family of secreted proteins and it plays a key role in synaptic plasticity, neuronal survival and cognitive functions[120]. These multiple biological functions are mediated by the activation of two receptors, tropomyosin receptor kinase B (TrkB) receptor and the p75 neurotrophin receptor.

In the brain, BDNF is widely expressed by glutamatergic neurons of many cortical areas, hippocampus, visual cortex and ventral tegmental area[121,122], and to a lesser extent in astrocytes and microglia, although in this cases the expression is highly context-dependent and usually tied to pathological or injury-related conditions[123].

The BDNF gene is located at chromosome 11 in humans, it has a complex structure with 11 different exons in humans, nine different exons in rodents, and nine alternative promoters for both groups[124,125]. The coding sequence is located in exon IX in both human and rodents, allowing for the encoding of the proBDNF protein. It is supposed that the nine alternative promoters can regulate the complex spatio-temporal expression of BDNF gene and allow BDNF to respond to a greater variety of stimuli.

Two forms of BDNF exists in the brain: the neurotrophin's precursor (proBDNF) and mature BDNF (mBDNF). Synthesis and maturation of BDNF is a multistage process, involving the formation of several precursor isoforms. The BDNF protein, discovered in 1982[126], is a highly conserved protein of 247 amino acids, synthesized and folded in the endoplasmic reticulum as preproBDNF (32–35 kDa). Upon translocation to the Golgi apparatus, the signal sequence of the pre-region is rapidly cleaved, and the isoform proBDNF (28–32 kDa) is generated[127]. proBDNF undergoes cleavage and is converted in the mature isoform mBDNF (13 kDa)[128], the pro-domain (BDNF pro-peptide, pBDNF) is removed intracellularly in neurons and astrocytes (by furin or PC1/3/7)[129,130] or extracellularly (by tPA/plasmin system or matrix metallopeptidases)[131,132].

BDNF can be released both by presynaptic and postsynaptic terminals[133]. In the latter case the release from the postsynaptic neuron can activate postsynaptic TrkB receptors in an autocrine fashion, promoting structural synaptic reinforcement. BDNF can also act as a retrograde messenger, modulating presynaptic vesicular release and glutamatergic transmission. In neurons, BDNF is released as a mixture of pro- and mature forms in different ratios, depending on the stage of brain development and region[134,135,136]. mBDNF binds with two kinds of plasma membrane receptors, the TrkB receptor[137] and the p75 neurotrophin receptor[138]. TrkB is considered to be the key receptor of mBDNF in adult brain since its wide range of expression and higher binding affinity to the neurotrophin with respect to p75, which binds preferentially the pro- form[139]. Activation of TrkB receptor promotes cell survival, facilitates long term potentiation (LTP) and increases spine complexity[140].

The binding of BDNF to TrkB receptor leads to phosphorylation of TrkB, activating different intracellular downstream signaling cascades, including phospholipase C gamma (PLC-γ), phosphatidylinositol 3-kinase/protein kinase B (PI3K/AKT), mitogen-activated protein kinase/extracellular signal-related kinase (MAPK/ERK) and guanosine triphosphate hydrolases (GTP-ases) of the Ras homolog (Rho) gene family pathways[141,142]. The BDNF/TrkB/PKC signaling is essential for synaptic function and maintenance[143], and it links pre- and postsynaptic activity to maintain neuromuscular function, which can be affected by a decrease in neuromuscular activity such in neuromuscular disorders[144]. BDNF/TrkB/PI3K/Akt pathway suppresses autophagy inhibiting the degradation of three important postsynaptic proteins (PSD-95, PICK1, and SHANK3) that are essential for N-methyl-D-aspartate receptor (NMDAR)-dependent synaptic plasticity[145]. BDNF also controls NMDA receptor subunits dynamic at different levels[146]. The PI3K/Akt/mTOR pathway promotes dendritic growing and branching through regulation of protein synthesis and cytoskeleton development[147]. The BDNF/TrkB/GTP-ases pathway promotes actin and microtubule synthesis, resulting in growth of neuronal fibers[148]. The MAPK/Ras-signaling cascade activates ERK 1/2 and

CREB, controlling immediate early genes expression such as c-Fos, and also cytoskeletal protein synthesis such as Arc[148]. Moreover, it plays a critical role in dendritic growth and branching of hippocampal neurons during neuronal differentiation[149]. During CNS development, the pro-BDNF/p75 neurotrophin receptor/sortilin binding complex initiates signaling cascades leading to activation of c-Jun amino terminal kinase (JNK), Ras homolog gene family member A (RhoA), and nuclear factor kappa B (NF-kB) downstream, which is involved in neuronal apoptosis, neuronal growth cone development and motility[139], and neuronal survival[132]. The specific role of BDNF in the regulation of numerous brain physiological processes depends on the interaction of its isoforms with different types of receptors. This, in turn, elicits the activation of signaling pathways that are critical for processes of brain development, synaptic plasticity, and protection and/or regeneration after damage. Perturbation of the BDNF synthesis, resulting in dysfunctions of its signaling cascades, may trigger several pathological processes. In fact, changes in BDNF levels in both peripheral blood and CNS, and the imbalance/insufficiency of pro-BDNF transformation into mBDNF, have been linked to several pathological conditions such as major depressive disorders, Alzheimer's disease, Parkinson's disease, Huntington's disease, amyotrophic lateral sclerosis, multiple sclerosis, and cerebral ischemic stroke[127,150].

1.3.2 – BDNF and synaptic plasticity

Neuroplasticity is the ability of the nervous system to reorganize its structure, function, and connections in response to extrinsic or intrinsic stimuli through different mechanisms[151]. Neuronal plasticity has been examined during critical periods, which represent specific early stages of brain development, when neural circuits are highly responsive to external stimuli and experiences that lead to lasting and widespread modifications. Although these circuits remain somewhat adaptable later in life, their capacity for change is significantly reduced. Once these critical periods conclude, the brain's ability to reorganize and reshape its network structure becomes more limited. One of the first evidence

of the neurotrophins' role in plasticity was observed in the visual cortex, where local BDNF synthesis is regulated by visual stimulation[152,153]. In this study, mice raised in the dark and resulting in lower levels of BDNF displayed a delay in visual plasticity[154]. Recent data indicate that many drugs used for the treatment of neuropsychiatric disorders (such as MDDs) can directly induce plasticity and reactivate a critical period-like plasticity in the adult brain by affecting the BDNF/TrkB pathway. Other mechanisms important for neuronal plasticity are the modification of mature neuronal morphology, involving axonal and dendritic arborization and pruning, an increase in spine density, and synaptogenesis[155]. Different studies suggest that intracellular overexpression of BDNF in hippocampal developing neurons induces maturation of excitatory and inhibitory synapses, with respect to exogenous application of BDNF[156]. Mice lacking BDNF die during the second postnatal week[157] and BDNF deficit causes inhibition of dendritic arborization[158] and reduction of expression of genes functionally related to vesicular tracking and synaptic communication[159]. BDNF is also required for several forms of LTP and LTD, the prototypical cellular models of synaptic plasticity. Many studies demonstrated that during LTP induction, BDNF is secreted and is functionally essential for acute signaling cascades leading to potentiation[160,161,162,163]. BDNF in LTP formation is best studied and understood in the hippocampus, but the effects of BDNF differ depending on the type of synapse and the brain region considered[160,141,164]. BDNF exerts fast effects on synaptic transmission by post-translational modifications of synaptic proteins, both at the pre- and post-synaptic levels[165,166]. BDNF-induced activation of TrkB receptors increases depolarization-evoked release of glutamate from isolated hippocampal and cerebrocortical nerve terminals[167,168,169]. The rapid effects of BDNF on neurotransmitter release are mediated, at least in part, by protein phosphorylation, downstream of TrkB receptor activation. Different studies reported the regulatory effects of BDNF toward the translation of specific mRNA[170]. Also, many dendritic transcripts are regulated by BDNF. The neurotrophin regulates glutamatergic synaptic transmission by acting at the pre- and post-synaptic level, where is sequestered in secretory vesicles and is released by a Ca^{2+}-dependent mechanism, following activation of glutamate receptors. BDNF can act also on pre-synaptic TrkB

receptors, potentiating glutamate release, and can induce the translocation of AMPA receptors to the synapse and increases the activity of NMDA receptors by phosphorylation-dependent mechanisms. Furthermore, BDNF induces local protein synthesis at the synapse from mRNAs transported along dendrites in RNA granules[171].

1.3.3 – BDNF-TrkB and memory

Due to its critical role in LTP, BDNF has been assumed to be an essential part of supporting memory formation and maintenance by promoting synaptic integration[160]. BDNF is involved in the formation of different types of memories and is also critical for maintaining long-lasting storage of information in hippocampus and in different cortical regions many hours after learning occurs. Different studies described BDNF as a key mediator of memory processing at different molecular levels: it regulates cation channels (several subtypes of Na+ and K+ channels) and ligand-gated channels (NMDA and AMPA receptors) after TrkB-mediated activation of intracellular signalling cascades, and it regulates transcription and translation of different proteins[172,173].

In hippocampus and amygdala-dependent memory processing, a fine control of BDNF release and processing is required. Recognition memory increases BDNF release and activates ERK1/2 in the dentate gyrus and in the perirhinal cortex[174], while hippocampal specific deletion of the BDNF gene impairs spatial learning and novel object recognition[175]. Interfering with BDNF/TrkB signaling in the amygdala has an effect on the acquisition and consolidation of fear memory conditioning, but the signaling cascade elicited by the two molecules is also necessary for extinction of aversive memories[176]. The downstream components of the BDNF-driven signaling pathway involved in memory consolidation are still under investigation, however an increased amount of experiments show that inhibition of ERK1/2 signalling before and/or after training sessions impairs long-term memory retention[177,178].

Many cortical areas are involved in BDNF/TrkB-driven memory processing. BDNF in prefrontal

cortex plays a dual role depending on the cortical region involved: in the prelimbic region BDNF is required for fear memory consolidation, while infralimbic BDNF is necessary for fear memory extinction. In perirhinal cortex, KO of BDNF translation impairs recognition memory consolidation[179]. In posterior parietal cortex the neurotrophin is important for fear memory, in insular cortex BDNF infusion rescues amnesia induced by protein synthesis inhibition, and in motor cortex BDNF has been demonstrated to be necessary in long lasting memories of motor map representation[180,181,182].

Different observation of the BDNF's role in memory has been obtained through the study of its unique polymorphism. The pro-domain of BDNF is the locus of a functional human BDNF polymorphism (SNPs) Val66Met, also known as rs6265 or G196Apolymorphism. This point mutation causes a substitution of Valine (Val) to Methionine (Met) at codon 66 (Val66Met) in the pro-domain of BDNF[183]. Since this SNP exists only in human, several attempts have been made to mimic the function of BDNF Val66Met in cellular models or in genetically engineered mouse models. In 2003 BDNF Val66Met polymorphism was shown to disrupt the episodic memory in humans[184]. In 2005 it was discovered that the BDNF Val66Met substitution also disrupts the sortilin-binding site, impairing activity-mediated secretion of BDNF[185]. The principle molecular mechanism associated with the polymorphism is the deficient activity-dependent release of BDNF, which consequently impacts the efficiency of BDNF-TrkB signaling.

This establish BDNF as a pivotal molecule in synaptic plasticity, required for the consolidation of LTM. Crucially, the persistence of memory requires not only the synthesis of new plasticity-related proteins but also the precise temporal and spatial regulation of neurotrophin signaling. While neuronal release of BDNF drives immediate plastic changes, astrocytes play a critical role in regulating the BDNF microenvironment through reuptake and recycling. The next chapter focuses on elucidating the specific mechanism by which astrocytes in the perirhinal cortex (PRC), a central region in recognition memory, maintain BDNF homeostasis, ensuring the necessary sustained signaling required for memory consolidation.

1.4 - The mechanism of BDNF recycling in astrocytes

To sustain the neurotrophin signaling required for LTM, astrocytes are essential regulators of BDNF concentration in the synaptic cleft. In 2016 Vignoli and colleagues described a new mechanism by which peri-synaptic glia provides proBDNF clearing and recycling via p75 receptor ($p75^{NTR}$), resulting in localized TrkB activation on adjacent neurons. The astrocytic BDNF recycling is relevant for LTP and LTM maintenance at cortical synapses, specifically in perirhinal cortex[129]. This work explores a novel mechanism of BDNF release which diverge from the classical activity-dependent secretion of BDNF from neurons.

To experimentally dissect the role of astrocytic BDNF recycling, this work utilizes a genetic approach for conditional deletion of the p75 receptor. The mouse model employed is the tamoxifen-inducible conditional p75lox/lox-GLASTCreERT2-R26R mutant mouse (hereafter referred to as p75-flox mice) [186].

This system is designed to selectively delete the astrocytic $p75^{NTR}$, which is responsible for the uptake of BDNF in astrocytes. The key steps of the deletion protocol are:

- Cell-Type Specificity: The expression of Cre recombinase is driven by the GLAST (Glutamate Aspartate Transporter) promoter, ensuring that expression is specific to astrocytes (GLAST positive cells).
- Inducible Deletion: The Cre activity is dependent on the ligand tamoxifen (CreERT2). Tamoxifen treatment is administered for five consecutive days, causing astrocytes to initiate the deletion of the p75lox allele.
- Receptor Depletion: After two additional weeks post-tamoxifen treatment, the complete depletion of already existing p75 receptor protein is observed due to the natural turnover of the protein.

This conditional knockout strategy allows for the precise temporal control of the genetic manipulation and ensures that the observed behavioural or molecular deficits can be causally linked to the loss of

astrocytic p75 ^{NTR} function in the adult animal, thereby isolating the role of this specific recycling mechanism during recognition memory consolidation.

Building upon this genetic manipulation, cortical slices derived from the p75-flox mice were analysed for synaptic plasticity. These slices exhibited an impairment in maintaining L-LTP induced by theta burst stimulation (TBS), showing a decline back to baseline levels approximately 140 minutes after the initial stimulation. Importantly, LTD remained unaffected by the glial p75 receptor deletion, indicating a specific deficit in the mechanisms underlying L-LTP maintenance. This selective synaptic deficit translated directly into an impairment in long-term recognition memory *in vivo*. When tested using the NOR task within a Y-arena, the p75-flox mice displayed no deficit in memory at the 1-hour time point following the sample phase, indicating intact STM. However, a significant memory impairment was observed at the 24-hour time point, confirming a defect in LTM consolidation. Crucially, the researchers successfully rescued the behavioural phenotype by re-expressing the p75 receptor specifically in cortical astrocytes using a lentiviral vector, establishing the causal role of astrocytic p75-mediated BDNF recycling in LTM maintenance. In fact, when cortical astrocytes are depleted form p75 receptor, astrocytic proBDNF internalization as well as TrkB phosphorylation in neighbouring neurons are impaired. However, neither TrkB phosphorylation nor the late phase LTP are directly regulated by proBDNF itself, but instead by its processing inside the astrocytes. It is known that cortical layer II/III astrocytes show a highly branched arborization and fine membrane extensions in the cell periphery[187]. The intricate ramifications of astrocytes allow them to tightly enwrap the synaptic terminals at organized microdomains[188,189,190], and proBDNF is specifically internalized in these small peri-synaptic regions[191].

Once internalized, astrocytic microdomains coordinate the recycling process. The proBDNF undergoes proteolytic cleavage and accumulate as both BDNFpro and mBDNF. These two components are then stored in the same vesicles and subsequently secreted back into the synaptic cleft for synaptic re-use via vesicle-associated membrane protein 3 (VAMP3), a key soluble N-ethylmaleimide-sensitive fusion protein attachment protein receptor (SNARE) protein that is

abundant in astrocytes[192]. Glial cells are reported to lack *de novo* proBDNF synthesis under physiological conditions[193], strongly suggesting that the BDNFpro and mBDNF detected in these cells originate solely from the proBDNF that was previously endocytosed and cleaved. This inactive-to-active processing of the pro-neurotrophin significantly increases mBDNF availability, thereby exceeding the transient, activity-dependent neurotrophin secretion provided by neurons. The BDNFpro exhibits a fundamental and independent role in this recycling mechanism, acting as an activator of TrkB/SorCS2 aggregation by targeting post-synaptic spines[194]. This facilitates TrkB translocation at post-synaptic regions, which is crucial for both synaptic tagging and LTP maintenance[195]. In this manner, an overall increase of both TrkB receptors and mBDNF can be observed at the level of activated synapses, ultimately amplifying the activated TrkB molecular cascade. Thus, astrocytic BDNFpro recruits TrkB expression on adjacent spines, ensuring tight temporal, spatial, and stimulus-dependent TrkB phosphorylation.

Recently, Losi, Vignoli and colleagues provided an additional and fundamental layer of complexity to the BDNF recycling system actuated by astrocytes. They demonstrated that spontaneous fluctuations of intracellular Ca^{2+} within astrocytic microdomains represent functional signals critical for the release of both mBDNF and BDNFpro[196].

The researchers investigated Ca^{2+} signal dynamics in astrocytes from the PRC layer II/III by injecting adeno-associated viral vectors for the transduction of the cytosolic Ca^{2+} indicator GCaMP6f and the reporter tdTomato. Ca^{2+} dynamics were studied both at rest and in response to TBS. This imaging revealed spontaneous and stochastic Ca^{2+} signals that were independent of neuronal activity. These signals exhibited a period of synchronization that coincided with TBS delivery before returning to basal activity. Importantly, these Ca^{2+} transients were demonstrated to be critical for LTP stabilization.

To prove this causality, the researchers employed a chemogenetic approach for silencing Ca^{2+}-microdomains. In this model, wild-type mice were injected with a viral vector (AAV5/2-GFAP-hM3D(Gq)-mCherry) that transduces the Gq-coupled receptor specifically in astrocytes. This allowed

for the selective activation of astrocytes by clozapine-N-oxide (CNO). CNO administration induced a biphasic response: an initial, transient increase of astrocytic intracellular Ca^{2+} levels, followed by a prolonged period of silencing. This biphasic pattern suggests that the subsequent inhibition of astrocytic Ca^{2+} signaling results from the depletion of intracellular Ca^{2+} stores[197]. Crucially, the use of this model allowed them to selectively impair spontaneous Ca^{2+} transients after the TBS delivery, while successfully sparing both the spontaneous activity before TBS and the evoked Ca^{2+} response to TBS.

Behaviourally, the impact of perturbing spontaneous Ca^{2+} dynamics on LTM was assessed using the NOR task. Ca^{2+} dynamics in *in vivo* cortical astrocytes transduced with AAV-hM3Dq are suppressed within 10 minutes of intraperitoneal CNO administration and remain inhibited for at least one hour[197]. When CNO was administered 30 minutes before the sample phase, mice displayed a significant reduction in the discrimination index at the 24-hour retention interval. This specific time window is critical, as administration immediately before the sample phase (t = 0) or 24 hours after the sample phase had no effect on LTM, thus strongly supporting the essential role of spontaneous astrocytic Ca^{2+} transients in the post-encoding consolidation phase of memory engrams. In summation, these findings position the astrocytic Ca^{2+} signaling machinery as a crucial regulator: a sustained, stochastic source of gliotransmitter release that is dynamically integrated with thousands of synaptic circuits to tailor memory engram consolidation to specific cortical states and behavioural contexts.

The astrocytic control over BDNF release adds a crucial, yet complex, layer to the engram consolidation system, requiring a high degree of spatial and temporal resolution to fully understand how BDNF-TrkB signaling is coordinated across distinct cellular compartments and memory phases. Therefore, the final introductory chapter details the development and utility of OptoTrkB, a cutting-edge optogenetic tool that we propose to utilize for the unprecedented, high-fidelity analysis of TrkB activity during memory consolidation.

1.5 - The OptoTrkB molecule

Until recent times, studies investigating TrkB signaling have largely relied on conventional genetic approaches (e.g., genetically mutated models[198,199,141,200,201,202]), the use of specific agonist and inhibitors[176,203], and truncated forms of TrkB[204]. Generally, these methodologies suffer from inherent limitations: they cannot be regulated or targeted to specific circuits or subcellular compartments, nor can they be activated or deactivated within restricted, physiologically relevant time frames. This lack of spatiotemporal precision makes it particularly challenging to dissect the BDNF-TrkB signalling events that underlie rapid, local processes such as synaptic plasticity and engram consolidation.

The emergence of optogenetics has provided a powerful alternative, utilizing light to precisely control cellular activities. This field has seen the development of numerous genetically encoded photoactivable channels and signaling proteins that have been successfully employed to study diverse cellular functions[205], including synaptic transmission[206,207,208]. However, optogenetic tools capable of directly inducing or manipulating intrinsic synaptic plasticity mechanisms, especially those involving complex receptor tyrosine kinases like TrkB, remain relatively rare[209,210]. This gap highlights the need for a targeted optogenetic approach to finally disentangle the spatial and temporal requirements of BDNF activity during memory formation.

In 2020, Huang and colleagues described the first optical tool to control the TrkB signalling, OptoTrkB[211], allowing for an unprecedented spatiotemporal control of this molecular pathway, even non-invasively in the mouse brain[212].

The endogenous TrkB receptor consists of three principal components[213]: an extracellular domain that function as the neurotrophin binding site, a transmembrane domain, and an intracellular catalytic domain (a tyrosine kinase). Ligand binding normally induces the dimerization of two TrkB monomers, thereby activating the intracellular kinase domain through trans-autophosphorylation.

Crucially, the OptoTrkB construct used in this work was specifically engineered to lack the native extracellular domain. This modification, coupled with improvements to increase its sensitivity to

light, provides a significant advantage by ensuring very low basal activity in the absence of light and completely decoupling its activation from endogenous BDNF concentration.

The genetic sequence has been designed to be incorporated in AAV (~4.9 kb limit). The expressed protein prevents its activation by endogenous ligands since only the cytoplasmic domain of TrkB (cytTrkB; aa 454-821) is present. A myristoylation sequence (Lyn signal peptide) is added at the N-terminus of cytTrkB to promote its localization to the plasma membrane, and a Cry2PHR domain is conjugated to the end of cytTrkB. The photolyase homology region (PHR) domain of cryptochrome 2 protein from *Arabidopsis thaliana* is one of the most widely used phototropins found in optogenetic modules, which induce or inhibit molecular functions in mammalian cells[214,215,216,217,218], and it is activated specifically by blue light (430 to 490nm)[219]. The group developed a Cry2PHR mutant, Cry2PHR(E281A), by structure prediction and showed that it exhibits reduced basal activity (spontaneous activity without light stimulation) upon linking to the target protein[220]. The OptoTrkB molecule is also equipped with a hemagglutinin-tag (HA) sequence to the C-terminus to facilitate its detection.

The utility of OptoTrkB is further enhanced by the precision of its delivery and operation. Regional specificity of OptoTrkB expression is controlled by site-specific viral vector injection and the use of cell-type-specific promoters, while temporal control is dictated by the precise regulation of the light source. By employing different light emission patterns, it is possible to activate downstream molecular cascades in a transient or more sustained way, even through the intact skull and fur of an *in vivo* mouse model[212,221]. This unprecedented spatiotemporal control is what allows us to precisely dissect the BDNF-TrkB signaling requirements during the discrete phases of memory engram consolidation.

AIMS OF THE THESIS

2.1 - Background

The transformation of fleeting experiences into stable, enduring knowledge - the very essence of learning - is critically dependent on memory consolidation. This post-encoding neurobiological process is the cornerstone of long-term memory formation, taking temporary, labile memory traces and reinforcing them into stable, enduring forms. Failures in consolidation underpin the cognitive deficits observed in numerous neurological and neurodegenerative disorders, emphasizing its fundamental importance to brain function and behaviour.

One of the most important molecular players implied in this process is BDNF and its high-affinity receptor, TrkB. TrkB signaling is a potent initiator of the structural and functional plasticity required to stabilize neuronal ensembles, or engrams, that physically represent the consolidated memory. Understanding how the precise timing and location of TrkB activation govern engram stability is crucial for unlocking the mechanisms of robust memory formation.

Despite the established importance of the BDNF-TrkB pathway, research into its real-time, functional contribution to consolidation *in vivo* faces significant hurdles. Traditional pharmacological and genetic approaches often lack the spatiotemporal precision required to definitively link a brief signaling event to a long-term behavioural outcome. To overcome these limitations, a methodology is required that can impose on-demand, precise temporal control over TrkB signaling specifically within identified engram circuits. This precise control is the essential prerequisite for dissecting the causal role of the BDNF-TrkB pathway in memory consolidation and translating these findings into therapeutic strategies.

2.2 - Objectives

To address the limitations in achieving spatiotemporal control over the BDNF-TrkB signaling pathway and to definitively test its causal role in long-term memory consolidation, we employed the innovative optogenetic tool, OptoTrkB. This light-inducible receptor allows for the non-invasive,

temporally precise activation of TrkB specifically within designated neuronal populations. The research presented in this doctoral thesis is structured around the following specific objectives:

- To validate the system of OptoTrkB activation *in vitro* by demonstrating acute, light-dependent phosphorylation (activation) of TrkB downstream signaling cascades (e.g., ERK1/2, CREB) in excitatory neurons following external blue-light delivery.
- To establish causal efficacy of OptoTrkB in LTP and memory consolidation rescue experiments. To determine if precise, on-demand TrkB signaling is sufficient to stabilize a fragile memory trace, we took advantage of several LTP and LTM-impaired mice models, and applied precise temporal OptoTrkB activation during critical post-encoding window required for memory stabilization.
- To causally determine the role of engram-specific consolidation in LTM maintenance by achieving selective rescue of an impaired long-term object recognition memory. We accomplished this through the targeted optogenetic manipulation of the BDNF/TrkB signaling axis exclusively within the perirhinal cortex engram neurons associated with a single, specific object memory, thereby bypassing astrocytic BDNF recycling deficiency and advancing the translational potential of this technology.

RESULTS

3.1 - Validation of OptoTrkB function in cortical neuronal culture

The central aim of this study required a tool capable of precise spatiotemporal control over TrkB signaling. Before proceeding to *in vivo* memory experiments, we first validated the light-dependent function of the OptoTrkB system in cultured neurons. Specifically, we assessed whether blue light delivery could efficiently activate the canonical TrkB downstream signaling cascade. For this validation, the OptoTrkB plasmid (pAAV-CaMK2a(0.4)-Opto-cytTrkB(E281A)-HA) was obtained from Addgene. The purified DNA was extracted using an EndoFree Plasmid Maxi kit, and its concentration and purity were verified using a Nanodrop spectrophotometer. The plasmid, encoding the CaMKIIa-OptoTrkB-HA construct, was then delivered to primary cortical neuronal cultures via nucleofection.

To induce OptoTrkB activity, we adapted a light-pulse pattern previously described by Huang and colleagues[211] to achieve transient phosphorylation of downstream molecules. This pattern consisted of 470-nm light pulses delivered at 5-s intervals for 10 min, using a 200-ms pulse duration at 9.7 W/cm^2. This light-pulse was delivered to specific regions of the cultures by using a Digital Light Processor (DLP) (Figure 3.a). The delivery was sufficient to induce phosphorylation of ERK1/2 and CREB in neurons located within the illuminated regions (Figure 3.b). Image analysis of fluorescence intensity was performed on fixed cultures, confirming that illuminated neurons showed significantly increased levels of ERK1/2 and CREB phosphorylation compared to control neurons (either kept in the dark or located immediately outside the illuminated area). The timing of this phosphorylation events are highly dependent on the experimental model and the specific stimulus applied. However, it is well-established that ERK1/2 phosphorylation is typically observed very quickly following receptor activation. This activation is transient, often peaking about 1-15 minutes after stimulus[222] [223] [224]. On the other side, CREB phosphorylation usually follows a more sustained time course, often displaying a first transient activation at 30 minutes and peaking hours later[225].

OptoTrkB signaling faithfully displayed this canonical temporal pattern: the initial phosphorylation of ERK1/2 peaked sharply at 10 minutes post-illumination, with a sparse signal visible in both the soma and nucleus. This was followed by a temporally shifted and predominantly nuclear phosphorylation of CREB peaking at 30 minutes after blue light delivery. In both cases, the signal of phosphorylated molecules decayed significantly with time (i.e., after 90 minutes post-illumination). To confirm the light-specificity of the activation, control neurons transfected with OptoTrkB and illuminated with green light pulses 546-nm showed minimal activation, with only a slight increase in signaling compared to the dark control condition (Figure 3.c). Taken together, these *in vitro* characterizations confirm that the OptoTrkB system functions as a tightly controlled, light-activated TrkB mimic that successfully recapitulates the canonical, biologically relevant temporal signaling dynamics of BDNF activation, making it a robust tool for our subsequent *ex vivo* and *in vivo* investigation of memory consolidation.

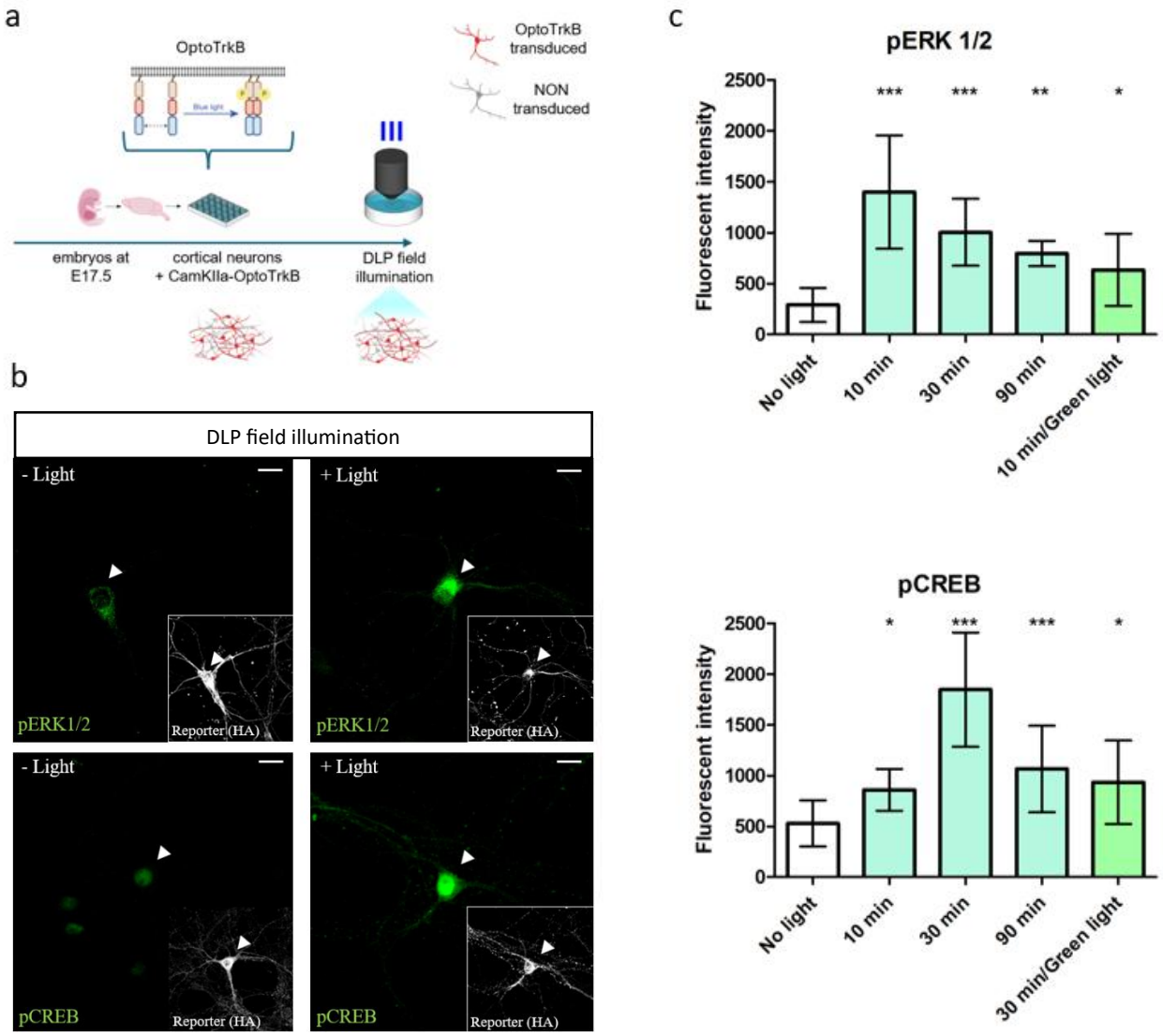

Figure 3. Light-activable OptoTrkB induces downstream molecules phosphorylation

a) *Schematic diagram of the experimental procedures.* ***b)*** *LSC images (60x) of OptoTrkB-HA expressing neurons immunostained for phosphorylated ERK1/2 or CREB not exposed to light (- Light) or illuminated by DLP (+ Light). Scale bar: 10µm.* ***c)*** *The bar-plots show mean fluorescent intensity of pERK1/2 and pCREB, plotted against time interval between illumination and time of PFA fixation. Coverslips from "No light" condition were kept in dark during the experiment and fixed without exposing neurons to any source of light. *p < 0.05, **p < 0.01, ***p < 0.001 (one way ANOVA with Tukey's multiple comparison test). (Number of neurons analysed in pERK1/2 plot, from left to right: n = 19, n = 14, n = 19, n = 11, n = 17. Number of neurons analysed in pCREB plot, from left to right: n = 9, n = 7, n = 9, n = 15, n = 11).*

3.2 - Restoring L-LTP in p75-flox mice using OptoTrkB

The successful *in vitro* validation of OptoTrkB as a precise "light-controlled TrkB" molecule prepared the groundwork for its application in addressing specific functional deficits *ex vivo*. As described in the introduction, LTP is the primary cellular model for examining the synaptic mechanisms underlying learning and memory. Field excitatory postsynaptic potential (fEPSP) recordings were used to investigate the stability of this synaptic transmission.

Our laboratory previously reported that astrocytic $p75^{NTR}$ is essential for long-lasting LTP (L-LTP) maintenance in brain slices from the PRC[129]. Normally, the application of TBS in wild-type (WT) or control slices induces a significant increase in fEPSP amplitude and slope that remains potentiated above baseline for the entire recording duration (e.g., 3 hours). Critically, however, TBS application in PRC slices from p75-flox mice results only in short-term potentiation (S-LTP), with the typical L-LTP being compromised; the electrical signals of the postsynaptic neurons reverse back to a basal state after TBS delivery.

This established deficit is caused by a failure in BDNF-TrkB signaling, normally critical for converting S-LTP into L-LTP. We therefore hypothesized that artificially bypassing the $p75^{NTR}$-mediated BDNF recycling mechanism by directly activating TrkB molecular cascade with OptoTrkB would be sufficient to rescue the L-LTP deficit in p75-flox slices.

In order to obtain the necessary high cellular specificity and expression of OptoTrkB in living animals, the adeno-associated viral vector AAV9-CaMKIIa-Opto-cytTrkB(E281A)-HA was produced by our collaborators. The combined tropism of the AAV9 capsid and the use of the CaMKIIa promoter ensured the precise regional expression of OptoTrkB specifically in CaMKIIa-positive excitatory neurons. We injected this vector into the perirhinal cortices of 3-month-old p75NTR-flox mice. After a 1-week recovery period, mice were treated with tamoxifen for 5 consecutive days to induce Cre recombination and achieve reliable depletion of astrocytic $p75^{NTR}$. We then waited an additional 3 weeks to allow for optimal vector expression and complete p75 receptor depletion in the

treated mice (Figure 4.a). Subsequently, we observed the effects of glial $p75^{NTR}$ deletion on LTP in cortical slices from p75-flox mice transduced with OptoTrkB and compared them to control slices (from WT mice injected with AAV9-CaMKIIa-tdTomato). LTP was induced applying TBS (100 Hz; four sets of stimulations delivered 15 s apart, each one consisting of ten bursts of five pulses at 100 Hz with inter-burst intervals of 150ms) in layer II/III of perirhinal cortices. LTP induction and maintenance were analysed for up to 180 min after stimulus.

Although direct light stimulation of OptoTrkB in acute brain slices had not been previously described, we leveraged protocols established for *in vivo* manipulation. Specifically, Hong and Heo demonstrated that a single 30-second exposure of blue light (473nm) delivered via an optic fiber was sufficient to activate ERK1/2 phosphorylation in the mouse brain[212]. Moreover, Lilja and colleagues employed a similar pattern (30 second of continuous blue light at 488nm and 0,5mW/mm^2 power) delivered through an external LED source on mice with transparent skull surgery; this stimulation was sufficient to activate CREB phosphorylation specifically in CaMKIIa-positive pyramidal neurons of the visual cortex[221]. We selected this latter 30-second continuous light-stimulation protocol to activate OptoTrkB by directly illuminating the PRC in brain slices with a focused laser, aiming for maximal TrkB activation to test rescue hypothesis.

The electrophysiological recordings confirmed our hypothesis: illuminated brain slices from p75-flox mice transduced with OptoTrkB displayed normal L-LTP stability, mirroring the sustained potentiation observed in illuminated brain slices from WT control mice expressing tdTomato. In contrast, p75-flox brain slices that were not exposed to blue light illumination displayed only a S-LTP, with the fEPSP signal decaying and returning to baseline conditions after approximately 120-140 minutes (figure 4.b). These findings conclusively demonstrate that the L-LTP maintenance deficit caused by a disrupted astrocytic BDNF-recycling can be fully rescued by the light-mediated and ligand-independent activation of neuronal TrkB signaling.

To provide molecular validation for these electrophysiological results, we performed immunohistochemical analysis to evaluate the expression levels of pCREB in perirhinal neurons as an index of successful OptoTrkB activation in the PRC layer II/III.

Brain slices exposed to illumination or electrical stimulation were fixed in PFA 4% at different time points. Slices from the following conditions: “light only”, “TBS only” and “TBS + light” were fixed 30 minutes after stimulus delivery, while slices from the “no light” condition were kept in the dark and used as the basal control. Slices from the long-term condition, “TBS + light (3h)”, were fixed after the full 3-hour LTP recording period. The fluorescent signal of pCREB was colocalized with NeuN, confirming that the analysis was restricted to mature neurons (Figure 4.c). Brain slices from transfected p75-flox mice kept in the dark were used as the control and reference for calculating the fold change difference among different conditions (Figure 4.d)

Image analysis revealed that illuminated neurons in the infected PRC area expressed pCREB at a significantly higher intensity than neurons kept in the dark, and these levels were similar to the pCREB levels observed in neurons that received TBS alone. Importantly, a plateau of pCREB expression seems to be reached in these conditions, as the combination of light and TBS stimulation in the same slice displayed the same maximal activation levels as the "only light" and "only TBS" conditions. Finally, pCREB levels in the illuminated and stimulated slices showed a natural decay after three hours (“TBS + light (3h)” condition), demonstrating that the transient activity of this molecular pattern diminishes in periods far from the electrical or optical stimulation.

The experiments presented in this chapter confirm that the L-LTP maintenance deficit following $p75^{NTR}$ deletion is attributable to a lack of sufficient TrkB activation. The ability of OptoTrkB to rescue L-LTP and induce a canonical molecular activation pattern (via pCREB) provides a robust foundation for our ultimate goal: to utilize this tool *in vivo* to temporally dissect the role of BDNF-TrkB signaling in memory consolidation.

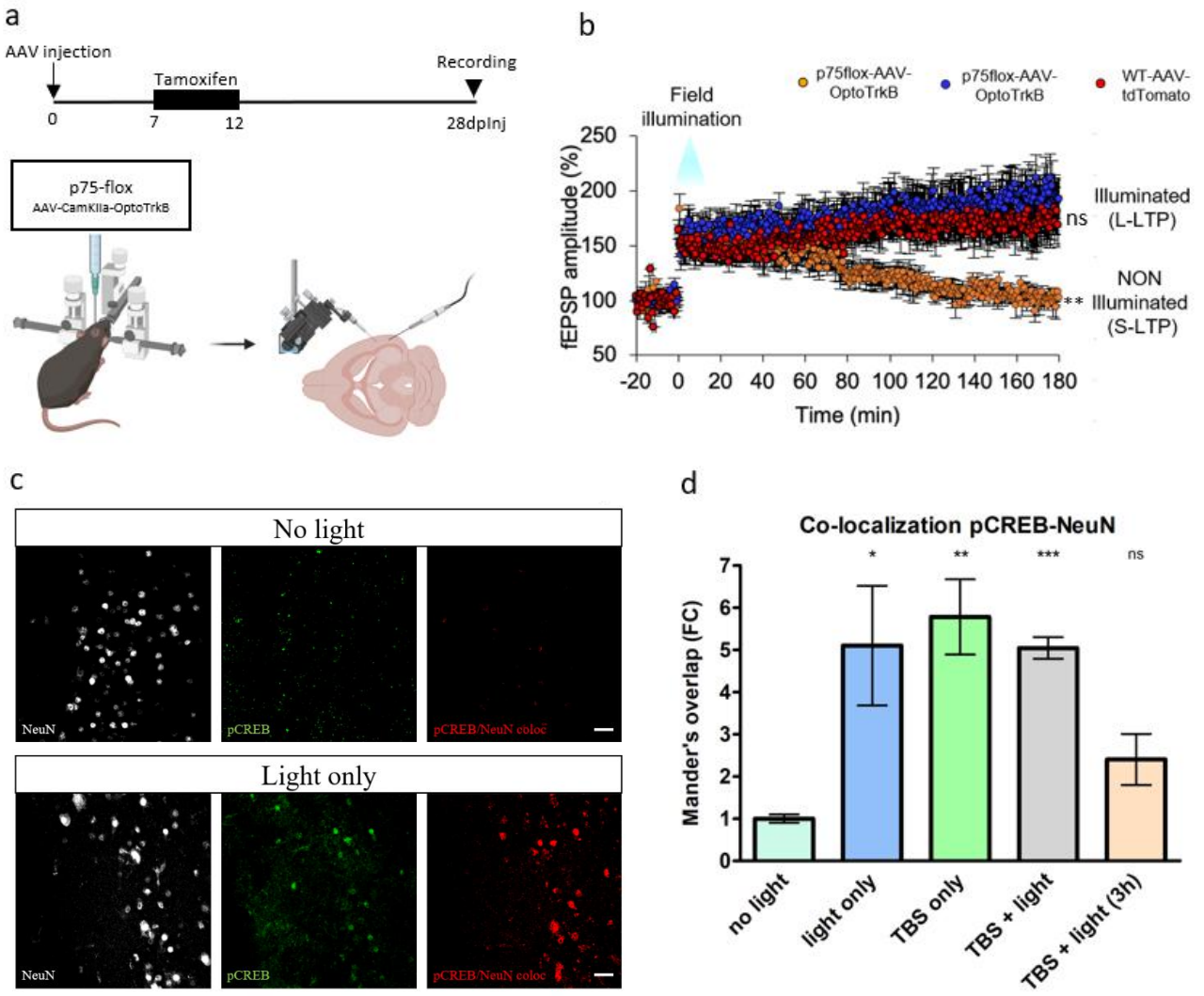

Figure 4. OptoTrkB activation rescues LTP deficit in p75-flox mice

a) *A schematic diagram shows the experimental paradigm used for virus injection and tamoxifen treatment in p75-flox mice. The AAV9-CaMKIIa-OptoTrkB vector was stereotaxically injected in PRC at day 0. Tamoxifen was administered for 5 consecutive days (day 7 to day 12) to induce* $p75^{NTR}$ *deletion in astrocytes. Electrophysiological recording was performed 28 days post injection (dpinj).* ***b)*** *The plot depicts the fEPSP amplitude, normalized to baseline, elicited in PRC slices. The graph shows the average fEPSP amplitude before (0-20 min) and after (20-180 min) TBS and the eventual illumination. Data are presented as mean ± SEM. Illuminated p75-flox-AAV-OptoTrkB slices (blue dots) showed maintenance comparable to WT controls (expressing tdTomato, red dots), while non-illuminated p75-flox-AAV-OptoTrkB slices exhibited only S-LTP and decayed back to baseline*

*(unpaired t test, ns p > 0,05, **p < 0,01). WT-tdTomato, n = 8 slices, 4 mice, p75-flox-OptoTrkB "illuminated", n = 8 slices, 6 mice, p75-flox-OptoTrkB "NON illuminated", n = 5 slices, 5 mice.* ***c)*** *LSC images (20x) of PRC slices depicting pCREB (green) and NeuN (white) expression, with a focus on the p75-flox-OptoTrkB "no light" control and "light only" conditions. pCREB/NeuN colocalization (red signal) serves as an index of successful OptoTrkB activation. Scale bar: 50µm.* ***d)*** *The bar-plot quantifies the pCREB and NeuN colocalization signal, expressed as Fold-Change (FC) relative to the p75-floxOptoTrkB "no light" control condition. Data show a strong increase in pCREB upon optical or electrical stimulation, which returns to baseline after 3h. Data are mean ± SEM (3 slices for each condition analysed). Statistics: *p < 0.05, **p < 0.01, ***p < 0.001, ns p > 0.05 (one-way ANOVA with Tukey's multiple comparison test).*

3.3 - Home-cage Novel Object Recognition (hcNOR) test

The NOR test is a standard behavioural assay used to evaluate non-spatial memory of object identity, a function critically dependent on the integrity of the PRC for both encoding and maintenance[226 227]. Typically, this test is performed within a dedicated testing arena (e.g., a square box or Y-maze) into which mice are introduced and habituated over several days prior to the object familiarization and test phases. This standard protocol, however, involves that the animals associate the object identity learning with the specific context of the arena. The required habituation and subsequent testing in this distinct environment engage an extended network of brain regions, including the sensory cortices and thalamus for filtering sensory information, and the hippocampus and amygdala for processing the emotional and contextual salience of the novel setting. Consequently, the resulting memory trace, or engram, is likely expansive, comprising neurons activated not only by the objects but also those encoding the contextual cues of the arena[228]. To restrict the population of encoding neurons primarily to those associated with the objects and thereby diminish the confounding contribution of the context, we designed a novel variant of the NOR test carried out directly within the mice's home cage (hcNOR).

For the hcNOR protocol, mice were singly housed (one mouse per cage) for a minimum of seven days prior to testing. This single housing condition was implemented to both facilitate unambiguous tracking of individual exploration behaviour during the test phases and eliminate potential variance or distraction arising from social interaction. During the sample phase, two identical, geometrically simple objects were introduced into opposite corners of the home cage (Figure 5.a). Object exploration time was recorded and quantified using a camera positioned directly above the cage. Objects were removed after a standardized five-minute exploration period. For the subsequent test phase, one of the familiar objects was substituted with a novel object. To preclude a priori "intrinsic" preferences, all objects used were carefully matched for physical properties, including shape, texture, and overall dimensions (Figure 5.b). A critical feature of the hcNOR method is that mouse

manipulation is entirely avoided between phases, and contextual pre-habituation is rendered unnecessary, as the test is performed directly within the animal's stable, familiar home environment.

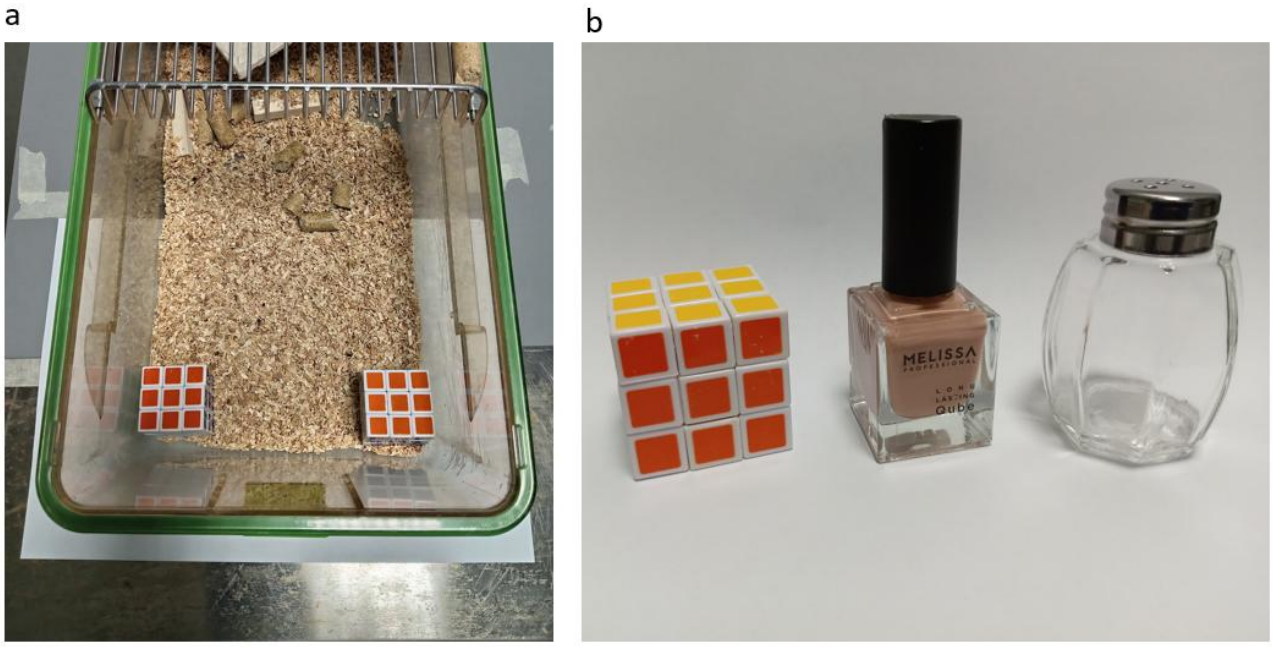

Figure 5. hcNOR protocol and stimuli matching

a) *Overhead view of a mouse home cage during the sample phase of the hcNOR protocol. Two identical, geometrically simple objects are placed in opposite corners of the bedding area.* ***b)*** *Example objects used for the task, matched for shape, texture, and overall dimensions to control for intrinsic preferences (e.g., small puzzle cube, nail polish bottle, and salt shaker).*

The functional integrity and specificity of the hcNOR method were assessed by testing wild-type C57BL/6J mice. These control experiments were essential to confirm that animals housed and tested under these conditions exhibit intact, canonical novel object recognition memory, providing a necessary baseline for comparison with experimental groups. To further characterize the memory retention profile supported by the hcNOR protocol and establish the time course of memory consolidation and natural decline, separate cohorts of WT mice were tested at four distinct retention intervals: 24 hours, 7, 10 and 14 days following the sample phase (figure 6.a). This approach aligns with the established understanding that long-term object recognition memory naturally undergoes a gradual decline over time. WT mice tested at 24 hours and 7 days following the sample phase successfully retained the object recognition memory, exhibiting a significantly positive and comparable Discrimination Index ($p > 0.05$). By 10 days post-sampling, a decline in the DI was evident although not significative, indicating a partial impairment or natural attenuation of the memory trace within this cohort. Furthermore, the cohort tested at 14 days demonstrated a complete loss of recognition memory, with the mean DI failing to reach statistical significance above the chance level ($DI \approx 0$, Figure 6.b). These results establish that the retention window for object recognition memory under the hcNOR protocol is reliably maintained up to 7 days and is substantially diminished by 14 days.

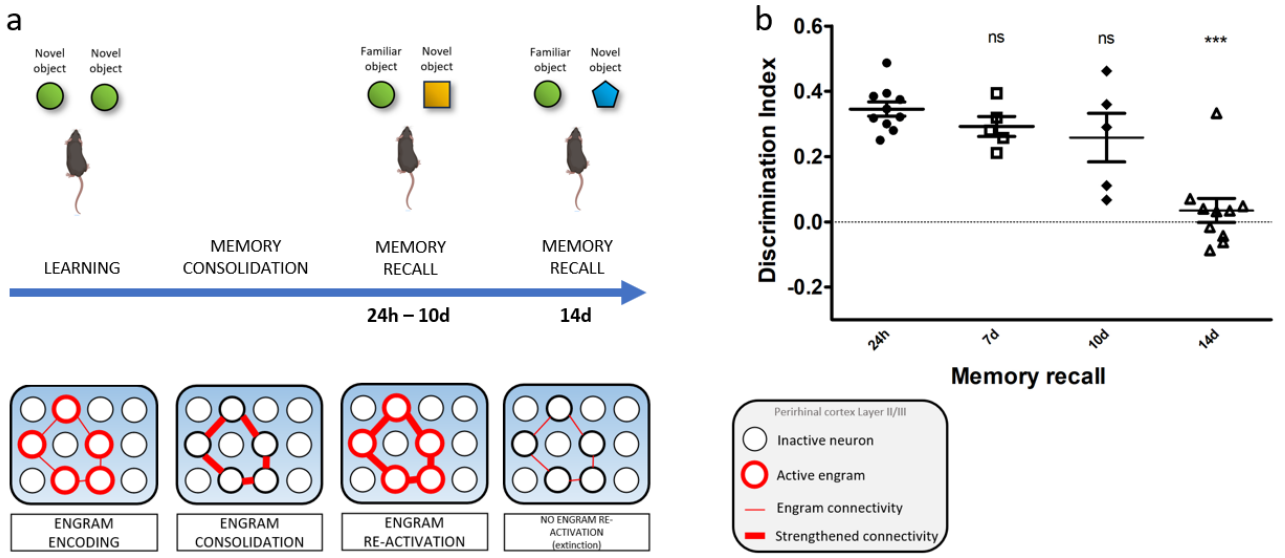

Figure 6. Memory retention profile using the home-cage Novel Object Recognition (hcNOR) test

a) *Schematic of the hcNOR behavioural paradigm and engram dynamics. Wild-type (WT) mice underwent the sample phase (learning phase) by exploring two identical familiar objects (green circles) placed in the home cage. Memory recall was assessed in separate cohorts at 24 hours, 7 days, 10 days, and 14 days after the sample phase. During the test phase (memory recall), one familiar object was replaced with a novel object (e.g., yellow square or light blue pentagon). The lower panel schematically illustrates the proposed underlying neuronal dynamics in the PRC (Layer II/III) across the phases: Engram Encoding (formation of object-specific ensemble), Consolidation (strengthening of connectivity), and Recall/Re-activation (successful memory retrieval) or Extinction/Loss (failure of engram re-activation).* ***b)*** *Discrimination Index across Retention intervals. The dot plot shows the mean Discrimination Index ± SEM for WT mice plotted against the time interval between the sample phase and test phases. Statistics: One-way ANOVA with Tukey's multiple comparison post-hoc test. Significant memory retention (DI > 0) was observed at 24 hours, 7 days, and 10 days. The memory trace was significantly diminished by 14 days. Specifically, ***$p < 0.001$ for the comparison of 14 days vs. 24 hours. Cohort sizes: n = 10 mice (24h), n = 5 mice (7d), n = 5 mice (10d), n = 10 mice (14d).*

In summary, the hcNOR paradigm represents a reliable and valid alternative to the classical NOR test. This method successfully supported canonical object recognition memory in WT mice, yielding a memory retention profile (up to 7 days) that is comparable to that established in conventional arenas. Crucially, the hcNOR protocol eliminates the confounding variables associated with handling stress and the formation of an arena-specific contextual engram. By avoiding animal manipulation and pre-test habituation to a novel environment, this method ensures a more specific and robust evaluation of object recognition memory, thereby establishing a highly sensitive and validated platform for studying the underlying neuronal mechanisms of engram formation and consolidation in subsequent experiments.

3.4 - Impaired astrocytic BDNF recycling selectively abolishes LTM: validation of the context-minimized hcNOR paradigm

As detailed in the introduction, the astrocytic recycling mechanism of proBDNF exerts a fundamental influence on the consolidation of long-term object recognition memory. Our previous laboratory findings have demonstrated that impairment of this mechanism at several key steps leads to a loss of LTM, while STM remains intact, when tested via the classical NOR paradigm. These disruptive manipulations include: (I) genetic ablation of the astrocytic proBDNF internalization receptor (p75-flox mice[129]), and (II) pharmacologically disrupting the vesicular release of mBDNF and BDNF propeptide through the use of the DREADD hM3Dq system[196]. Given the reported LTM deficits in these models tested under conventional conditions, we hypothesized that the hcNOR paradigm, which minimizes contextual encoding, would similarly reveal the phenotypic LTM impairment across these established mouse models, thereby validating the hcNOR system for subsequent mechanistic investigation.

To investigate the behavioural phenotype associated with the astrocytic $p75^{NTR}$ depletion, three-month-old p75-flox mice were treated with tamoxifen for five consecutive days. A two-week period followed the final dose to ensure the complete and widespread deletion of astrocytic $p75^{NTR}$. During this period, all mice were singly housed in preparation for the hcNOR test. Following the $p75^{NTR}$ depletion, mice were subjected to the hcNOR paradigm, with memory assessed at three retention intervals: 1 hour (to evaluate STM), 4 hours and 24 hours (to assess LTM) post-sample phase (Figure 7.a).

Consistent with their intact STM, p75-flox mice exhibited a significantly positive Discrimination Index at the 1-hour retention interval, demonstrating a strong preference for the novel object. However, by the 4-hour retention interval and continuing to 24 hours post-learning, p75-flox mice were unable to discriminate between the familiar and novel objects ($DI \approx 0$). Consequently, the Discrimination Index recorded at both the 4-hour and 24-hour time points was significantly lower

compared to the 1-hour DI ($p < 0.01$, Figure 7.b). These results validate that the p75-flox model displays a rapid transition from intact STM to LTM failure when tested using the context-minimized hcNOR.

To test the effect of acute pharmacological disruption of astrocytic release, three-month-old WT mice received stereotaxic injection of AAV5-GFAP-hM3Dq. A minimum of four weeks was allowed post-injection to ensure robust, astrocyte-specific expression driven by the GFAP promoter. Throughout this period, mice were singly housed in preparation for the hcNOR test. On the test day, five minutes prior to the sample phase, hM3Dq-expressing mice received an intraperitoneal injection of CNO. The CNO activates the hM3Dq DREADD, leading to the depletion of intracellular Ca^{2+} within astrocytic microdomains, thereby preventing the Ca^{2+}-dependent vesicular release of mBDNF and BDNF propeptide. Mice were then subjected to the hcNOR paradigm, with memory assessed at two retention intervals: 1 hour (STM evaluation) and 24 hours (LTM evaluation) post-sample phase (Figure 7.c).

Consistent with their intact STM, the CNO-treated WT-hM3Dq mice exhibited a significantly positive Discrimination Index at the 1-hour retention interval, demonstrating a robust preference for the novel object. However, at the 24 hours post-learning, mice were unable to discriminate between the familiar and novel objects ($DI \approx 0$). Consequently, the Discrimination Index recorded at 24-hour time points was significantly lower compared to the 1-hour DI ($p < 0.001$, Figure 7.d). These data further confirm that acute astrocytic disruption of BDNF release results in a specific failure of LTM consolidation, a phenotype which is reliably captured by the hcNOR paradigm.

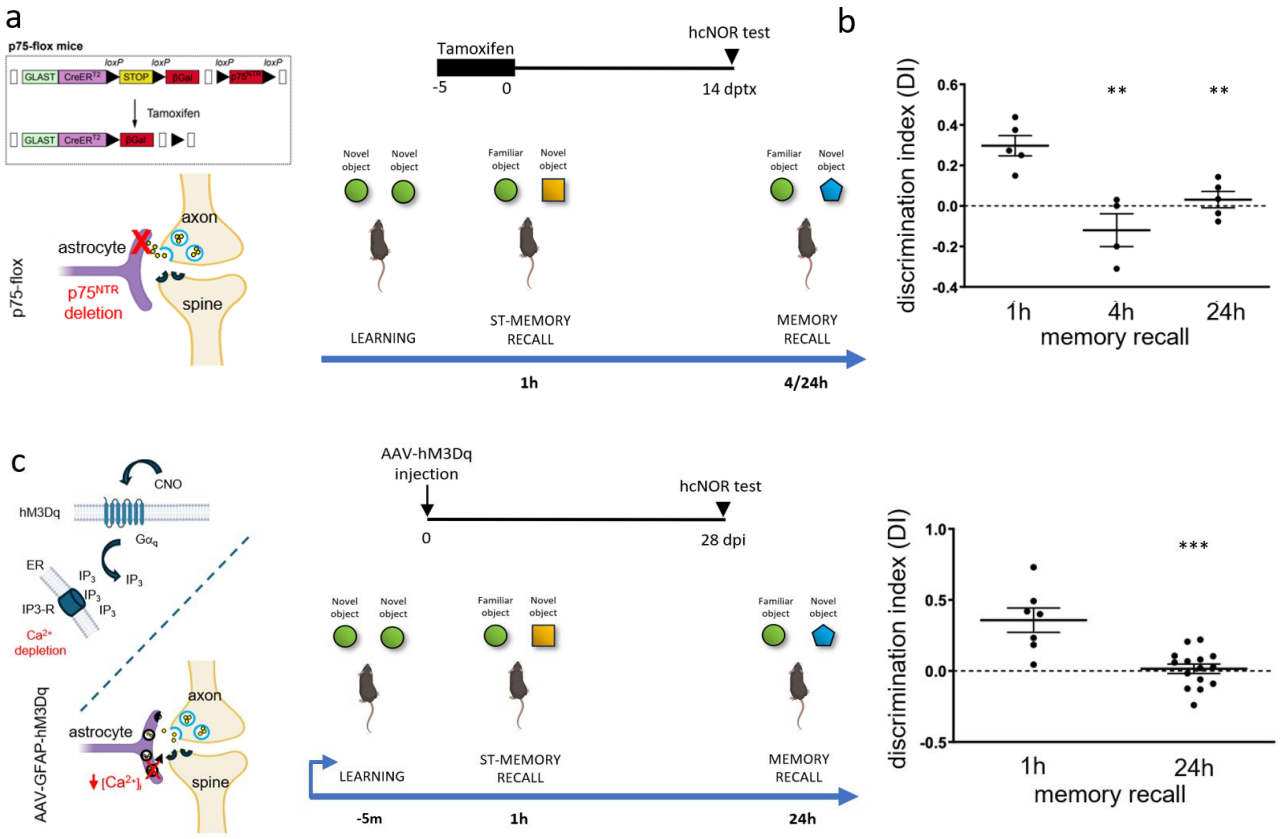

Figure 7. Validation of the hcNOR paradigm in mouse models of impaired astrocytic BDNF recycling

a) *Experimental design and mechanism for p75-flox mice, schematic illustrating the genetic deletion of astrocytic* $p75^{NTR}$ *(which mediates proBDNF internalization). Three-month-old p75-flox mice were treated with Tamoxifen (5 days), leading to GLAST-CreER-mediated deletion of* $p75^{NTR}$ *in astrocytes. Fourteen days post-tamoxifen treatment (dptx), mice were subjected to the hcNOR test, with memory retention assessed at 1 hour (STM), 4 hours, and 24 hours (LTM) post-sample phase. The left panel shows the resulting impairment of proBDNF uptake and recycling by the astrocyte.* ***b)*** *Short-Term and Long-Term Memory deficits in p75-flox mice. The dot plot shows the mean Discrimination Index ± SEM for p75-flox mice at different retention intervals. While STM was intact (DI > 0 at 1h), LTM was significantly impaired at both 4h and 24h. Statistics: One-way ANOVA with Tukey's multiple comparison post-hoc test. DI at 4h and 24h were significantly lower compared to the 1h DI (**p < 0.01 vs. 1h DI). Cohort sizes: n = 5 mice (1h); n = 4 mice (4h); n = 5 mice (24h).* ***c)*** *Experimental design and mechanism for WT-AAV-GFAP-hM3Dq mice. Schematic illustrating the acute*

pharmacological depletion of astrocytic Ca^{2+} via DREADD hM3Dq activation. WT mice received stereotaxic injections of AAV-GFAP-hM3Dq to achieve astrocyte-specific expression. Twenty-eight days post-injection (dpi), mice were injected with CNO 5 minutes before the sample phase to activate the DREADD. This activation sequesters intracellular Ca^{2+}, preventing the Ca^{2+}-dependent vesicular release of mBDNF and BDNF propeptide. Memory was assessed at 1 hour (STM) and 24 hours (LTM). ***d)*** *LTM deficit in WT-AAV-GFAP-hM3Dq mice. The dot plot shows the mean Discrimination Index ± SEM for CNO-treated WT-AAV-GFAP-hM3Dq mice. STM was intact (DI > 0 at 1h), but LTM was impaired. Statistics: Paired t-test comparing the 1h and 24h retention intervals. The DI at 24h was significantly lower than the DI at 1h (***p < 0.001). Cohort sizes: n = 7 mice (1h); n = 15 mice (24h).*

The successful recapitulation of the known LTM deficits in both p75-flox and AAV-GFAP-hM3Dq mouse models using the novel hcNOR paradigm validates this context-minimized method as a robust platform for studying the underlying neuronal mechanisms of recognition memory consolidation. Our data confirm that disrupting the astrocytic BDNF recycling axis rapidly and specifically abolishes LTM. Having demonstrated that the LTM loss stems from impaired astrocytic signaling to the post-synaptic compartment, the subsequent chapter focuses on directly restoring the TrkB signaling cascade. We will employ an innovative, non-invasive chemiluminescent approach, utilizing the luciferase-luciferin interaction within astrocytes to drive the activation of OptoTrkB in post-synaptic neurons, thereby simulating the astrocytic release of BDNF to restore LTM in these impaired mouse models.

3.5 - Bioluminescent Optogenetic for non-invasive OptoTrkB activation

The phenomenon of bioluminescence, involving the catalytic activity of enzymes such as luciferase to emit light upon the oxidation of specific substrates (e.g., luciferin), has been broadly utilized *in vitro* and *in vivo* to non-invasively activate light-gated ion channels and pumps in excitable cells[229]. This approach, termed Bioluminescent Optogenetics ("BL-OG"), represents a chemogenetic strategy capable of driving optogenetic reactions deep within the brain[230,231]. Photosensory proteins that rely on light-dependent dimerization or conformational changes can be activated by bioluminescence to modulate diverse cellular processes, ranging from protein localization and regulation of intracellular signaling pathways to gene transcription.

We sought to leverage BL-OG to achieve non-invasive, targeted activation of OptoTrkB in post-synaptic neurons. To mechanistically recapitulate the physiological function of astrocytes, specifically the peri-synaptic storage and subsequent Ca^{2+}-dependent release of endocytic vesicles containing mBDNF and its pro-peptide, which activate post-synaptic TrkB, we engineered astrocytes to express a luciferase-releasing vesicle system.

To achieve this, we utilized the following AAV vector construct, provided by our collaborators: AAV5-GFAP-hPOMC1-26-sbGLuc-P2A-dTomato. This construct is designed to ensure astrocyte-specific expression (via the GFAP promoter) of the following components: (I) sbGLuc, a highly optimized, blue light-emitting *Gaussia* luciferase variant engineered to resist low pH[232,233,234]; and (II) a vesicle-targeting sequence derived from the human pro-opiomelanocortin pro-peptide ($hPOMC_{1-26}$)[235,236], which directs the sbGLuc cargo into astrocytic endocytic vesicles. The entire coding sequence is linked via a self-cleaving P2A sequence to a reporter gene, tdTomato, enabling identification of transduced astrocytes.

To facilitate tracking of the specific genetic tools used in the bioluminescent optogenetic experiments, the constructs are summarized in Table 1.

Viral Vector	Target Promoter	Vector key functions
AAV9-CaMKIIa-Opto-cytTrkB(E281A)-HA	CaMKIIa (excitatory neurons)	OptoTrkB (photosensitive TrkB variant)
AAV5-GFAP-hPOMC1-26-sbGLuc-P2A-dTomato	GFAP (astrocyte-specific)	sbGLuc (blue light-emitting luciferase) hPOMC1-26 (vesicular targeting sequence)
AAV5-GFAP-Synb-sbGLuc	GFAP (astrocyte-specific)	hSyn-sbGLuc (The luminal end of synaptobrevin/VAMP2 expose the luciferase to the cleft with activity driven vesicle fusion to the astrocytic membrane, but without releasing it)
AAV5-GFAP-hM3Dq	GFAP (astrocyte-specific)	hM3Dq (deplete intracellular Ca^{2+} from astrocytic microdomains, blocking vesicular release)

Table 1. List of viral vectors used and their key functions

To test the efficacy of the Bioluminescent Optogenetic (BL-OG) system in rescuing memory consolidation deficits, we employed the p75-flox mouse model. Three-month-old p75-flox mice received bilateral stereotaxic injections into the PRC layer II/III of two distinct viral vectors:

AAV5-GFAP-hPOMC$_{1-26}$-sbGLuc-P2A-dTomato (to express the vesicle-targeted luciferase in astrocytes) and AAV9-CaMKIIa-Opto-cytTrkB(E281A)-HA (to express the photosensitive TrkB variant in excitatory neurons). One week following vector injection, mice were treated with Tamoxifen for five consecutive days to induce astrocytic $p75^{NTR}$ depletion. A minimum of four weeks post-injection was allowed for viral expression and Cre-recombination to complete (figure 8.a). Mice were then subjected to the first hcNOR test (Trial 1). Immediately following the 5-minute sample phase, mice received an intraperitoneal injection of Coelenterazine (CTZ), a BBB-permeable substrate for sbGLuc[237 238] (Figure 8.b). The activation of OptoTrkB by the resultant bioluminescence was expected to drive LTM consolidation.

To confirm that the rescue was dependent on the CTZ-induced light signal, the same cohort of mice underwent a second hcNOR test (Trial 2) one week after Trial 1, using two novel objects. In Trial 2, the post-sample treatment consisted of a vehicle injection (saline) instead of CTZ. Finally, to assess the durability and physiological decay of the rescued memory, a subset of the Trial 1 cohort was tested at 14 days post-first learning (Figure 8.b).

The p75-flox mice that received the CTZ injection immediately following the Trial 1 learning phase displayed a significant rescue of LTM, exhibiting a positive Discrimination Index at the 24-hour retention interval, successfully overcoming the characteristic LTM impairment observed in this model. In contrast, during Trial 2, when the same mice were subjected to the vehicle injection after learning, they were unable to discriminate between the familiar and novel objects at 24 hours post-second learning. The DI for this group was statistically indistinguishable from zero, recapitulating the typical LTM failure phenotype of the p75-flox model, also indicating that the OptoTrkB activation in Trial 1 was not affecting subsequent learning events. When tested for remote memory retention at 14 days post-first learning, the rescued memory trace exhibited a physiological decay, with the mice showing a loss of recognition memory (DI ≈ 0). These results collectively demonstrate that the BL-OG system efficiently and acutely rescues the LTM consolidation deficit by activating OptoTrkB, and that the resulting memory follows a normal decay profile (Figure 8.c).

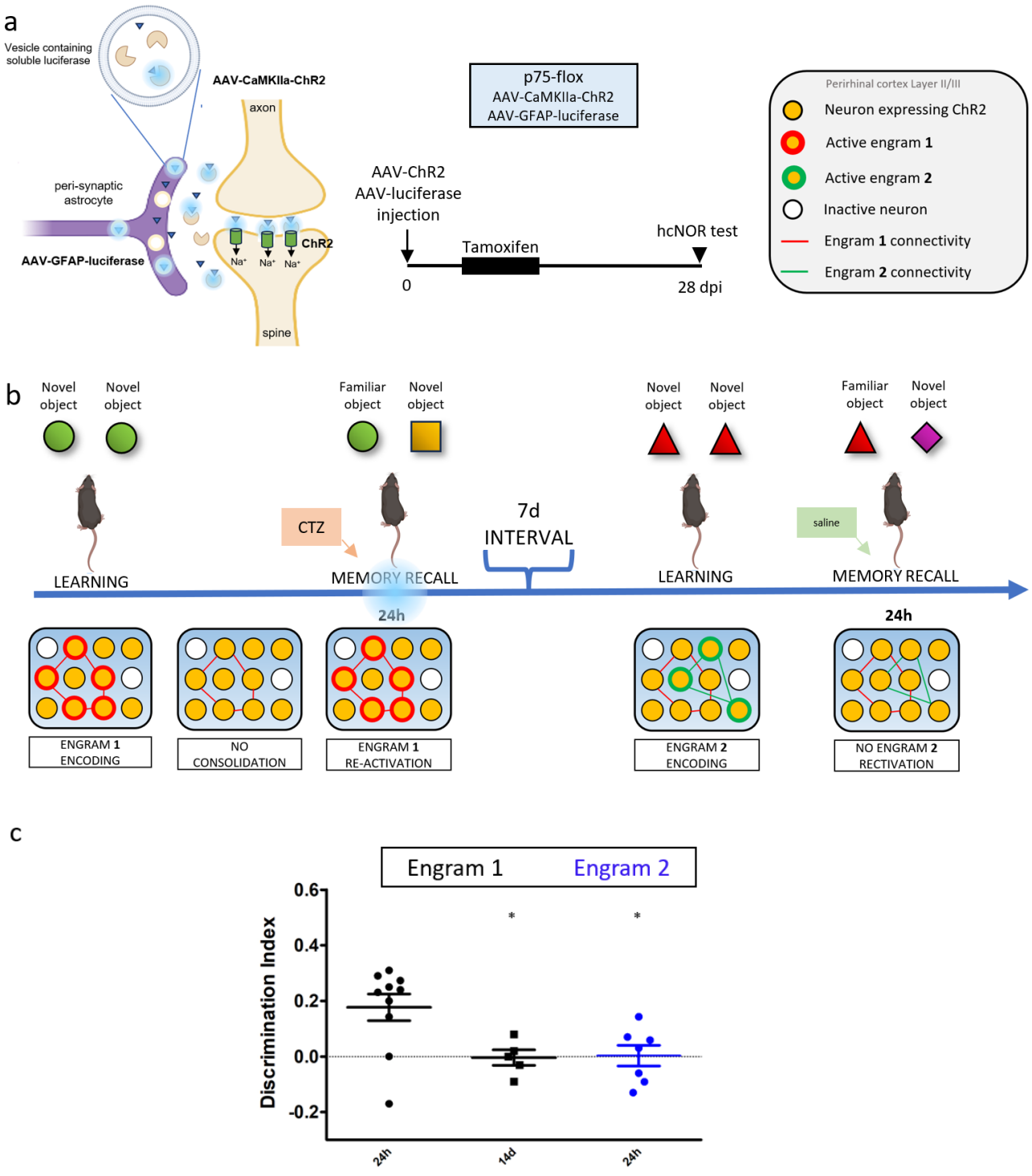

Figure 8. Bioluminescent activation of OptoTrkB rescues LTM in p75-flox mice with a physiological decay kinetic

a) *BL-OG vector strategy and experimental timeline. Schematic illustration of the molecular strategy and general timeline. Astrocytes in the PRC of p75-flox mice were transduced with the vector AAV-*

GFAP-hPOMC-sbGLuc and excitatory neurons were transduced with the vector AAV-CaMKIIa-OptoTrkB. p75^{NTR} deletion was induced by Tamoxifen. The mechanism shows Coelenterazine (CTZ) activating the astrocytic luciferase, which emits light to activate post-synaptic OptoTrkB, mimicking endogenous BDNF signaling. The test begins 28 days post-injection (dpi) ***b)*** *Multi-trial hcNOR paradigm and engram dynamics. Trial 1 (Engram 1, Rescue): mice learned Object set-1 (green circles). Immediately post-learning, they received CTZ injection to activate OptoTrkB and induce consolidation. Memory was tested 24 hours later. Trial 2 (Engram 2, Control): seven days later, the same mice learned Object set-2 (red triangles) but received a vehicle (saline) injection, serving as an intra-animal, non-rescued control. Memory was tested 24 hours later. Remote Memory: A subset of mice from Trial 1 was tested 14 days after the initial learning of Engram 1. The lower panel illustrates the hypothesized engram dynamics: successful consolidation and re-activation for Engram 1 (rescued) and consolidation failure for Engram 2 (non-rescued). At 14 days, the Engram 1 connectivity is weakened and the memory trace is not recalled.* ***c)*** *Discrimination Index for rescued and non-rescued engrams. The dot plot shows the mean Discrimination Index* ± SEM. *LTM consolidation was successfully rescued in Engram 1 (24h DI > 0), while the non-rescued Engram 2 failed to consolidate (24h DI ≈ 0). Furthermore, the rescued memory in Engram 1 exhibited physiological decay, with the DI at 14 days post-learning being near 0. Statistics: One-way ANOVA with Tukey's multiple comparison post-hoc test. The 24h DI for Engram 1 was significantly higher than both the 14d DI for Engram 1 and the 24h DI for Engram 2 (*p < 0.05). Cohort Sizes: Engram 1 (24h rescue): n = 10 mice; Engram 1 (14d remote): n = 5 mice; Engram 2 (24h non-rescued): n = 7 mice.*

In summary, the non-invasive, acute activation of post-synaptic OptoTrkB via the astrocytic BL-OG system proved highly efficient in stabilizing the consolidation phase of Engram 1, resulting in a robust memory trace that nonetheless followed a physiological decay timeline. These results demonstrate that the BL-OG system is a potent and precise chemiluminescent tool capable of functionally mimicking the BDNF recycling and release mechanism carried out by astrocytes, thereby allowing for the selective study of consolidation dynamics.

3.6 - Necessity of vesicular release for BL-OG rescue

Effective LTM consolidation requires the tight temporal, spatial, and stimulus-dependent processing and release of glial mBDNF and its pro-peptide onto adjacent neurons, leading to post-synaptic TrkB phosphorylation. Prior results using WT mice expressing GFAP-hM3Dq demonstrated that the stochastic astrocytic vesicular release of endocytic vesicles containing mBDNF and pro-peptide is essential for physiological engram consolidation.

To directly test whether the vesicular release of the luciferase is necessary for memory consolidation, we designed a triple-vector experiment. We combined the p75-flox model's deficiency with the hM3Dq release-blocking mechanism:

1. Express vesicular luciferase: AAV5-GFAP-hPOMC-sbGLuc to load luciferase into astrocytic vesicles.

2. Express photosensitive receptor: AAV9-CaMKIIa-OptoTrkB to express the receptor in excitatory neurons.

3. Block vesicular release: AAV5-GFAP-hM3Dq to sequester astrocytic Ca^{2+} upon CNO treatment.

Three-month-old p75-flox mice received bilateral stereotaxic injections of all three vectors into the PRC. Tamoxifen treatment followed one week later to induce the $p75^{NTR}$ depletion (Figure 9.a). After

four weeks post-injection for expression and recombination, mice were subjected to the hcNOR test, consisting of two trials one week apart (Figure 9.b).

Trial 1 (Blocked Release): Mice were treated with CNO (5 minutes pre-sample phase) to acutely deplete astrocytic Ca^{2+} stores and block vesicular release of all contents, including sbGLuc. Immediately after the learning phase, the CTZ substrate was administered intraperitoneally. LTM recall was assessed 24 hours later.

Trial 2 (Restored Release): Seven days later, the same mice underwent a second hcNOR trial using new objects. In this trial, a saline vehicle was administered instead of CNO, thereby allowing the sbGLuc-filled vesicles to be released during learning-induced synaptic activity, functionally restoring the BL-OG rescue mechanism.

When tested for LTM 24 hours after Trial 1 (Blocked Release), mice that received CNO treatment showed no ability to discriminate between the familiar and novel objects (Engram 1, DI $\approx$ 0). This crucial finding confirms that even with the OptoTrkB receptor and luciferase substrate present, the physical blockade of astrocytic vesicular release, which prevents the sbGLuc from reaching the synaptic cleft, ablates the memory rescue effect. However, when the same cohort of mice underwent the second learning trial (Trial 2, Restored Release) one week later, with the confounding CNO administration omitted (vehicle treatment), they were able to discriminate the novel and familiar objects at the 24-hour retention interval. The DI for this rescued memory (Engram 2) was significantly positive and comparable to the rescue previously observed in the p75-flox model (Figure 8.c). Collectively, these data provide direct and compelling evidence that the astrocytic vesicular release of sbGLuc is a mandatory requirement for the activation of the post-synaptic OptoTrkB, thereby functionally confirming that the BL-OG system precisely mimics the physiological secretion and signaling pathway of astrocytic BDNF recycling (Figure 9.c).

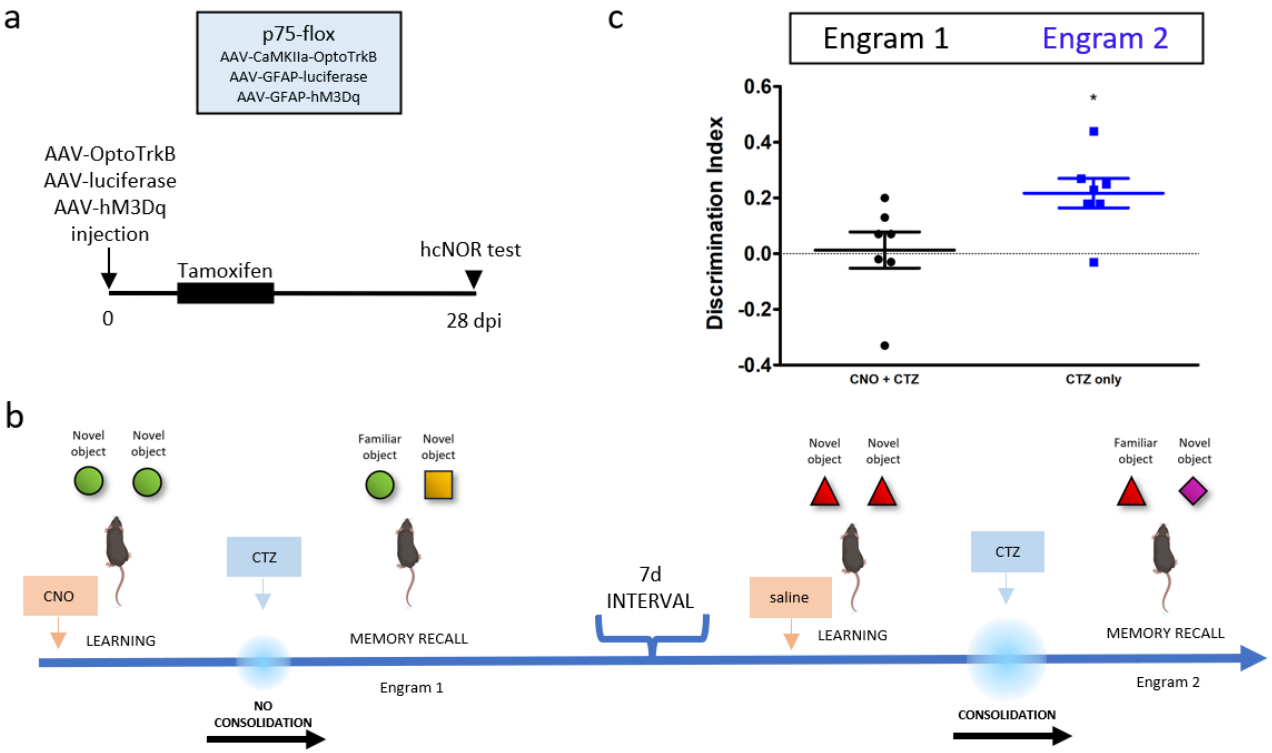

Figure 9. Chemogenetic inhibition of Ca^{2+} dependent vesicular release prevents memory consolidation rescue

a) *Triple-vector strategy and timeline. Schematic showing the combined genetic approach in p75-flox mice. Mice received stereotaxic injections of three AAVs: effector (CaMKIIa-OptoTrkB), generator (GFAP-luciferase), and inhibitor (GFAP-hM3Dq) into the PRC. Tamoxifen treatment followed to deplete $p75^{NTR}$. Testing started 28 days post-injection (dpi).* ***b)*** *BL-OG paradigm with vesicular release modulation. Trial 1 (Engram 1, Blocked Release): 5 minutes before learning Object Set-1, mice received CNO to activate hM3Dq, leading to Ca^{2+} depletion and the inhibition of vesicular release (including the sbGLuc luciferase). CTZ was administered immediately after learning. LTM recall was tested 24 hours later, showing failed consolidation. Trial 2 (Engram 2, Restored Release): seven days later, the same mice learned Object Set-2. CNO was replaced with saline vehicle, allowing sbGLuc release and catalysis at the synaptic cleft upon CTZ injection and subsequent OptoTrkB activation, leading to consolidation. LTM recall was tested 24 hours later.* ***c)*** *Vesicular secretion is required for LTM rescue. The dot plot shows the mean Discrimination Index ± SEM for the two*

memory engrams. In the CNO + CTZ condition (Engram 1, Blocked Release), the DI was ≈ 0. In the CTZ only condition (Engram 2, Restored Release), the DI was significantly positive, indicating successful LTM rescue. Statistics: The two conditions (CNO + CTZ vs. CTZ only) were compared using a Paired t-test (as the same animals served as both experimental and control trials). The DI in the CTZ only condition was significantly higher than the DI in the CNO + CTZ condition ($p < 0.05$). Cohort Sizes: n = 7 mice were tested in both the CNO + CTZ condition (Engram 1) and the CTZ only condition (Engram 2).*

To provide definitive corroboration that the physical vesicular targeting of the luciferase is mandatory for the BL-OG-mediated memory rescue, we conducted an additional control trial. Here, we used a synaptobrevin-gated luciferase construct that utilizes an expose-retreat strategy. In this case, the luciferase is linked to the luminal end of synaptobrevin/VAMP2[239], allowing the exposure of the enzyme to the cleft, without releasing it.

Three-month-old p75-flox mice received stereotaxic injections of AAV5-GFAP-Synb-sbGLuc, alongside the AAV9-CaMKIIa-OptoTrkB vector. After Tamoxifen treatment and the standard four-week expression period, these mice were subjected to the hcNOR test. Immediately following the sample phase, mice received the standard CTZ injection. LTM recall was assessed 24 hours later (Figure 10.a).

When tested for LTM 24 hours after learning CTZ administration, this cohort displayed a complete failure of memory consolidation. The mice were unable to discriminate between the familiar and novel objects (DI ≈ 0) (Figure 10.b). This finding definitively confirms that the mere presence of the luciferase enzyme within the astrocyte, and the subsequent generation of bioluminescent light upon CTZ administration, is insufficient to activate the post-synaptic OptoTrkB receptor. Instead, the results robustly establish that the specific packaging and localized, perisynaptic release of the luciferase into the synaptic cleft, as a surrogate for endogenous mBDNF and pro-peptide release, is a critical prerequisite for successful LTM consolidation.

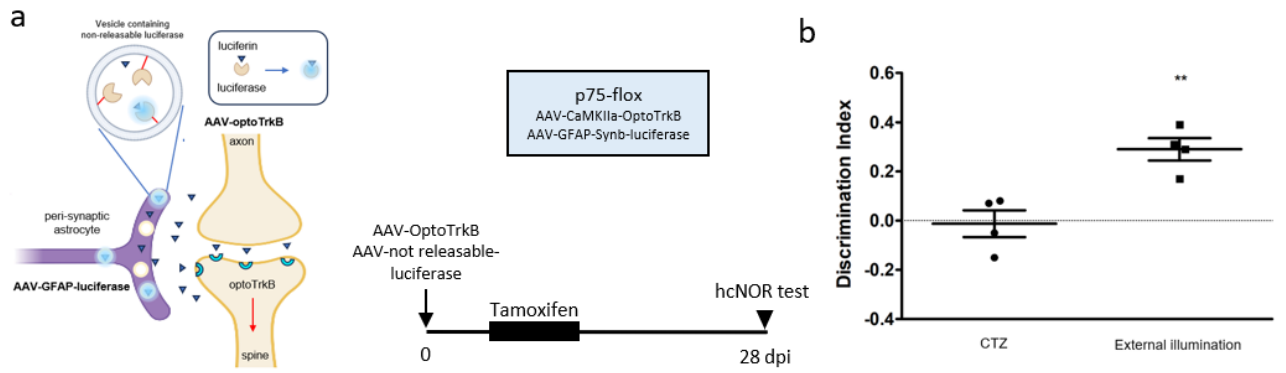

Figure 10. Requirement of luciferase secretion for OptoTrkB activation and LTM consolidation

a) *Experimental paradigm with non-releasable luciferase. Schematic illustrating the double-component strategy to confirm the necessity of localized luciferase release. p75-flox mice were injected with effector vector (CaMKIIa-OptoTrkB) and a modified generator vector (GFAP-Synb-sbGLuc). In this construct, the Synaptobrevin (Synb) targeting sequence directs the luciferase to vesicles but renders them non-releasable from the astrocyte. Tamoxifen treatment and a 28-day post-injection (dpi) period followed. The experiment involved two trials: one treated with CTZ and one with external illumination (positive control).* ***b)*** *Non-releasable luciferase fails to rescue LTM consolidation. The dot plot shows the mean Discrimination Index ± SEM at the 24-hour retention interval for two separate conditions. CTZ condition (internal light failure): Mice treated with the CTZ substrate (which activates the non-releasable luciferase) failed to consolidate LTM, exhibiting a DI ≈ 0. This demonstrates that non-releasable luciferase is ineffective at activating the post-synaptic OptoTrkB. External illumination condition (positive control): mice were subjected to external blue light illumination instead of CTZ. Mice treated this way successfully rescued LTM, showing a significantly positive DI. Statistics: the two conditions (CTZ vs. External illumination) were compared using a Paired t-test (as the same animals served as both experimental and control trials). The DI in the CTZ only condition was significantly lower than the DI in the External illumination condition (**$p < 0.01$). Cohort Sizes: n = 4 mice were tested in both the CTZ and External light condition.*

The Bioluminescent Optogenetic (BL-OG) system proved to be an extremely powerful and precise tool capable of functionally substituting for the endogenous astrocytic BDNF recycling pathway, successfully rescuing LTM consolidation in genetically impaired mouse models. This non-invasive chemical-genetic approach offers unprecedented control over the molecular machinery necessary for memory stabilization. However, the current BL-OG strategy presents significant practical limitations: namely, the uncontrolled pharmacokinetics of the CTZ substrate compromises the precise temporal window of TrkB activation, and, crucially, the system is incompatible with engram-specific consolidation rescue. Given that the ultimate goal is to achieve engram-specific control over consolidation, restoring stability only to the neurons that encode the specific memory, a mechanism allowing for precise spatial and temporal light delivery is required. Therefore, the subsequent chapter evaluates the utility of external, targeted optical illumination to activate OptoTrkB in a highly localized, engram-specific manner, thereby overcoming the systemic constraints of the BL-OG paradigm.

3.7 - Non-invasive *in-vivo* OptoTrkB activation rescues memory consolidation in impaired mouse models

In order to refine a system for non-invasive, engram specific activation of OptoTrkB in the PRC we started exploring the possibility of delivery blue light as an external source.

The success of this strategy relied on a light-delivery method capable of activating OptoTrkB through the intact skull and fur of a mouse head, a feasibility previously demonstrated by Hong and Heo[212] and Lilja and colleagues[221]. To achieve this, we employed a custom-designed LED cage lid (Figure 11) configured to fit the standard home cage and deliver blue light from above. The light pattern was carefully selected to ensure efficient OptoTrkB activation while maintaining animal welfare and system stability. Based on established optogenetic protocols[212,221], we utilized a pulsed pattern of 488 nm blue LED light delivered for 1 second every 5 seconds, for a total duration of 30 minutes, at an average power density of approximately 1mW/mm^2 at the cage floor. This pattern ensures robust photon delivery for OptoTrkB activation inside the PRC while preventing potential side effects such as photo-toxicity, visual over-stimulation, or excessive thermal accumulation in the cage environment.

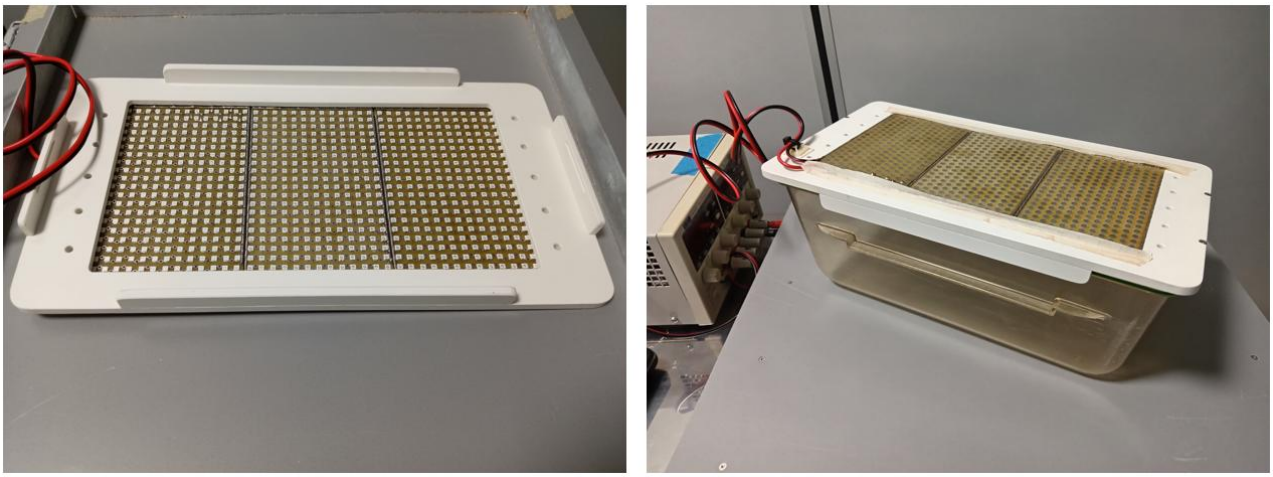

Figure 11. Custom designed LED cage lid for external optogenetic activation

a) *The custom-built LED array lid, designed to fit a standard mouse home cage and deliver blue light from above. The grid pattern ensures uniform light delivery across the cage floor.* ***b)*** *The LED lid mounted on a mouse home cage, connected to a power source for controlled delivery of 488 nm blue light to activate OptoTrkB through the intact skull.*

To assess the efficacy of the non-invasive illumination system, we tested its ability to rescue the LTM consolidation deficit in the p75-flox mouse model. Three-month-old p75-flox mice received bilateral stereotaxic injections of the OptoTrkB vector (AAV9-CaMKIIa-Opto-cytTrkB(E281A)-HA) into the PRC. Following a one-week recovery, $p75^{NTR}$ depletion was induced with five consecutive days of tamoxifen treatment. Mice were then singly housed. After four weeks for optimal vector expression and $p75^{NTR}$ deletion, mice were subjected to the hcNOR paradigm (figure 12.a). Immediately following the 5-minute sample phase, the mice received the 30-minute patterned blue light pulse delivered via the custom LED cage lid (Figure 12.b and c). The illuminated p75-flox mice displayed a robust rescue of LTM, exhibiting a significantly positive Discrimination Index (DI > 0) at the 24-hour retention interval (Figure 12.d, left column). To ensure the OptoTrkB activation effect was circumscribed to the consolidation window and did not impact subsequent learning, the same cohort of mice underwent a second hcNOR trial one week later using a new set of objects. In this control trial, no illumination was applied post-sample phase. Consistent with the model's LTM deficit, mice were unable to discriminate between the familiar and novel objects at 24 hours post-second learning. This confirms that the initial OptoTrkB activation produced a memory-specific and transient effect, which did not occlude subsequent learning or permanently alter synaptic function (Figure 12.d, right column).

We further validated the non-invasive rescue in the model of acute pharmacological disruption of astrocytic release. WT mice received bilateral PRC injections of both the OptoTrkB vector (AAV9-CaMKIIa-Opto-cytTrkB-HA) and the astrocytic chemogenetic inhibitor vector (AAV5-GFAP-hM3Dq) (Figure 12.a). After a four-week expression period, mice were tested with the hcNOR paradigm. On the test day, mice received an intraperitoneal injection of CNO five minutes prior to the sample phase to inhibit Ca^{2+}-dependent astrocytic vesicular release, which is known to cause LTM failure (Section 3.4). Immediately following the sample phase, the mice received the 30-minute patterned blue light pulse (Figure 12.c). As observed in the p75-flox model, the CNO-treated WT-

hM3Dq mice that received the post-learning blue light displayed a successful rescue of LTM (DI > 0 at 24 hours post-learning). In a subsequent non-illuminated control trial one week later (where mice received CNO but no light), LTM rescue failed (DI ≈ 0). These results demonstrate that the OptoTrkB activation via non-invasive external light is potent enough to overcome the acute astrocytic deficit caused by CNO and restore LTM consolidation (Figure 12.e).

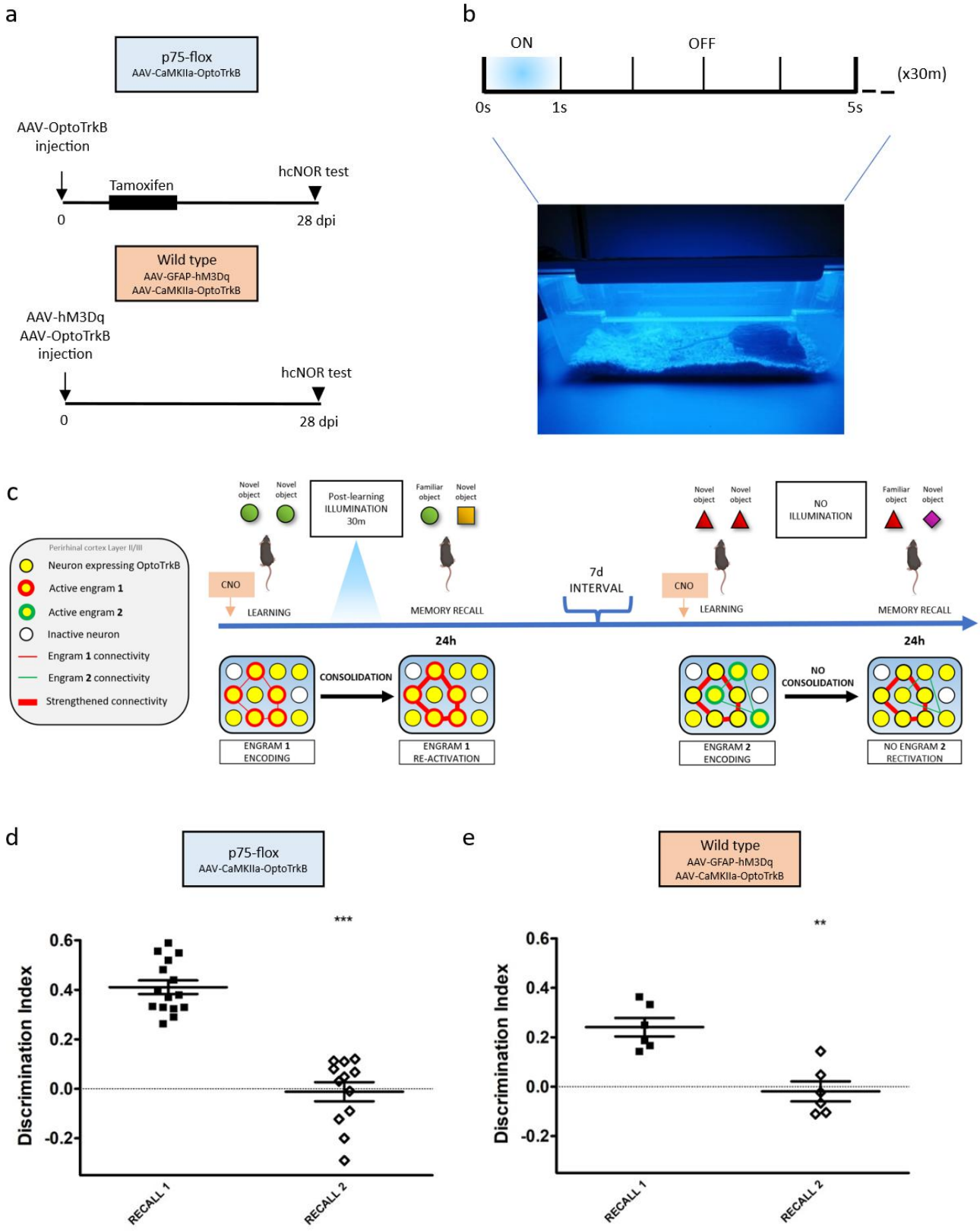

Figure 12. Non-invasive external optical illumination enables LTM consolidation rescue

a) *Experimental timelines for OptoTrkB rescue in LTM deficit models. Top: p75-flox mice received stereotaxic injection of AAV-CaMKIIa-OptoTrkB into the PRC, followed by tamoxifen treatment for* $p75^{NTR}$ *deletion. Bottom: WT mice received stereotaxic injection of both AAV-GFAP-hM3Dq (to block astrocyte vesicular release) and AAV-CaMKIIa-OptoTrkB. hcNOR testing begins 28 days post-injection (dpi).* ***b)*** *Non-invasive illumination system and pattern. Top: schematic of the 30-minute pulsed blue light pattern (1s ON, 4s OFF) used for OptoTrkB activation. Bottom: Photograph of the custom LED cage lid system delivering blue light to the mouse within its home cage.* ***c)*** *Multi-trial hcNOR paradigm for LTM rescue and engram specificity. Trial 1 (Recall 1): mice (pre-treated with CNO in the hM3Dq model) learn objects of Engram 1 (green circles). Immediately post-learning, they receive 30 min of patterned blue light illumination. LTM is tested 24 hours later. Trial 2 (Recall 2): seven days later, the same mice learn objects of Engram 2 (red triangle) using a new set of novel objects but receive no post-learning illumination. LTM is tested 24 hours later. The lower panel illustrates the hypothesized outcome: successful Engram 1 consolidation (strengthened connectivity) and Engram 2 consolidation failure (no strengthening).* ***d)*** *LTM rescue in p75-flox mice is light dependent. The dot plot shows the mean Discrimination Index ± SEM. The DI at 24 hours post-learning is significantly positive for Recall 1 (illuminated) but not for Recall 2 (not illuminated). Statistic: Paired t-test (***p < 0.001). Cohort sizes: n = 15 mice for Recall 1, n = 12 mice for Recall 2.* ***e)*** *LTM rescue in WT-hM3Dq mice is light dependent. CNO-treated mice show a significantly positive DI for Recall 1 (illuminated) compared to Recall 2 Data are mean Discrimination Index ± SEM. Statistic: Paired t-test (**p < 0.01). Cohort sizes: n = 6 for both recalls.*

3.8 - Control experiments confirm specificity and physiology of OptoTrkB-mediated LTM rescue

A critical test for the validity of the OptoTrkB rescue mechanism is to confirm that the restored LTM trace follows the natural time-course of memory decay and is not pathologically stabilized. As previously established (Section 3.3), object recognition memory acquired via the hcNOR paradigm in WT mice typically undergoes a gradual, physiological decline, becoming undetectable by 14 days post-learning. To assess the decay profile of the OptoTrkB-rescued memory, separate cohorts of p75-flox mice expressing OptoTrkB were subjected to the hcNOR test and received the post-learning patterned blue light illumination. Memory retention was then tested at four distinct retention intervals: 24 hours, 7 days, 10 days, and 14 days post-learning (Figure 13.a). Consistent with the natural memory profile, the p75-flox mice successfully retained the rescued LTM up to 7 days post-illumination, showing a strong Discrimination Index comparable to WT controls. Memory performance began to decline by 10 days, and by 14 days post-learning the DI was significantly reduced (DI ≈ 0). These results conclusively demonstrate that while OptoTrkB activation is sufficient for LTM restoration, the consolidated memory trace is not permanently fixed and follows a canonical, transient physiological decay profile (Figure 13.b).

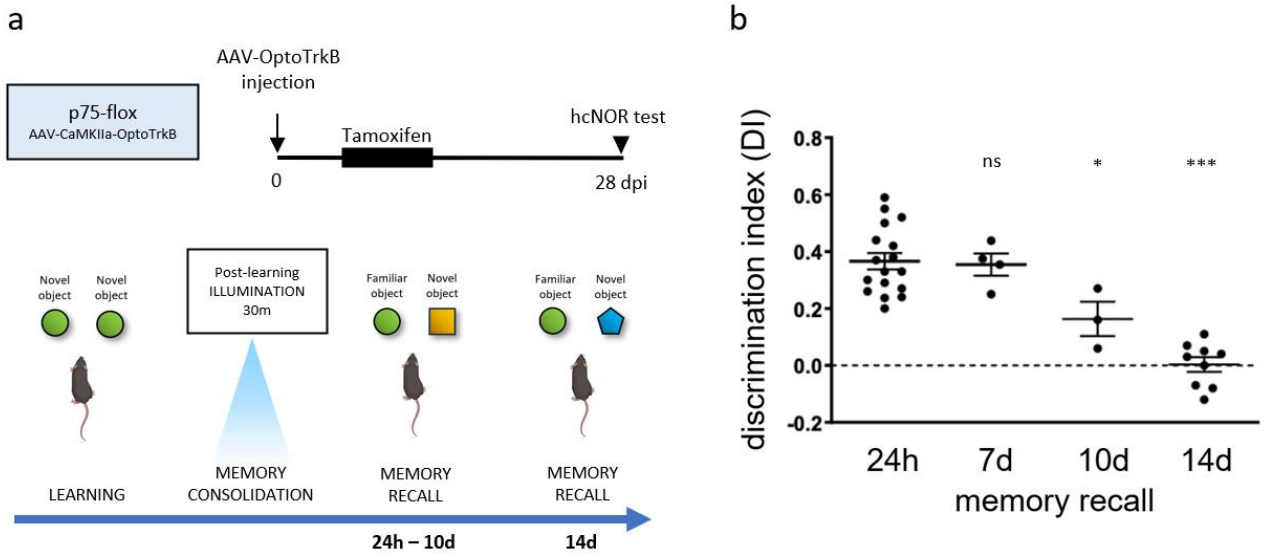

Figure 13. OptoTrkB-rescued LTM follows canonical physiological decay kinetics

a) *Experimental timeline for remote memory testing. p75-flox mice injected with AAV9-CaMKIIa-OptoTrkB underwent Tamoxifen treatment and were subjected to the hcNOR paradigm. The memory trace was established by post-learning external light illumination (30 min patterned blue light). Separate cohorts were then tested for memory recall at 24 hours, 7 days, 10 days, and 14 days post-learning.* ***b)*** *Time-dependent decay of OptoTrkB-rescued LTM. The Discrimination Index (DI) shows successful memory retention up to 7 days, with a significant decline evident by 10 days (*p < 0,05 vs 24h DI) and complete loss of recognition memory by 14 days (***p < 0.001 vs 24h DI). Data are mean DI ± SEM. Statistics: One-way ANOVA with Tukey's multiple comparison post-hoc test. Cohort sizes: n = 17 mice (24h), n = 4 mice (7d), n = 3 mice (10d), n = 9 mice (14d).*

To conclusively demonstrate that the observed LTM rescue is specifically mediated by the light-activated OptoTrkB construct and not by non-specific effects of the illumination, we conducted two essential control experiments:

1. Optogenetic Specificity Control (Non-Functional Vector): we tested whether the light pulse itself, when delivered to p75-flox mice, could rescue LTM without the functional OptoTrkB receptor. p75-flox mice were injected with a control vector expressing the fluorescent reporter tdTomato (AAV9-CaMKIIa-tdTomato) in excitatory neurons, instead of OptoTrkB. Following tamoxifen treatment and the hcNOR sample phase, these mice received the standard 30-minute blue light illumination. As expected, this cohort exhibited the characteristic LTM failure (DI ≈ 0) at the 24-hour retention interval (Figure 14.a). This finding serves as a definitive negative control, confirming that the LTM rescue is dependent specifically on the presence and activation of the OptoTrkB construct and not on any non-specific effects of the light (e.g., photo-thermal or visual artifacts).

2. Physiological perturbation control (intact BDNF-TrkB pathway): we investigated whether the activation of OptoTrkB could artificially enhance or interfere with memory consolidation when the endogenous astrocytic BDNF recycling pathway was intact. WT mice were injected with AAV9-CaMKIIa-OptoTrkB. After the hcNOR sample phase, these WT mice also received the standard blue light illumination. The WT mice displayed a robust and significantly positive DI at 24 hours, statistically indistinguishable from unilluminated WT controls (Figure 14.b). This confirms that activating OptoTrkB in excitatory neurons does not pathologically enhance or interfere with normal memory consolidation. It establishes OptoTrkB as a substitute/rescue tool, designed to functionally bypass a deficit, rather than a general memory enhancer.

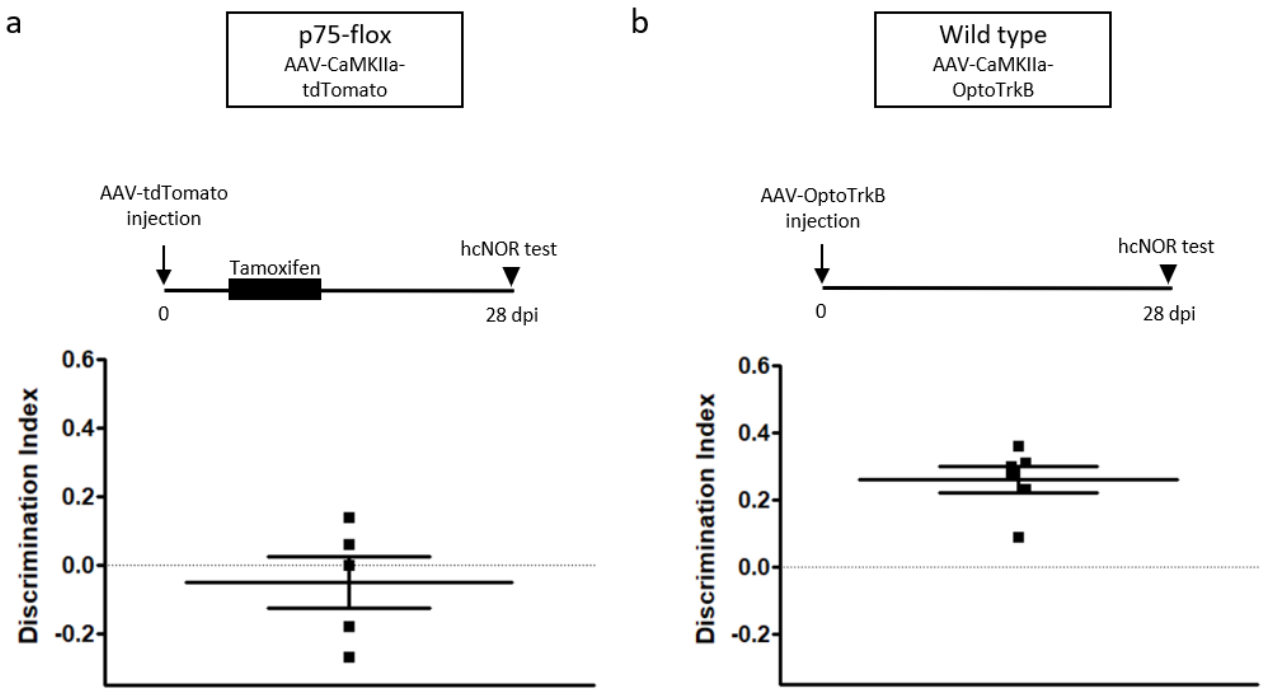

Figure 14. OptoTrkB activation is necessary to rescue LTM deficits but has no impact on normal memory retention

a) *LTM rescue requires the OptoTrkB construct. Schematic showing p75-flox mice injected with the control vector AAV-CaMKIIa-tdTomato and treated with Tamoxifen. The dot plot shows the Discrimination Index at 24 hours post-learning following external illumination. p75-flox mice with the non-functional control vector failed to consolidate LTM (DI ≈ 0), confirming the rescue effect is OptoTrkB-dependent. Data are mean DI ± SEM (n = 6 mice).* ***b)*** *OptoTrkB activation does not alter normal LTM in WT mice. Schematic showing WT mice injected with AAV9-CaMKIIa-OptoTrkB. The dot plot shows the DI at 24 hours post-learning following external illumination. WT mice exhibited normal LTM retention (DI > 0) at 24h, demonstrating that OptoTrkB activation does not interfere with or pathologically enhance the endogenous consolidation pathway. Data are mean DI ± SEM (n = 6 mice).*

3.9 - Temporal dissection of the consolidation critical window

The preceding results established that light-mediated OptoTrkB activation successfully rescues LTM consolidation in astrocytic-impaired mouse models. However, the 30-minute post-learning illumination used so far only demonstrates the sufficiency of the TrkB signal within the immediate post-learning phase. A critical question in memory research is the precise temporal window during which the BDNF-TrkB signal is necessary to convert a transient memory trace (STM) into a stable engram (LTM).

Here, we leveraged the acute temporal precision of the external optical system to define the critical consolidation period dependent on TrkB activation. We hypothesized that delaying the OptoTrkB rescue signal beyond the natural consolidation window would lead to a failure of LTM formation.

To test this, singly housed p75-flox mice, depleted of $p75^{NTR}$ and expressing OptoTrkB, were subjected to the hcNOR sample phase. The 30-minute patterned blue light pulse was then delivered at five distinct time points, relative to the end of the sample phase, plus a non-illuminated control group:

- Immediate (0 h): light pulse administered immediately (within 5 min) post-sample phase.

- Late delay (9, 13, 16, 18) h: Light pulse administered 9-, 13-, 16- or 18-hour post-sample phase.

LTM retention was assessed 24 hours after the sample phase for all cohorts (Figure 15.a).

Mice that received the OptoTrkB activation immediately (0 h) and even at the late time points of 9 h and 13 h post-learning exhibited a robust rescue of LTM, with a significantly positive Discrimination Index ($DI > 0$). This striking finding suggests that the molecular machinery necessary to support LTM consolidation remains permissive for TrkB signaling for many hours following the initial encoding event.

However, delaying the OptoTrkB activation until 16 hours post-learning resulted in a complete failure of LTM consolidation. The mean DI for this cohort was statistically comparable to the "Not illuminated" group (DI ≈ 0). Furthermore, by 18 hours post-learning, the rescue effect was completely lost, with the DI returning to the baseline failure levels (Figure 15.b).

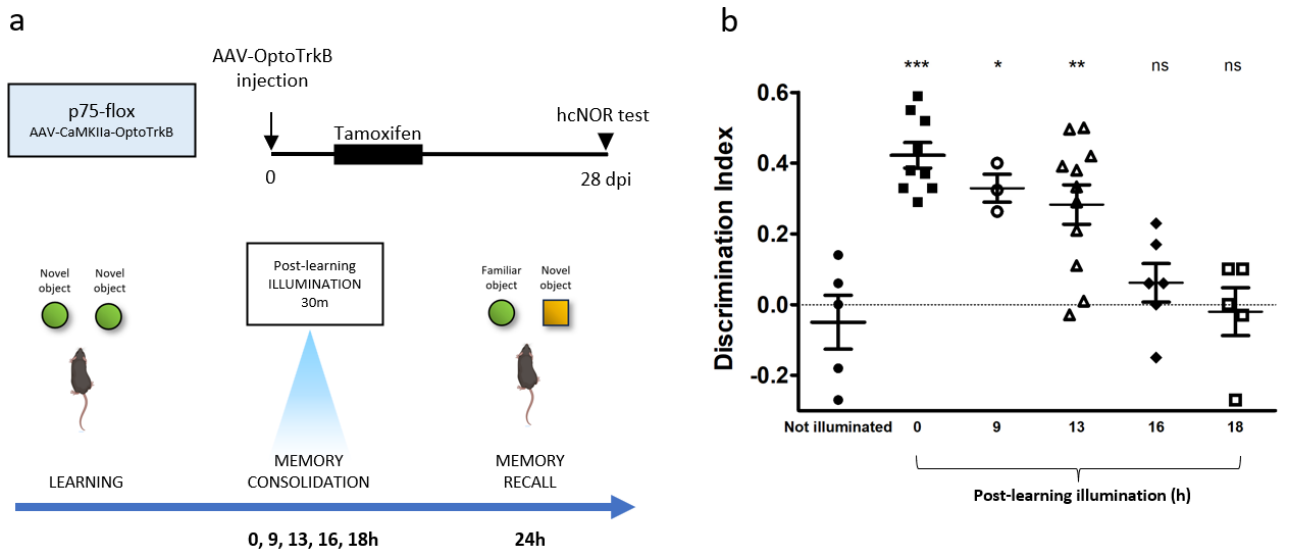

Figure 15. Delayed OptoTrkB activation rescues LTM consolidation up to 13 hours post-learning

a) *Experimental timeline for temporal dissection of TrkB-dependent consolidation. p75-flox mice received stereotaxic injections of AAV9-CaMKIIa-OptoTrkB into the PRC, followed by Tamoxifen treatment for $p75^{NTR}$ depletion. After 28 days post-injection (dpi), mice underwent the hcNOR sample phase. The 30-minute patterned blue light illumination was delivered at various post-learning delays: immediately (0 h), or at 9, 13, 16, or 18 hours. LTM retention was assessed 24 hours after the sample phase.* ***b)*** *Discrimination Index reveals an extended TrkB-dependent consolidation window. The dot plot shows mean DI ± SEM at 24 hours post-learning for mice receiving illumination at different delays, compared to a non-illuminated control. LTM consolidation was successfully rescued when OptoTrkB was activated up to 13 hours post-learning (***$p < 0.001$ 0h vs. Not illuminated; *$p < 0.05$ 9h vs. Not illuminated; **$p < 0.01$ 13h vs. Not illuminated). However, by 16h and 18h, the rescue effect was lost (ns $p > 0,05$ 16- and 18-h vs. Not illuminated). Statistics: One-way ANOVA with Tukey's multiple comparison post-hoc test. Cohort sizes: n = 5 mice (Not illuminated), n = 8 mice (0 h), n = 3 mice (9h), n = 11 mice (13h), n = 6 mice (16h), n = 5 mice (18h).*

These results challenge the conventional view of a narrow, early post-learning critical period for TrkB-dependent consolidation. Instead, they define a remarkably extended consolidation window of up to 13 hours during which a single optical TrkB activation is sufficient to rescue LTM formation in the absence of astrocytic BDNF recycling mechanism. This suggests that the initial synaptic tag or intermediate memory trace remains functional for a far longer period than previously appreciated, serving as a substrate for late-onset TrkB rescue.

4. - Engram-specific activation of OptoTrkB rescues LTM consolidation impaired mice

The ultimate goal of this study was to achieve engram-specific control over consolidation, allowing the stabilization of the LTM trace only within the specific neuronal ensemble that encoded the memory. To accomplish this, we integrated the OptoTrkB system with the Targeted Recombination in Active Population (TRAP) technique, which provides genetic access to neurons active during a defined behavioural window.

We employed the cFos-TRAP2 mouse line[240] (which utilizes a cFos promoter-driven iCre-ERT2 and a Cre-dependent tdTomato reporter allele) to permanently tag PRC neurons active during the hcNOR sample phase. This approach allows for the indelible fluorescent labelling of the object-specific engram by restricting Cre recombination to active neurons during the 4-Hydrotamoxifen (4-OHT) administration window. To validate the specificity of this labelling under the context-minimized hcNOR protocol, Fos-TRAP mice were divided into two cohorts:

1. Object-Trained cohort: Mice received an intraperitoneal injection of 4-OHT and were then subjected to the hcNOR sample phase (5 minutes exploration of two objects) to activate the object-encoding engram.

2. Handling-control cohort: Mice received the 4-OHT injection but were subjected to a control procedure where the home cage lid was opened and closed, but no objects were introduced (5 minutes

exploration of empty cage). This controlled for background neuronal activity triggered by handling, 4-OHT administration, and minimal environmental changes.

After 7 days (to allow proper tdTomato expression), brain slices were analysed for tdTomato expression in the PRC (Figure 16.a). Quantification revealed a significantly higher density of tdTomato-positive (TRAPped) neurons in the PRC of the Object-trained cohort compared to the Handling-control cohort. This confirms that the hcNOR paradigm successfully induces a specific, measurable cFos response within the PRC and that the cFos-TRAP system effectively and specifically labels the neuronal ensemble (engram) responsible for object encoding.

The goal of this final experiment was to test whether the rescue of LTM consolidation could be achieved by activating OptoTrkB exclusively in the subset of PRC neurons comprising the memory engram, thereby overcoming a systemic memory impairment caused by astrocytic deficit. To achieve this specific control, we utilized a triple-manipulation strategy in cFos-TRAP mice:

1. Impairment: AAV5-GFAP-hM3Dq was injected into the PRC to acutely block astrocytic BDNF release upon CNO administration, inducing LTM failure.

2. Engram-specific receptor expression: AAV9-CaMKIIa-DIO-Opto-cytTrkB(E281A)-HA was injected. This DIO (Double-Inverted Open reading frame) construct ensures that OptoTrkB is expressed only in excitatory neurons (CaMKIIa promoter) that have undergone Cre recombination (i.e., the engram neurons TRAPped by the cFos-CreERT2 system).

3. Engram TRAPping and rescue: Mice received 4-OHT (to TRAP the engram) and CNO (to impair LTM) before the hcNOR sample phase. The OptoTrkB activation via external illumination was then delivered later to rescue the specific engram (Figure 16.b).

Based on the temporal dissection results (Section 3.9), we utilized a 13-hour delay between the learning phase and the external light illumination. This window ensured two critical criteria were met: (I) it provided sufficient time for 4-OHT to be cleared and the TRAPping window to close, preventing

non-specific labelling; and (II) it provided the required time for the Cre-driven OptoTrkB expression to reach functional levels, while still being within the maximal 13-hour critical period permissive for LTM rescue. LTM was assessed using a multi-trial paradigm (Figure 16.c):

- Trial 1 (Engram 1, rescue): mice received CNO and 4-OHT pre-learning, and were illuminated 13 hours post-learning.

- Trial 2 (Engram 2, control): one week later, the same mice learned a new engram (Engram 2) but received CNO and 4-OHT without post-learning illumination.

- Remote memory: a subset was tested 14 days after Trial 1.

At 24 hours post-first learning (Engram 1), the illuminated mice were able to discriminate between the familiar and novel objects, demonstrating a significantly positive Discrimination Index ($DI > 0$). This crucial finding confirms that activating TrkB exclusively in the cFos-defined engram neurons is sufficient to rescue LTM consolidation, when the underlying astrocytic BDNF recycling mechanism is prevented. In contrast, the same cohort of mice failed to consolidate LTM for Engram 2 (Trial 2), showing a DI statistically indistinguishable from zero ($DI \approx 0$). This confirms that the TrkB activation effect was circumscribed and engram-specific, having no lasting impact on subsequent learning or the ability of the same animal to form a new, but non-rescued engram one week later. Finally, the rescued Engram 1 memory followed a normal physiological decay profile, with LTM failing by the 14-day remote memory test (Figure 16.d).

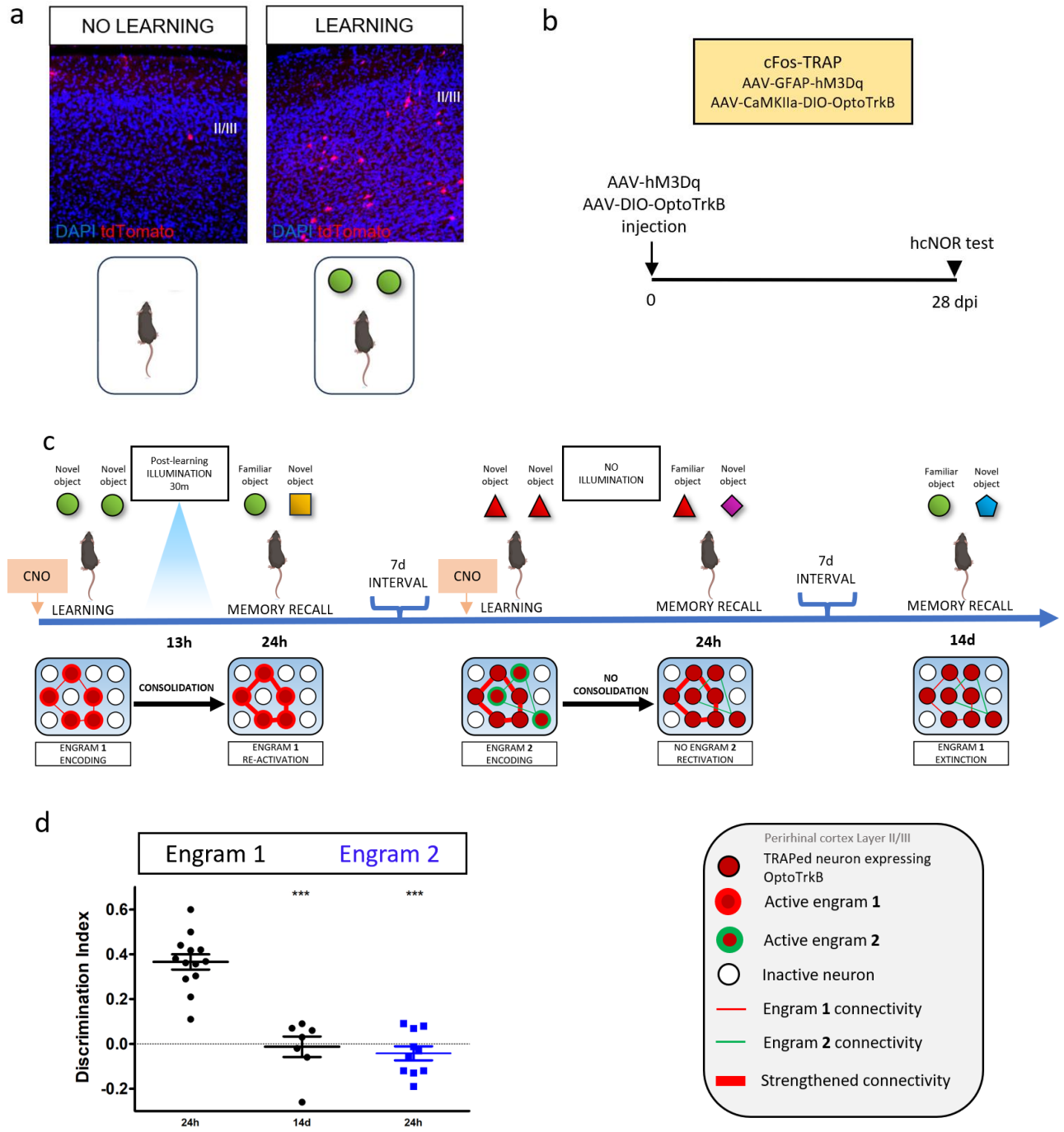

Figure 16. Engram-specific activation of OptoTrkB rescues LTM consolidation

a) *Validation of cFos-TRAP engram labelling in PRC. Confocal images of PRC layer II/III in cFos-TRAP mice, immunostained for tdTomato (red, TRAPped neurons) and DAPI (blue, nuclei). Neurons active during the hcNOR sample phase (Object-trained, right) show a significantly higher density of tdTomato+ neurons compared to the No Learning (Handling-control, left) condition, confirming the specificity of the engram labelling.* ***b)*** *Triple-manipulation experimental timeline. cFos-TRAP mice*

received bilateral PRC injections of the impairment vector (AAV5-GFAP-hM3Dq) and the engram-specific rescue vector (AAV9-CaMKIIa-DIO-OptoTrkB). hcNOR testing begins 28 days post-injection (dpi). ***c)*** *Multi-trial engram-specific rescue paradigm. Trial 1 (Engram 1, Rescue): CNO and 4-OHT are administered pre-learning. LTM impairment is induced by CNO and the engram is TRAPped by 4-OHT. OptoTrkB is activated via illumination (30 minutes blue light pattern) 13 hours post-learning to specifically rescue the TRAPped neurons. Trial 2 (Engram 2, Control): one week later, mice learn a new engram with CNO/4-OHT but no illumination, serving as the non-rescued control.* ***d)*** *LTM rescue is engram specific and follows a physiological decay. The dot plot shows the mean Discrimination Index ± SEM. Engram 1 (24h) showed successful LTM consolidation (*** $p < 0.001$ vs. Engram 2 (24 h) and Engram 1 (14 d). Engram 2 failed to consolidate ($DI \approx 0$), demonstrating the specificity of the rescue. Engram 1 also exhibited physiological decay by 14 days. Statistics: One-way ANOVA with Tukey's multiple comparison post-hoc test. Cohort sizes: n = 13 mice (Engram 1 24h), n = 7 mice (Engram 1 14d), n = 10 mice (Engram 2 24h).*

These results collectively provide the most direct evidence that the astrocytic BDNF-TrkB axis acts to strengthen connectivity within the specific engram ensemble and that this cellular-level process is both necessary and sufficient for the conversion of short-term object recognition memory into a stable long-term trace.

DISCUSSION

Memory consolidation is a multifaceted and highly coordinated process, involving a complex interplay of synaptic tagging and capture, *de novo* protein synthesis, and various neuromodulatory systems. Rather than suggesting that memory is "fundamentally dependent" on a single pathway in an absolute sense, this work highlights the BDNF-TrkB signaling axis as a critical causal lever within the Perirhinal Cortex (PRC). In our specific models of astrocytic recycling deficit, TrkB signaling emerges as a limiting factor whose precise temporal activation is sufficient to drive the transition from short-term to long-term memory. While these observations are currently focused on the mnemonic processes of the PRC, we acknowledge that different brain regions may rely on distinct molecular signatures and metabolic requirements for consolidation[241,242]. Rather than acting in isolation, TrkB serves as a master regulator of the late-phase plasticity required to stabilize the memory trace.

The investigation into the causal role of TrkB was made possible by the implementation of light-sensitive Tropomyosin receptor kinase B (OptoTrkB). While the molecular foundation of OptoTrkB was established over a decade ago[243], and subsequent variants have been applied in various *in vivo* contexts, its utility in probing the temporal dynamics of memory consolidation has remained largely unexplored. The novelty of the current work, therefore, lies not in the introduction of OptoTrkB as a molecular concept, but in its strategic application as a tool for the manipulation of engram-specific consolidation. By integrating OptoTrkB with TRAP-mediated genetic labelling and non-invasive bioluminescent-optogenetic (BL-OG) stimulation, we have successfully moved beyond general pathway activation to achieve a level of post-encoding control within defined neuronal ensembles that was previously unattainable with systemic pharmacology or traditional optogenetic interventions.

Our findings establish that precise TrkB signaling is both necessary and sufficient to stabilize memory traces when endogenous consolidation mechanisms are impaired. We first confirmed the functional fidelity of the OptoTrkB system i*n vitro*, where acute blue-light delivery successfully induced the

phosphorylation of critical downstream signaling cascades, specifically ERK1/2 and CREB. Crucially, this activation followed a physiological pattern: a rapid, transient phosphorylation of ERK1/2 followed by the delayed, prolonged activation of CREB, which is the signature required for initiating gene expression and synaptic plasticity.

To determine the causal efficacy of OptoTrkB in a fragile memory state, we utilized a p75-flox mouse model, which exhibits impaired long-term potentiation and memory due to a disruption in the astrocytic recycling mechanism crucial for BDNF availability. This model highlights a critical emerging concept: the essential non-neuronal contribution to sustained BDNF signaling that supports engram stability. Using *ex vivo* slice preparations, we demonstrated that optical activation of OptoTrkB immediately following tetanus stimulation rescued Long-lasting LTP (L-LTP). While these results are robust, a rigorous interpretation requires us to consider the molecular specificity of the rescue. Further validation, such as the use of a kinase-dead OptoTrkB variant or the pharmacological blockade of TrkB during the light-delivery window, would provide definitive proof that the observed rescue is mediated exclusively by the receptor's catalytic activity. However, the necessity of TrkB signaling for long-term object recognition memory is well-supported by literature. Previous studies using pharmacological inhibition (e.g., K252a or ANA-12) or conditional genetic deletion of BDNF/TrkB in the PRC have consistently shown that disrupting this axis selectively impairs long-term, but not short-term, object memory[244,245]. Furthermore, evidence suggests that BDNF release and subsequent TrkB activation are required specifically during the post-encoding consolidation window to stabilize the memory trace[246]. Our work builds upon these established "loss-of-function" findings by providing the critical "gain-of-function" counterpart, reinforcing the centrality of this pathway as the essential molecular switch for engram consolidation.

Translating these findings to behaviour, we achieved the first effective rescue of impaired memory consolidation *in vivo*. The adoption of a home-cage Novel Object Recognition (hcNOR) paradigm, rather than the standard arena-based NOR, was a deliberate methodological choice aimed at isolating

the molecular mechanisms of memory consolidation within a restricted neural circuit. Standard NOR necessitates the formation of a complex, multi-modal engram in which an object identity is linked to spatial context[247]. This engages a broad, distributed network including the PRC, the hippocampus, the visual association area Te2, and various sensory cortices[248]. By conducting the task within the animal's familiar environment, we minimized "contextual contamination", ensuring that the behavioural readout and the TRAP-mediated labelling were primarily driven by object-associated plasticity specifically within the PRC. However, the requirement for single housing to facilitate automated tracking and eliminate social variance introduces a potential confounding factor that warrants critical consideration. Social deprivation in male mice is well-documented to induce psychological distress, often manifesting as increased anxiety-like behaviour in assays such as the open field or elevated plus maze, and is frequently correlated with reduced endogenous BDNF levels[249]. While social isolation is a significant factor, the home-cage environment simultaneously mitigates the acute stress associated with a novel arena, which is a confound factor in standard NOR protocols[250,251]. Furthermore, evidence suggesting a detrimental impact specifically on NOR performance in wild-type mice remains inconsistent, with recent studies showing social influence in specific disease models but not in control groups[252]. Nevertheless, we must acknowledge that prolonged isolation may have established a unique "plasticity baseline" that potentially sensitized the circuit to our OptoTrkB intervention. Future research could address this by comparing these findings with results obtained in classical squared or Y-shaped arenas, albeit at the likely cost of reduced engram specificity. A promising alternative to avoid the stressors of isolation would be the use of female mice, which can be group-housed more safely than males. However, this approach introduces its own technical complexities; specifically, the use of CNO for DREADD-based or p75-flox systems must be carefully weighed against its potential interactions with estrogen receptor signaling and subsequent behavioural effects.

A significant outcome of this study was the validation of a Bioluminescent Optogenetics (BL-OG) technique aimed at restoring memory deficits caused by BDNF-recycling impairments. We

successfully implemented a self-contained, non-invasive system by co-expressing OptoTrkB with a genetically encoded bioluminescent light source (luciferase). This approach not only removes the necessity for implanted optic fibers, marking a significant step toward translational applicability, but also mechanistically reinforces the astrocytic hypothesis. We reinforced this hypothesis by showing that if the astrocytic vesicular release of the luciferase was chemically inhibited, the rescue of consolidation failed, underscoring the necessity of the astrocytic machinery for localized, perisynaptic delivery of the TrkB activating signal. Our results provide two major mechanistic insights into memory consolidation that fundamentally advance the field: (I) Causality in consolidation, not just recall: unlike previous optogenetic approaches that forced artificial engram reactivation to induce recall, the OptoTrkB system restores the functional consolidation itself. The recovered LTM is a physiological memory trace that can be recalled days later without concomitant light activation, definitively proving that TrkB signaling is one of the central signaling hub driving consolidation. (II) Extended therapeutic window: we observed that the "therapeutic" window for OptoTrkB activation extended remarkably, up to 13 hours post-encoding. This extended temporal flexibility is likely explained by the sustained presence of the intermediate memory trace (the synaptic tag) which remains receptive to late TrkB signaling, likely feeding into the prolonged activity of the transcriptional activator CREB. This finding challenges the strictly time-limited view of consolidation and suggests a protracted period during which gene-expression-dependent stabilization mechanisms remain amenable to intervention, opening a substantially longer window for potential pharmacological or optical therapies.

To achieve maximum cellular precision, we combined OptoTrkB with the cFos-TRAP line. In this model, light delivery rescued only the memory linked to a specific, tagged engram. This demonstrates the ability to act on the consolidation of a single memory without interfering with surrounding neurons or subsequent memories, providing the strongest causal evidence to date that the astrocytic BDNF/TrkB axis works to selectively strengthen the connectivity of the already active neuronal ensemble, defining the cellular unit of memory stabilization.

Finally, we must address the conceptual precision of the term "engram." While our TRAP-based approach captures the ensemble active during encoding, the term "engram" must be applied with rigorous distinction between a correlative ensemble and a functional substrate. In our systemic experiments, where TrkB signaling was manipulated across broader populations of CaMKIIa-positive excitatory neurons, we likely observed a general modulation of cortical plasticity rather than a precise “engram-specific” intervention. It is statistically certain that not all excitatory neurons expressing OptoTrkB participate in the encoding of a specific object; rather, the engram is “nested” within this larger activated population. Interestingly, these systemic findings demonstrate that the simultaneous activation of OptoTrkB across a broad excitatory network does not degrade the signal-to-noise ratio or the specificity of the memory trace, suggesting a degree of functional autonomy. By transitioning from these systemic observations to engram-specific rescue, we provide robust causal evidence for a functional engram. However, we propose that the engram likely extends beyond the cellular level; the "synaptic engram", defined by specific synapses receiving stochastic proBDNF release, may represent the ultimate unit of consolidation in PRC engrams.

In conclusion, this thesis presents a robust and comprehensively validated OptoTrkB system, establishing one of the first effective *in vivo* optogenetic control over the TrkB signaling pathway to causally manipulate memory engram consolidation. By precisely applying TrkB activation during the post-encoding window, we have rescued LTM deficits in multiple impaired models, highlighted the crucial role of the astrocytic-neuronal unit in maintaining TrkB availability, and demonstrated that the therapeutic window for intervention is surprisingly long. The use of the BL-OG platform and the successful demonstration of engram-specific rescue offer powerful new tools for both basic research and translational application. Future work should focus on utilizing this precision tool to dissect the role of TrkB signaling in specific brain sub-regions, offering a novel therapeutic avenue for neurological and neurodegenerative conditions marked by cognitive decline.

MATERIAL and METHODS

5.1 - Primary cell culture

All experiments were performed in accordance with the Italian Animal Welfare legislation (D.L. 26/2014) that was implemented by the European Committee Council Directive (2010/63 EEC) and were approved by local veterinary authorities and the Italian Ministry of Health (3FAF3.N.1JY).

Primary neuronal cultures: cortices were isolated from C57BL6 mouse embryos at embryonic day 17 (E17). In brief, cortical tissues were collected and placed in ice-cold Hank's balanced salt solution (HBSS) supplemented with 10 mM HEPES. Tissues were incubated with 0.25% trypsin-EDTA at 37°C for 20 min. Subsequently, trypsin was carefully aspirated, and the tissues were washed twice with a phosphate-buffered saline (PBS) solution. 1 ml Dulbecco's modified Eagle's medium (DMEM) containing 10% fetal bovine serum (FBS) and penicillin-streptomycin 10000 U/ml (P/S) was added to neutralize the trypsin. Cortical cells were gently dissociated using a P1000 pipette, collected by centrifugation (1900 RPM for 5 min), and resuspended in DMEM supplemented with 10% FBS and P/S. The cells were eventually transfected with 3µg of DNA using the Amaxa Nucleofector system following the manufacturer's instructions. The transfected cells were plated on glass coverslips pre-coated with poly-L-lysine (0.1 mg/ml) (200·000 cells per coverslip). 3 hours after plating, the medium was replaced with Neurobasal supplemented with B-27, penicillin-streptomycin, and Glutamax. Half of the culture media was refreshed every 3-4 days until DIV 11, when coverslips were used for the experiments.

5.2 - Constructs and viral vectors

The following AAVs plasmids and vectors were used:

Plasmid/Vector	**Source**
pAAV-CamK2a(0.4)-Opto-cytTrkB(E281A)-HA	Addgene #180589
pAAV-Camk2a(0.4)-DIO-Opto-cytTrkB(E281A)-HA	Addgene #180588
pAAV-Helper	Was a gift from Alessandra Denti (University of Trento, IT)
pAAV2/9 (rep/cap)	Addgene #112865
pAAV2/5 (rep/cap)	Addgene #104964
AAV9-CamK2a(0.4)-Opto-cytTrkB(E281A)-HA	Was produced by the laboratory of Michele Simonato (Vita-Salute San Raffaele University, Milan, IT)
AAV9-Camk2a(0.4)-DIO-Opto-cytTrkB(E281A)-HA	Was produced by the laboratory of Michele Simonato (Vita-Salute San Raffaele University, Milan, IT)
AAV5-GFAP-hM3D(Gq)-mCherry (AAV-hM3Dq)	Was a gift from Bryan Roth (University of North Carolina-Chapel Hill, USA), (Addgene plasmid # 50478 ; http://n2t.net/addgene:50478 ; RRID:Addgene_50478)
AAV5-GFAP-tdTomato	Was a gift from Baljit Khakh (University of California, Los Angeles, USA)
AAV5-GFAP-hPOMC1-26-sbGLuc-P2A-dTomato	Was a gift from Ute Hochgeschwender (Neuroscience Program and College of Medicine, Central Michigan University, Mt Pleasant, USA)
AAV5-GFAP-Synb-sbGLuc	Was a gift from Ute Hochgeschwender (Neuroscience Program and College of Medicine, Central Michigan University, Mt Pleasant, USA)
CamK2a(0.4)-Opto-cytTrkB(E281A)-HA DNA (used in Section 3.1) was purified and extracted using an EndoFree Plasmid Maxi kit from Qiagen® (Cat. N°12362)	

Viral titers were determined by qPCR.

5.3 - Intracranial Viral Injection

For virus delivery, three-month-old mice were injected with the following volumes of AAV (1,5 µl in volume for a single vector injection, 0,8 µl per vector for double vectors injection, 0,6 µl per vector for triple vectors injection). Injections were performed in deeply anesthetized animals (with isoflurane; 4% for the induction and 1.5% for maintenance) after drilling a hole (0.5 mm diameter) into the skull above the perirhinal cortices (coordinates from Bregma: anteroposterior −2 mm, mediolateral ±4.2 mm, dorsoventral −2.8/−2.6 mm). Viral vectors were infused into the PRC of each hemisphere by inserting a pulled glass capillary containing the viral vectors mix and connected to a manual syringe pump or an automated syringe pump (Pump 11 Elite, Harvard Apparatus). After injections, the skin was sutured and mice were revitalized under a heat lamp, returned to their cage and housed in standard conditions until the day of the experiment.

5.4 - Experimental plan for DLP light stimulation experiments

A Digital Light Processor device (DLP) E4500 purchased from E.K.B Technologies Ltd. equipped with 3 LEDs, optics, a WXGA DMD (Wide Extended Graphics Array Digital Micromirror Device), and a driver board was integrated into the EPI-fluorescence port of SD microscope. The DLP's light engine can generate approximately 150 lumens at 15 W of LED power consumption. Specifically, a blue LED with a wavelength of 460 ± 14 nm and a power output of 600 mW was utilized. The DMD features 1039680 mirrors arranged in a diamond array configuration of 912 columns by 1140 rows, enabling patterned illumination using preloaded and custom patterns. The system supports temporal pulsing of light with internal and external triggers, with a minimum exposure time ranging from 235 µs to 8333 µs, depending on the bit depth of the projected image. It handles 1 to 8-bit images at a resolution of 912 columns × 1140 rows, ensuring pixel accuracy where each pixel corresponds to a micromirror on the DMD. The emitted light from the DLP system is aligned with the microscope's optical path via the system's rear port. A dichroic mirror (Chroma T505lpxr-UF1) serves as a high-

pass filter, reflecting wavelengths smaller than 505 nm. This setup enables simultaneous DLP illumination and signal recording at longer wavelengths.

At DIV11 cortical neurons expressing OptoTrkB were placed under the microscope in a 35 mm dish with a dark bottom containing HBSS supplemented with 2mM CaCl2 and 1mM MgCl2. Target illumination regions were selected based on optimal cellular density and visual confirmation of neuronal health.

Light excitations were conducted using the following pattern: 470-nm light pulses delivered at 5-s intervals for 10 min, using a 200-ms pulse duration at 9.7 W/cm^2. Following light stimulation, coverslips were returned to the incubator in culture media and fixed with cold 4% paraformaldehyde (PFA) for 20 min. Non-illuminated cultures were kept in the dark throughout the entire experimental period.

5.5 - Immunostaining

Immunocytochemistry: Cultured cells were fixed in cold 4% para-formaldehyde (PFA) for 20 min and washed with PBS. Cells were permeabilized with 0.1% Triton X-100 in PBS for 20 min and blocked with 3% bovine serum albumin (BSA) in PBS for 60 min. Neurons were incubated with primary antibodies diluted into 3% BSA at 4°C overnight. Following the incubation, cells were washed multiple times with 3% BSA before incubating with secondary antibodies conjugated with fluorophores for 2h at room temperature. Post-incubation, cells were washed with PBS, counterstained with DAPI (Sigma-Aldrich,Cat#D9542) and mounted with Aqua Poly/mount (Polysciences, Inc., Cat#18606). The primary antibody used and dilutions are listed below:

HA (Chicken, Abcam ab#9111, 1:1000), pERK1/2 (P-p44/42 MAPK) (Rabbit, Cell Signaling Technology ab#91015, 1:500), pCREB (Rabbit, Santa Cruz Biotechnology ab#7978R, 1:200)

Immunohistochemistry: Brain slices from electrophysiology experiments were fixed in 4% PFA for 1 h. Slices were treated with 0,5% Triton X-100 for 20 min, blocked with 3% Bovine Serum Albumin (BSA) in Phosphate-buffered saline for 1 h, and incubated overnight free-floating with primary antibodies diluted in blocking buffer. Slices were washed in Phosphate-buffered saline and incubated for 2 h at room temperature with secondary antibodies diluted in a blocking buffer. Slices were eventually counterstained with DAPI (Sigma-Aldrich, Cat#D9542) and mounted with Aqua Poly/mount (Polysciences, Inc., Cat#18606). The primary antibody used and dilutions are listed below:

NeuN (Mouse, Abcam ab#77315, 1:1000), pCREB (Rabbit, Santa Cruz Biotechnology ab#7978R, 1:200)

5.6 - Confocal microscopy for *in-vitro* images

The microscopy setup consists of a system purchased from Crisel Instruments Company, integrating the X-Light V2 top-performance confocal spinning disk module and an integrated VCS (Video Confocal Super-resolution) super-resolution module based on structured illumination microscopy. The SIM module achieves a lateral resolution of 115 nm and an axial resolution of approximately 250 nm. The entire system is configured in an upright position. It incorporates 7 solid state LED sources covering the spectrum from 395 nm to 640 nm, arranged in the Lumencore Spectra X LED-based light engine. The imaging system is equipped with a Prime Back-side Illuminated (BSI) Scientific CMOS camera with 2048x2048 pixels and a pixel area of 6.5µmx6.5µm. Three objectives are integrated into the system: a dry long-working-distance 10x (LMPLFLN10XLWD, NA 0.25, WD 21mm), a water immersion 60x (LUMPLFLN60XW, NA 1, WD 2mm) and an oil 100X (UP objectives UPLSAPO100XO, NA 1.4, WD 0.13 mm). The confocal setup includes spinning disks with double pinhole patterns: one with 40 µm holes, and another with 70 µm holes which can be inserted in the path or kept aside.

5.7 - Laser scanning Confocal Microscopy

Confocal imaging was performed using a laser-scanning motorized confocal system (Nikon A1) equipped with an Eclipse Ti-E inverted microscope and four laser lines (405, 488, 561 and 638 nm). Z-series images were taken with an inter-stack interval of 0.5 µm using a 60X oil immersion objective (Nikon APO 60x 1.4).

Confocal imaging was performed using a laser-scanning motorized confocal system (Nikon A1) equipped with an Eclipse Ti-E inverted microscope and four laser lines (405, 488, 561 and 638 nm). For each type of quantification, laser intensities and camera settings were maintained identically within the same experiment to allow comparison of different experimental groups and treatments. Image processing were performed using the software NIS Element (Nikon). For the analysis of CREB phosphorylation in *ex vivo* preparations, 3 regions of interest (ROIs) were acquired for each slice and the percentage of pCREB and NeuN co-localization was calculated. Co-localization was quantified calculating Mander's overlap using the software NIS Element (Nikon).

5.8 - Quantitative image analysis

For each type of quantification, laser intensities and camera settings were maintained identical within the same experiment to allow the comparison of different experimental groups and treatments. Image processing was performed using the ImageJ software or the NIS Element software (Nikon).

- Quantification of pERK1/2 and pCREB *in vitro*: Image processing was conducted using ImageJ software. For the confocal image analysis, neurons were first classified based on their light exposure: "illuminated" (exposed to light stimulation) or "non-illuminated" (maintained in the dark throughout the experiment). Critically, the quantification was restricted exclusively to HA-positive (HA+) neurons to ensure the analysis focused only on cells efficiently transfected and expressing OptoTrkB. A circular area was drawn in order to cover the soma (for pERK1/2) or the

nucleus (for pCREB), maintaining the same radius for all the cells analysed. The mean pixel value was calculated by the software.

- *ex vivo*: Colocalization of pCREB and NeuN signals was quantified by calculating Mander's overlap using the software NIS Element.

5.9 - Electrophysiological recording

Brain slices were prepared from p75-flox, control littermates, or wild-type mice (7–9 weeks old). The brain was removed and placed in cold (5°C) oxygenated (95% O2 and 5% CO2) artificial cerebrospinal fluid (ACSF) containing 124.0 mM NaCl, 4.4 mM KCl, 1 mM NaH2PO4, 2.5 mM CaCl2, 1.3 mM MgCl2, 26.2 mM NaHCO3, 10 mM glucose, and 2 mM L-ascorbic acid (Sigma-Aldrich). Horizontal cortex slices (300 mm thick) were prepared using a vibratome and maintained in a chamber containing oxygenated ACSF at room temperature. After a minimum recovery period of at least 1 hr, a single slice was transferred into a submersion recording chamber perfused (3 mL/min) with oxygenated ACSF at 32°C ± 0.2°C and square current pulses (duration 0.2 ms) were applied every 30 s (0.033 Hz) using a stimulus generator (WPI, stimulus isolator A360) connected through a stimulus isolation unit to a concentric bipolar electrode (40–80 KU, FHC) positioned in layers II/III on the temporal side of the rhinal sulcus. Evoked extracellular fEPSPs were recorded using an Axoclamp-2B amplifier (Axon Instruments) with ACSF-filled glass micropipette pulled on a vertical puller (Narishige PC-10, resistance [<5 MU]), inserted in layers II/III at around 500 mm from the stimulation electrode, and analyzed using Axoscope 8.0 software (Axon Instruments). Baseline responses were obtained every 30 s with a stimulus intensity adjusted to induce ≈50% of the maximal synaptic response. After 20 min of stable baseline, LTP was evoked by TBS (100 Hz; four sets of stimulations delivered 15 s apart, each one consisting of ten bursts of five pulses at 100 Hz with inter-burst intervals of 150 ms). LTD was evoked by LFS of either 3,000 stimuli (10 min) or 1,950 stimuli (6.5 min) at 5 Hz. fEPSPs were plotted as amplitude and slope and we selected only

those showing similar trend. Each point represents the responses every 30 s expressed as means ± SEM.

6. - Animal models

All experiments were performed in accordance with the Italian Animal Welfare legislation (D.L. 26/2014) that was implemented by the European Committee Council Directive (2010/63 EEC) and were approved by local veterinary authorities and the Italian Ministry of Health (3FAF3.73).

Wild type mice (C57 BL/6 RRID:IMSR_JAX:000664) were obtained from Charles River Laboratories. p75-flox mice were generated by crossing p75lox/lox mice with Glast::CreERT2 R26R mice (RRID:IMSR_JAX:012586; IMSR_JAX:002192). Animals were housed in a 12 h light/dark cycle with unrestricted access to food and water. In the behavioural experiments, only male mice were used.

p75-flox mice and control littermates were treated with one milligram of tamoxifen (Sigma Aldrich) dissolved in corn oil (Sigma Aldrich) twice a day for 5 consecutive days.

For “BL-OG” experiments, mice expressing *Gaussia* luciferase received a single intraperitoneal injection of coelenterazine (CTZ).

Mice injected with AAV5-GFAP-hM3Dq received a single intraperitoneal injection of clozapine-N-oxide (CNO) before the sample phase.

cFos-TRAP mice received a single intraperitoneal injection of 4-Hydrotamoxifen before the sample phase.

To minimize potential variability associated with the estrous cycle, only male mice were used in this study.

6.1 - Home-cage Novel Object Recognition (hcNOR) test

For the hcNOR protocol, mice were singly housed (one mouse per cage) for a minimum of seven days prior to testing. During the sample phase, two identical, geometrically simple objects were introduced into opposite corners of the home cage, and mice were free to explore the objects for 5 minutes. To test STM or LTM the retention period between sample and test phases was changed accordingly. For the test phase, one of the familiar objects was substituted with a novel object, and exploration was allowed for 5 minutes. The objects were cleaned up with ethanol 70% between trials to stop the build-up of olfactory cues.

The discrimination index (DI) was calculated as follows:

$$DI = \frac{(\text{time with novel location or object} - \text{time with familiar location or object})}{(\text{time with novel location or object} + \text{time with familiar location or object})}$$

A video camera was mounted above the cage to record trials. The exploration time was the time during which mice approached the objects with muzzles and paws.

6.2 - Light stimulation

ex-vivo: brain slices were illuminated using a focus laser emitting 30 second of continuous blue light at 488nm and 0,5mW/mm^2 power registered at the surface of the slice-containing chamber.

in vivo: for external LED light stimulation of mice injected bilaterally with AAV9-OptoTrkB (E281A), the blue light stimulation was applied atop the head with an intact skull and fur. A 488 nm blue LED light pulse was given for one second every five seconds, for a total duration of 30 min, with 0,5mW/mm^2. A custom-designed LED cage lid was used for this non-invasive light stimulation.

6.3 - Statistical analysis

Sample sizes and statistical tests can be found in figure legends. Statistical analysis was carried out using Graphpad Prism 9. Comparison between the two groups was assessed by the unpaired t test. Comparison between two dependent groups was evaluated by the paired t test. We used one-way ANOVA with Tukey's multiple comparison post-hoc test (behavioural experiments) or Bonferroni's test (LTP experiments) for multiple comparisons. Data were excluded from the analysis following the outlier analysis. The level of significance used was $P < 0.05$.

REFERENCES

1. Aggleton, J. P. & Brown, M. W. Episodic memory, amnesia, and the hippocampal–anterior thalamic axis. *Behav. Brain Sci.* **22**, 425 (1999).
2. Ennaceur, A. & Delacour, J. A new one-trial test for neurobiological studies of memory in rats. 1: Behavioral data. *Behav. Brain Res.* **31**, 47–59 (1988).
3. Antunes, M. & Biala, G. The novel object recognition memory: neurobiology, test procedure, and its modifications. *Cogn. Process.* **13**, 93–110 (2012).
4. Balderas, I., Rodriguez-Ortiz, C. J. & Bermudez-Rattoni, F. Consolidation and reconsolidation of object recognition memory. *Behav. Brain Res.* **285**, 213–222 (2015).
5. Tanimizu, T., Kono, K. & Kida, S. Brain networks activated to form object recognition memory. *Brain Res. Bull.* **141**, 27–34 (2018).
6. Neural substrates of tactile object recognition: An fMRI study. https://onlinelibrary.wiley.com/doi/epdf/10.1002/hbm.10162?getft_integrator=sciencedirect_contenthosting&src=getftr&utm_source=sciencedirect_contenthosting doi:10.1002/hbm.10162.
7. Malkova, L. & Mishkin, M. One-Trial Memory for Object-Place Associations after Separate Lesions of Hippocampus and Posterior Parahippocampal Region in the Monkey. *J. Neurosci.* **23**, 1956–1965 (2003).
8. Ennaceur, A. & Delacour, J. A new one-trial test for neurobiological studies of memory in rats. 1: Behavioral data. *Behav. Brain Res.* **31**, 47–59 (1988).
9. Semon: Die Mneme als erhaltendes Prinzip im Wechsel... - Google Scholar. https://scholar.google.com/scholar_lookup?title=Die%20Mneme%20als%20erhaltendes%20Prinzip%20im%20Wechsel%20des%20organischen%20Geschehens&author=R%20Semon&author=W%20Engelmann&publication_year=1904&.
10. Morris, R. G. D.O. Hebb: The Organization of Behavior, Wiley: New York; 1949. *Brain Res. Bull.* **50**, 437 (1999).

11. Josselyn, S. A., Köhler, S. & Frankland, P. W. Finding the engram. *Nat. Rev. Neurosci.* **16**, 521–534 (2015).

12. Tonegawa, S., Liu, X., Ramirez, S. & Redondo, R. Memory Engram Cells Have Come of Age. *Neuron* **87**, 918–931 (2015).

13. Josselyn, S. A. & Tonegawa, S. Memory engrams: Recalling the past and imagining the future. *Science* **367**, eaaw4325 (2020).

14. Eichenbaum, H. Barlow versus Hebb: When is it time to abandon the notion of feature detectors and adopt the cell assembly as the unit of cognition? *Neurosci. Lett.* **680**, 88–93 (2018).

15. Yuste, R. From the neuron doctrine to neural networks. *Nat. Rev. Neurosci.* **16**, 487–497 (2015).

16. Sun, X. *et al.* Functionally Distinct Neuronal Ensembles within the Memory Engram. *Cell* **181**, 410-423.e17 (2020).

17. Poon, C. H., Chan, Y.-S., Fung, M. L. & Lim, L. W. Memory and neuromodulation: A perspective of DNA methylation. *Neurosci. Biobehav. Rev.* **111**, 57–68 (2020).

18. Singewald, N. Altered brain activity processing in high-anxiety rodents revealed by challenge paradigms and functional mapping. *Neurosci. Biobehav. Rev.* **31**, 18–40 (2007).

19. Guzowski, J. F. *et al.* Mapping behaviorally relevant neural circuits with immediate-early gene expression. *Curr. Opin. Neurobiol.* **15**, 599–606 (2005).

20. Sternson, S. M. Exploring internal state-coding across the rodent brain. *Curr. Opin. Neurobiol.* **65**, 20–26 (2020).

21. Guenthner, C. J., Miyamichi, K., Yang, H. H., Heller, H. C. & Luo, L. Permanent Genetic Access to Transiently Active Neurons via TRAP: Targeted Recombination in Active Populations. *Neuron* **78**, 773–784 (2013).

22. Tonegawa, S., Morrissey, M. D. & Kitamura, T. The role of engram cells in the systems consolidation of memory. *Nat. Rev. Neurosci.* **19**, 485–498 (2018).

23. Schacter, D. L. *Forgotten Ideas, Neglected Pioneers: Richard Semon and the Story of Memory*. (Psychology Press, New York, 2012). doi:10.4324/9780203720134.

24. Dudai, Y. Consolidation: fragility on the road to the engram. *Neuron* **17**, 367–370 (1996).

25. Kandel, E. R. & Tauc, L. Mechanism of heterosynaptic facilitation in the giant cell of the abdominal ganglion of Aplysia depilans. *J. Physiol.* **181**, 28–47 (1965).

26. Bliss, T. V. & Lomo, T. Long-lasting potentiation of synaptic transmission in the dentate area of the anaesthetized rabbit following stimulation of the perforant path. *J. Physiol.* **232**, 331–356 (1973).

27. Ito, M. Cerebellar control of the vestibulo-ocular reflex--around the flocculus hypothesis. *Annu. Rev. Neurosci.* **5**, 275–296 (1982).

28. Asok, A., Leroy, F., Rayman, J. B. & Kandel, E. R. Molecular Mechanisms of the Memory Trace. *Trends Neurosci.* **42**, 14–22 (2019).

29. Lisman, J., Yasuda, R. & Raghavachari, S. Mechanisms of CaMKII action in long-term potentiation. *Nat. Rev. Neurosci.* **13**, 169–182 (2012).

30. Lisman, J., Schulman, H. & Cline, H. The molecular basis of CaMKII function in synaptic and behavioural memory. *Nat. Rev. Neurosci.* **3**, 175–190 (2002).

31. Benke, T. A., Lüthi, A., Isaac, J. T. & Collingridge, G. L. Modulation of AMPA receptor unitary conductance by synaptic activity. *Nature* **393**, 793–797 (1998).

32. Derkach, V., Barria, A. & Soderling, T. R. Ca2+/calmodulin-kinase II enhances channel conductance of alpha-amino-3-hydroxy-5-methyl-4-isoxazolepropionate type glutamate receptors. *Proc. Natl. Acad. Sci. U. S. A.* **96**, 3269–3274 (1999).

33. Shirke, A. M. & Malinow, R. Mechanisms of potentiation by calcium-calmodulin kinase II of postsynaptic sensitivity in rat hippocampal CA1 neurons. *J. Neurophysiol.* **78**, 2682–2692 (1997).

34. Matus, A. Actin-based plasticity in dendritic spines. *Science* **290**, 754–758 (2000).

35. Zhang, H., Ben Zablah, Y., Zhang, H. & Jia, Z. Rho Signaling in Synaptic Plasticity, Memory, and Brain Disorders. *Front. Cell Dev. Biol.* **9**, 729076 (2021).

36. Carlisle, H. J. & Kennedy, M. B. Spine architecture and synaptic plasticity. *Trends Neurosci.* **28**, 182–187 (2005).

37. Lamprecht, R. & LeDoux, J. Structural plasticity and memory. *Nat. Rev. Neurosci.* **5**, 45–54 (2004).

38. Okamoto, K.-I., Nagai, T., Miyawaki, A. & Hayashi, Y. Rapid and persistent modulation of actin dynamics regulates postsynaptic reorganization underlying bidirectional plasticity. *Nat. Neurosci.* **7**, 1104–1112 (2004).

39. Nägerl, U. V., Eberhorn, N., Cambridge, S. B. & Bonhoeffer, T. Bidirectional activity-dependent morphological plasticity in hippocampal neurons. *Neuron* **44**, 759–767 (2004).

40. Guskjolen, A. & Cembrowski, M. S. Engram neurons: Encoding, consolidation, retrieval, and forgetting of memory. *Mol. Psychiatry* **28**, 3207–3219 (2023).

41. Gouty-Colomer, L. A. *et al.* Arc expression identifies the lateral amygdala fear memory trace. *Mol. Psychiatry* **21**, 364–375 (2016).

42. Parsons, R. G. Behavioral and neural mechanisms by which prior experience impacts subsequent learning. *Neurobiol. Learn. Mem.* **154**, 22–29 (2018).

43. Mozzachiodi, R. & Byrne, J. H. More than synaptic plasticity: role of nonsynaptic plasticity in learning and memory. *Trends Neurosci.* **33**, 17–26 (2010).

44. Benito, E. & Barco, A. CREB's control of intrinsic and synaptic plasticity: implications for CREB-dependent memory models. *Trends Neurosci.* **33**, 230–240 (2010).

45. Silva, A. J., Zhou, Y., Rogerson, T., Shobe, J. & Balaji, J. Molecular and Cellular Approaches to Memory Allocation in Neural Circuits. *Science* https://doi.org/10.1126/science.1174519 (2009) doi:10.1126/science.1174519.

46. Dong, Y. *et al.* CREB modulates excitability of nucleus accumbens neurons. *Nat. Neurosci.* **9**, 475–477 (2006).

47. Wallace, D. L. *et al.* CREB regulation of nucleus accumbens excitability mediates social isolation–induced behavioral deficits. *Nat. Neurosci.* **12**, 200–209 (2009).

48. Han, J.-H. *et al.* Neuronal Competition and Selection During Memory Formation. *Science* https://doi.org/10.1126/science.1139438 (2007) doi:10.1126/science.1139438.

49. Zhou, Y. *et al.* CREB regulates excitability and the allocation of memory to subsets of neurons in the amygdala. *Nat. Neurosci.* **12**, 1438–1443 (2009).

50. Yiu, A. P. *et al.* Neurons Are Recruited to a Memory Trace Based on Relative Neuronal Excitability Immediately before Training. *Neuron* **83**, 722–735 (2014).

51. Abraham, W. C., Jones, O. D. & Glanzman, D. L. Is plasticity of synapses the mechanism of long-term memory storage? *Npj Sci. Learn.* **4**, 9 (2019).

52. Frankland, P. W. & Josselyn, S. A. In search of the memory molecule. *Nature* **535**, 41–42 (2016).

53. Kandel, E. R. The Molecular Biology of Memory Storage: A Dialogue Between Genes and Synapses. *Science* https://doi.org/10.1126/science.1067020 (2001) doi:10.1126/science.1067020.

54. Dudai, Y. The Neurobiology of Consolidations, Or, How Stable is the Engram? *Annu. Rev. Psychol.* **55**, 51–86 (2004).

55. Alberini, C. M. Transcription Factors in Long-Term Memory and Synaptic Plasticity. *Physiol. Rev.* https://doi.org/10.1152/physrev.00017.2008 (2009) doi:10.1152/physrev.00017.2008.

56. Frankland, P. W., Josselyn, S. A. & Köhler, S. The neurobiological foundation of memory retrieval. *Nat. Neurosci.* **22**, 1576–1585 (2019).

57. Tulving, E. & Thomson, D. M. Encoding specificity and retrieval processes in episodic memory. *Psychol. Rev.* **80**, 352–373 (1973).

58. Han, J.-H. *et al.* Selective Erasure of a Fear Memory. *Science* https://doi.org/10.1126/science.1164139 (2009) doi:10.1126/science.1164139.

59. Ryan, T. J., Roy, D. S., Pignatelli, M., Arons, A. & Tonegawa, S. Engram cells retain memory under retrograde amnesia. *Science* https://doi.org/10.1126/science.aaa5542 (2015) doi:10.1126/science.aaa5542.

60. Garner, A. R. *et al.* Generation of a Synthetic Memory Trace. *Science* https://doi.org/10.1126/science.1214985 (2012) doi:10.1126/science.1214985.

61. Ramirez, S. *et al.* Creating a False Memory in the Hippocampus. *Science* https://doi.org/10.1126/science.1239073 (2013) doi:10.1126/science.1239073.

62. Liu, X. *et al.* Optogenetic stimulation of a hippocampal engram activates fear memory recall. *Nature* **484**, 381–385 (2012).

63. Carrillo-Reid, L., Han, S., Yang, W., Akrouh, A. & Yuste, R. Controlling Visually Guided Behavior by Holographic Recalling of Cortical Ensembles. *Cell* **178**, 447-457.e5 (2019).

64. Hardt, O., Nader, K. & Nadel, L. Decay happens: the role of active forgetting in memory. *Trends Cogn. Sci.* **17**, 111–120 (2013).

65. Nørby, S. Why Forget? On the Adaptive Value of Memory Loss. *Perspect. Psychol. Sci.* https://doi.org/10.1177/1745691615596787 (2015) doi:10.1177/1745691615596787.

66. Lee, J.-H. *et al.* Astrocytes phagocytose adult hippocampal synapses for circuit homeostasis. *Nature* **590**, 612–617 (2021).

67. Wang, C. *et al.* Microglia mediate forgetting via complement-dependent synaptic elimination. *Science* https://doi.org/10.1126/science.aaz2288 (2020) doi:10.1126/science.aaz2288.

68. Redondo, R. L. *et al.* Bidirectional switch of the valence associated with a hippocampal contextual memory engram. *Nature* **513**, 426–430 (2014).

69. Richards, B. A. & Frankland, P. W. The conjunctive trace. *Hippocampus* **23**, 207–212 (2013).

70. Tulving, E. & Thomson, D. M. Encoding specificity and retrieval processes in episodic memory. *Psychol. Rev.* **80**, 352–373 (1973).

71. Bartlett, S. F. C. *Remembering: A Study in Experimental and Social Psychology*. (Cambridge University Press, 1995).

72. Schacter, D. L. Constructive memory: past and future. *Dialogues Clin. Neurosci.* **14**, 7–18 (2012).

73. Dudai, Y. & Eisenberg, M. Rites of passage of the engram: reconsolidation and the lingering consolidation hypothesis. *Neuron* **44**, 93–100 (2004).

74. Squire, L. R., Genzel, L., Wixted, J. T. & Morris, R. G. Memory consolidation. *Cold Spring Harb. Perspect. Biol.* **7**, a021766 (2015).

75. Sutton, M. A. & Schuman, E. M. Dendritic protein synthesis, synaptic plasticity, and memory. *Cell* **127**, 49–58 (2006).

76. Raymond, C. R., Thompson, V. L., Tate, W. P. & Abraham, W. C. Metabotropic glutamate receptors trigger homosynaptic protein synthesis to prolong long-term potentiation. *J. Neurosci. Off. J. Soc. Neurosci.* **20**, 969–976 (2000).

77. Alberini, C. M., Ghirardi, M., Metz, R. & Kandel, E. R. C/EBP is an immediate-early gene required for the consolidation of long-term facilitation in Aplysia. *Cell* **76**, 1099–1114 (1994).

78. Abraham, W. C., Jones, O. D. & Glanzman, D. L. Is plasticity of synapses the mechanism of long-term memory storage? *NPJ Sci. Learn.* **4**, 9 (2019).

79. Frey, U. & Morris, R. G. Synaptic tagging and long-term potentiation. *Nature* **385**, 533–536 (1997).

80. Rao-Ruiz, P. *et al.* Engram-specific transcriptome profiling of contextual memory consolidation. *Nat. Commun.* **10**, 2232 (2019).

81. Mercer, T. R. *et al.* Noncoding RNAs in Long-Term Memory Formation. *Neurosci. Rev. J. Bringing Neurobiol. Neurol. Psychiatry* **14**, 434–445 (2008).

82. Smalheiser, N. R. The RNA-centred view of the synapse: non-coding RNAs and synaptic plasticity. *Philos. Trans. R. Soc. Lond. B. Biol. Sci.* **369**, 20130504 (2014).

83. Renner, M., Choquet, D. & Triller, A. Control of the postsynaptic membrane viscosity. *J. Neurosci. Off. J. Soc. Neurosci.* **29**, 2926–2937 (2009).

84. Sheng, M. & Kim, M. J. Postsynaptic signaling and plasticity mechanisms. *Science* **298**, 776–780 (2002).

85. Kreutzberg, G. W. Microglia: a sensor for pathological events in the CNS. *Trends Neurosci.* **19**, 312–318 (1996).

86. Salter, M. W. & Stevens, B. Microglia emerge as central players in brain disease. *Nat. Med.* **23**, 1018–1027 (2017).

87. Bachiller, S. *et al.* Microglia in Neurological Diseases: A Road Map to Brain-Disease Dependent-Inflammatory Response. *Front. Cell. Neurosci.* **12**, 488 (2018).

88. Frost, J. L. & Schafer, D. P. Microglia: Architects of the Developing Nervous System. *Trends Cell Biol.* **26**, 587–597 (2016).

89. Wang, C. *et al.* Microglia mediate forgetting via complement-dependent synaptic elimination. *Science* **367**, 688–694 (2020).

90. Gibson, E. M. *et al.* Neuronal activity promotes oligodendrogenesis and adaptive myelination in the mammalian brain. *Science* **344**, 1252304 (2014).

91. Steadman, P. E. *et al.* Disruption of Oligodendrogenesis Impairs Memory Consolidation in Adult Mice. *Neuron* **105**, 150-164.e6 (2020).

92. Sofroniew, M. V. & Vinters, H. V. Astrocytes: biology and pathology. *Acta Neuropathol. (Berl.)* **119**, 7–35 (2010).

93. Allaman, I., Bélanger, M. & Magistretti, P. J. Astrocyte-neuron metabolic relationships: for better and for worse. *Trends Neurosci.* **34**, 76–87 (2011).

94. Abbott, N. J. Developmental neurobiology. The milieu is the message. *Nature* **332**, 490–491 (1988).

95. Vasile, F., Dossi, E. & Rouach, N. Human astrocytes: structure and functions in the healthy brain. *Brain Struct. Funct.* **222**, 2017–2029 (2017).

96. Okamoto, M. *et al.* Reduction in paracrine Wnt3 factors during aging causes impaired adult neurogenesis. *FASEB J. Off. Publ. Fed. Am. Soc. Exp. Biol.* **25**, 3570–3582 (2011).

97. Lie, D.-C. *et al.* Wnt signalling regulates adult hippocampal neurogenesis. *Nature* **437**, 1370–1375 (2005).

98. Ojeda, S. R. *et al.* Glia-to-neuron signaling and the neuroendocrine control of female puberty. *Ann. Med.* **35**, 244–255 (2003).

99. Rudge, J. S. *et al.* Expression of Ciliary Neurotrophic Factor and the Neurotrophins-Nerve Growth Factor, Brain-Derived Neurotrophic Factor and Neurotrophin 3-in Cultured Rat Hippocampal Astrocytes. *Eur. J. Neurosci.* **4**, 459–471 (1992).

100. Cornell-Bell, A. H., Finkbeiner, S. M., Cooper, M. S. & Smith, S. J. Glutamate Induces Calcium Waves in Cultured Astrocytes: Long-Range Glial Signaling. *Science* **247**, 470–473 (1990).

101. Porter, J. T. & McCarthy, K. D. Hippocampal Astrocytes In Situ Respond to Glutamate Released from Synaptic Terminals. *J. Neurosci.* **16**, 5073–5081 (1996).

102. Kanemaru, K. *et al.* In Vivo Visualization of Subtle, Transient, and Local Activity of Astrocytes Using an Ultrasensitive Ca2+ Indicator. *Cell Rep.* **8**, 311–318 (2014).

103. Di Castro, M. A. *et al.* Local Ca2+ detection and modulation of synaptic release by astrocytes. *Nat. Neurosci.* **14**, 1276–1284 (2011).

104. Panatier, A. *et al.* Astrocytes Are Endogenous Regulators of Basal Transmission at Central Synapses. *Cell* **146**, 785–798 (2011).

105. Perea, G. & Araque, A. Astrocytes Potentiate Transmitter Release at Single Hippocampal Synapses. *Science* **317**, 1083–1086 (2007).

106. Sasaki, T., Matsuki, N. & Ikegaya, Y. Action-Potential Modulation During Axonal Conduction. *Science* **331**, 599–601 (2011).

107. Chever, O., Lee, C.-Y. & Rouach, N. Astroglial connexin43 hemichannels tune basal excitatory synaptic transmission. *J. Neurosci. Off. J. Soc. Neurosci.* **34**, 11228–11232 (2014).

108. Gerlai, R., Wojtowicz, J. M., Marks, A. & Roder, J. Overexpression of a calcium-binding protein, S100 beta, in astrocytes alters synaptic plasticity and impairs spatial learning in transgenic mice. *Learn. Mem. Cold Spring Harb. N* **2**, 26–39 (1995).

109. Gibbs, M. E., Anderson, D. G. & Hertz, L. Inhibition of glycogenolysis in astrocytes interrupts memory consolidation in young chickens. *Glia* **54**, 214–222 (2006).

110. Newman, L. A., Korol, D. L. & Gold, P. E. Lactate produced by glycogenolysis in astrocytes regulates memory processing. *PloS One* **6**, e28427 (2011).

111. Suzuki, A. *et al.* Astrocyte-neuron lactate transport is required for long-term memory formation. *Cell* **144**, 810–823 (2011).

112. Tadi, M., Allaman, I., Lengacher, S., Grenningloh, G. & Magistretti, P. J. Learning-Induced Gene Expression in the Hippocampus Reveals a Role of Neuron -Astrocyte Metabolic Coupling in Long Term Memory. *PloS One* **10**, e0141568 (2015).

113. Ostroff, L. E., Manzur, M. K., Cain, C. K. & Ledoux, J. E. Synapses lacking astrocyte appear in the amygdala during consolidation of Pavlovian threat conditioning. *J. Comp. Neurol.* **522**, 2152–2163 (2014).

114. Kuchibhotla, K. V., Lattarulo, C. R., Hyman, B. T. & Bacskai, B. J. Synchronous hyperactivity and intercellular calcium waves in astrocytes in Alzheimer mice. *Science* **323**, 1211–1215 (2009).

115. Olabarria, M., Noristani, H. N., Verkhratsky, A. & Rodríguez, J. J. Concomitant astroglial atrophy and astrogliosis in a triple transgenic animal model of Alzheimer's disease. *Glia* **58**, 831–838 (2010).

116. Simpson, J. E. *et al.* Astrocyte phenotype in relation to Alzheimer-type pathology in the ageing brain. *Neurobiol. Aging* **31**, 578–590 (2010).

117. Halassa, M. M. *et al.* Astrocytic modulation of sleep homeostasis and cognitive consequences of sleep loss. *Neuron* **61**, 213–219 (2009).

118. Lee, H. S. *et al.* Astrocytes contribute to gamma oscillations and recognition memory. *Proc. Natl. Acad. Sci. U. S. A.* **111**, E3343-3352 (2014).

119. Adamsky, A. *et al.* Astrocytic Activation Generates De Novo Neuronal Potentiation and Memory Enhancement. *Cell* **174**, 59-71.e14 (2018).

120. Kowiański, P. *et al.* BDNF: A Key Factor with Multipotent Impact on Brain Signaling and Synaptic Plasticity. *Cell. Mol. Neurobiol.* **38**, 579–593 (2018).

121. Leßmann, V. & Brigadski, T. Mechanisms, locations, and kinetics of synaptic BDNF secretion: An update. *Neurosci. Res.* **65**, 11–22 (2009).

122. Andreska, T., Aufmkolk, S., Sauer, M. & Blum, R. High abundance of BDNF within glutamatergic presynapses of cultured hippocampal neurons. *Front. Cell. Neurosci.* **8**, 107 (2014).

123. Huang, L. *et al.* BDNF produced by cerebral microglia promotes cortical plasticity and pain hypersensitivity after peripheral nerve injury. *PLoS Biol.* **19**, e3001337 (2021).

124. Pruunsild, P., Kazantseva, A., Aid, T., Palm, K. & Timmusk, T. Dissecting the human BDNF locus: bidirectional transcription, complex splicing, and multiple promoters. *Genomics* **90**, 397–406 (2007).

125. Aid, T., Kazantseva, A., Piirsoo, M., Palm, K. & Timmusk, T. Mouse and rat BDNF gene structure and expression revisited. *J. Neurosci. Res.* **85**, 525–535 (2007).

126. Barde, Y. A., Edgar, D. & Thoenen, H. Purification of a new neurotrophic factor from mammalian brain. *EMBO J.* **1**, 549–553 (1982).

127. Wang, M., Xie, Y. & Qin, D. Proteolytic cleavage of proBDNF to mBDNF in neuropsychiatric and neurodegenerative diseases. *Brain Res. Bull.* **166**, 172–184 (2021).

128. Foltran, R. B. & Diaz, S. L. BDNF isoforms: a round trip ticket between neurogenesis and serotonin? *J. Neurochem.* **138**, 204–221 (2016).

129. Vignoli, B. *et al.* Peri-Synaptic Glia Recycles Brain-Derived Neurotrophic Factor for LTP Stabilization and Memory Retention. *Neuron* **92**, 873–887 (2016).

130. Han, J., Yoon, S. & Park, H. Endocytic BDNF secretion regulated by Vamp3 in astrocytes. *Sci. Rep.* **11**, 21203 (2021).

131. Mowla, S. J. *et al.* Biosynthesis and post-translational processing of the precursor to brain-derived neurotrophic factor. *J. Biol. Chem.* **276**, 12660–12666 (2001).

132. Lee, R., Kermani, P., Teng, K. K. & Hempstead, B. L. Regulation of cell survival by secreted proneurotrophins. *Science* **294**, 1945–1948 (2001).

133. Matsuda, N. *et al.* Differential activity-dependent secretion of brain-derived neurotrophic factor from axon and dendrite. *J. Neurosci. Off. J. Soc. Neurosci.* **29**, 14185–14198 (2009).

134. Yang, J. *et al.* Neuronal release of proBDNF. *Nat. Neurosci.* **12**, 113–115 (2009).

135. Yang, J. *et al.* proBDNF negatively regulates neuronal remodeling, synaptic transmission, and synaptic plasticity in hippocampus. *Cell Rep.* **7**, 796–806 (2014).

136. Pang, P. T. *et al.* Cleavage of proBDNF by tPA/Plasmin Is Essential for Long-Term Hippocampal Plasticity. *Science* **306**, 487–491 (2004).

137. Martin-Zanca, D., Hughes, S. H. & Barbacid, M. A human oncogene formed by the fusion of truncated tropomyosin and protein tyrosine kinase sequences. *Nature* **319**, 743–748 (1986).

138. Dechant, G. & Barde, Y.-A. The neurotrophin receptor p75NTR: novel functions and implications for diseases of the nervous system. *Nat. Neurosci.* **5**, 1131–1136 (2002).

139. Meeker, R. B. & Williams, K. S. The p75 neurotrophin receptor: at the crossroad of neural repair and death. *Neural Regen. Res.* **10**, 721–725 (2015).

140. Volosin, M. *et al.* Interaction of survival and death signaling in basal forebrain neurons: roles of neurotrophins and proneurotrophins. *J. Neurosci. Off. J. Soc. Neurosci.* **26**, 7756–7766 (2006).

141. Minichiello, L. TrkB signalling pathways in LTP and learning. *Nat. Rev. Neurosci.* **10**, 850–860 (2009).

142. Mohammadi, A., Amooeian, V. G. & Rashidi, E. Dysfunction in Brain-Derived Neurotrophic Factor Signaling Pathway and Susceptibility to Schizophrenia, Parkinson's and Alzheimer's Diseases. *Curr. Gene Ther.* **18**, 45–63 (2018).

143. Lanuza, M. A. *et al.* The Impact of Kinases in Amyotrophic Lateral Sclerosis at the Neuromuscular Synapse: Insights into BDNF/TrkB and PKC Signaling. *Cells* **8**, 1578 (2019).

144. Hurtado, E. *et al.* Muscle Contraction Regulates BDNF/TrkB Signaling to Modulate Synaptic Function through Presynaptic cPKCα and cPKCβI. *Front. Mol. Neurosci.* **10**, 147 (2017).

145. Nikoletopoulou, V., Sidiropoulou, K., Kallergi, E., Dalezios, Y. & Tavernarakis, N. Modulation of Autophagy by BDNF Underlies Synaptic Plasticity. *Cell Metab.* **26**, 230-242.e5 (2017).

146. Nakai, T. *et al.* Girdin phosphorylation is crucial for synaptic plasticity and memory: a potential role in the interaction of BDNF/TrkB/Akt signaling with NMDA receptor. *J. Neurosci. Off. J. Soc. Neurosci.* **34**, 14995–15008 (2014).

147. Kumar, V., Zhang, M.-X., Swank, M. W., Kunz, J. & Wu, G.-Y. Regulation of dendritic morphogenesis by Ras-PI3K-Akt-mTOR and Ras-MAPK signaling pathways. *J. Neurosci. Off. J. Soc. Neurosci.* **25**, 11288–11299 (2005).

148. Gonzalez, A., Moya-Alvarado, G., Gonzalez-Billaut, C. & Bronfman, F. C. Cellular and molecular mechanisms regulating neuronal growth by brain-derived neurotrophic factor. *Cytoskelet. Hoboken NJ* **73**, 612–628 (2016).

149. Kwon, M., Fernández, J. R., Zegarek, G. F., Lo, S. B. & Firestein, B. L. BDNF-promoted increases in proximal dendrites occur via CREB-dependent transcriptional regulation of cypin. *J. Neurosci. Off. J. Soc. Neurosci.* **31**, 9735–9745 (2011).

150. Eyileten, C. *et al.* The Relation of the Brain-Derived Neurotrophic Factor with MicroRNAs in Neurodegenerative Diseases and Ischemic Stroke. *Mol. Neurobiol.* **58**, 329–347 (2021).

151. Cramer, S. C. *et al.* Harnessing neuroplasticity for clinical applications. *Brain J. Neurol.* **134**, 1591–1609 (2011).

152. Castrén, E. & Antila, H. Neuronal plasticity and neurotrophic factors in drug responses. *Mol. Psychiatry* **22**, 1085–1095 (2017).

153. Castrén, E., Berninger, B., Leingärtner, A. & Lindholm, D. Regulation of brain-derived neurotrophic factor mRNA levels in hippocampus by neuronal activity. *Prog. Brain Res.* **117**, 57–64 (1998).

154. Gianfranceschi, L. *et al.* Visual cortex is rescued from the effects of dark rearing by overexpression of BDNF. *Proc. Natl. Acad. Sci. U. S. A.* **100**, 12486–12491 (2003).

155. Hong, E. J., McCord, A. E. & Greenberg, M. E. A biological function for the neuronal activity-dependent component of Bdnf transcription in the development of cortical inhibition. *Neuron* **60**, 610–624 (2008).

156. Rauti, R. *et al.* BDNF impact on synaptic dynamics: extra or intracellular long-term release differently regulates cultured hippocampal synapses. *Mol. Brain* **13**, 43 (2020).

157. Ernfors, P., Lee, K.-F. & Jaenisch, R. Mice lacking brain-derived neurotrophic factor develop with sensory deficits. *Nature* **368**, 147–150 (1994).

158. Gao, X., Smith, G. M. & Chen, J. Impaired dendritic development and synaptic formation of postnatal-born dentate gyrus granular neurons in the absence of brain-derived neurotrophic factor signaling. *Exp. Neurol.* **215**, 178–190 (2009).

159. Mariga, A., Zavadil, J., Ginsberg, S. D. & Chao, M. V. Withdrawal of BDNF from hippocampal cultures leads to changes in genes involved in synaptic function. *Dev. Neurobiol.* **75**, 173–192 (2015).

160. Bramham, C. R. & Messaoudi, E. BDNF function in adult synaptic plasticity: the synaptic consolidation hypothesis. *Prog. Neurobiol.* **76**, 99–125 (2005).

161. Edelmann, E. *et al.* Theta Burst Firing Recruits BDNF Release and Signaling in Postsynaptic CA1 Neurons in Spike-Timing-Dependent LTP. *Neuron* **86**, 1041–1054 (2015).

162. Edelmann, E., Lessmann, V. & Brigadski, T. Pre- and postsynaptic twists in BDNF secretion and action in synaptic plasticity. *Neuropharmacology* **76 Pt C**, 610–627 (2014).

163. Korte, M. *et al.* Hippocampal long-term potentiation is impaired in mice lacking brain-derived neurotrophic factor. *Proc. Natl. Acad. Sci. U. S. A.* **92**, 8856–8860 (1995).

164. Cowansage, K. K., LeDoux, J. E. & Monfils, M.-H. Brain-derived neurotrophic factor: a dynamic gatekeeper of neural plasticity. *Curr. Mol. Pharmacol.* **3**, 12–29 (2010).

165. Levine, E. S., Dreyfus, C. F., Black, I. B. & Plummer, M. R. Brain-derived neurotrophic factor rapidly enhances synaptic transmission in hippocampal neurons via postsynaptic tyrosine kinase receptors. *Proc. Natl. Acad. Sci. U. S. A.* **92**, 8074–8077 (1995).

166. Lohof, A. M., Ip, N. Y. & Poo, M. M. Potentiation of developing neuromuscular synapses by the neurotrophins NT-3 and BDNF. *Nature* **363**, 350–353 (1993).

167. Pascual, M., Climent, E. & Guerri, C. BDNF induces glutamate release in cerebrocortical nerve terminals and in cortical astrocytes. *Neuroreport* **12**, 2673–2677 (2001).

168. Pereira, D. B. *et al.* Trkb receptors modulation of glutamate release is limited to a subset of nerve terminals in the adult rat hippocampus. *J. Neurosci. Res.* **83**, 832–844 (2006).

169. Jovanovic, J. N., Czernik, A. J., Fienberg, A. A., Greengard, P. & Sihra, T. S. Synapsins as mediators of BDNF-enhanced neurotransmitter release. *Nat. Neurosci.* **3**, 323–329 (2000).

170. Jourdi, H. *et al.* Positive AMPA receptor modulation rapidly stimulates BDNF release and increases dendritic mRNA translation. *J. Neurosci. Off. J. Soc. Neurosci.* **29**, 8688–8697 (2009).

171. Santos, A. R., Comprido, D. & Duarte, C. B. Regulation of local translation at the synapse by BDNF. *Prog. Neurobiol.* **92**, 505–516 (2010).

172. Cunha, C., Brambilla, R. & Thomas, K. L. A simple role for BDNF in learning and memory? *Front. Mol. Neurosci.* **3**, 1 (2010).

173. Rattiner, L. M., Davis, M. & Ressler, K. J. Differential regulation of brain-derived neurotrophic factor transcripts during the consolidation of fear learning. *Learn. Mem. Cold Spring Harb. N* **11**, 727–731 (2004).

174. Callaghan, C. K. & Kelly, Á. M. Differential BDNF signaling in dentate gyrus and perirhinal cortex during consolidation of recognition memory in the rat. *Hippocampus* **22**, 2127–2135 (2012).

175. Heldt, S. A., Stanek, L., Chhatwal, J. P. & Ressler, K. J. Hippocampus-specific deletion of BDNF in adult mice impairs spatial memory and extinction of aversive memories. *Mol. Psychiatry* **12**, 656–670 (2007).

176. Andero, R. & Ressler, K. J. Fear extinction and BDNF: Translating animal models of PTSD to the clinic. *Genes Brain Behav.* **11**, 503–512 (2012).

177. Bekinschtein, P. *et al.* BDNF is essential to promote persistence of long-term memory storage. *Proc. Natl. Acad. Sci. U. S. A.* **105**, 2711–2716 (2008).

178. Gupta, A. K. *et al.* Exploring the Connection Between BDNF/TrkB and AC/cAMP/PKA/CREB Signaling Pathways: Potential for Neuroprotection and Therapeutic Targets for Neurological Disorders. *Mol. Neurobiol.* https://doi.org/10.1007/s12035-025-05001-5 (2025) doi:10.1007/s12035-025-05001-5.

179. Seoane, A., Tinsley, C. J. & Brown, M. W. Interfering with perirhinal brain-derived neurotrophic factor (BDNF) expression impairs recognition memory in rats. *Hippocampus* **21**, 121–126 (2011).

180. Seoane, A., Tinsley, C. J. & Brown, M. W. Interfering with perirhinal brain-derived neurotrophic factor expression impairs recognition memory in rats. *Hippocampus* **21**, 121–126 (2011).

181. Alonso, M. *et al.* Endogenous BDNF is required for long-term memory formation in the rat parietal cortex. *Learn. Mem.* **12**, 504–510 (2005).

182. Castillo, D. V. & Escobar, M. L. A role for MAPK and PI-3K signaling pathways in brain-derived neurotrophic factor modification of conditioned taste aversion retention. *Behav. Brain Res.* **217**, 248–252 (2011).

183. Petryshen, T. L. *et al.* Population genetic study of the brain-derived neurotrophic factor (BDNF) gene. *Mol. Psychiatry* **15**, 810–815 (2010).

184. Egan, M. F. *et al.* The BDNF val66met polymorphism affects activity-dependent secretion of BDNF and human memory and hippocampal function. *Cell* **112**, 257–269 (2003).

185. Chen, Z.-Y. *et al.* Variant brain-derived neurotrophic factor (BDNF) (Met66) alters the intracellular trafficking and activity-dependent secretion of wild-type BDNF in neurosecretory cells and cortical neurons. *J. Neurosci. Off. J. Soc. Neurosci.* **24**, 4401–4411 (2004).

186. Bogenmann, E. *et al.* Generation of mice with a conditional allele for the p75(NTR) neurotrophin receptor gene. *Genes. N. Y. N 2000* **49**, 862–869 (2011).

187. Lanjakornsiripan, D. *et al.* Layer-specific morphological and molecular differences in neocortical astrocytes and their dependence on neuronal layers. *Nat. Commun.* **9**, 1623 (2018).

188. Oheim, M., Schmidt, E. & Hirrlinger, J. Local energy on demand: Are 'spontaneous' astrocytic Ca2+-microdomains the regulatory unit for astrocyte-neuron metabolic cooperation? *Brain Res. Bull.* **136**, 54–64 (2018).

189. Grosche, J. *et al.* Microdomains for neuron–glia interaction: parallel fiber signaling to Bergmann glial cells. *Nat. Neurosci.* **2**, 139–143 (1999).

190. Lia, A. *et al.* Calcium Signals in Astrocyte Microdomains, a Decade of Great Advances. *Front. Cell. Neurosci.* **15**, 673433 (2021).

191. Vignoli, B. *et al.* Astrocytic microdomains from mouse cortex gain molecular control over long-term information storage and memory retention. *Commun. Biol.* **4**, 1152 (2021).

192. Han, J., Yoon, S. & Park, H. Endocytic BDNF secretion regulated by Vamp3 in astrocytes. *Sci. Rep.* **11**, 21203 (2021).

193. Lessmann, V., Gottmann, K. & Malcangio, M. Neurotrophin secretion: current facts and future prospects. *Prog. Neurobiol.* **69**, 341–374 (2003).

194. Anastasia, A. *et al.* Val66Met polymorphism of BDNF alters prodomain structure to induce neuronal growth cone retraction. *Nat. Commun.* **4**, 2490 (2013).

195. Glerup, S. *et al.* SorCS2 is required for BDNF-dependent plasticity in the hippocampus. *Mol. Psychiatry* **21**, 1740–1751 (2016).

196. Losi, G. *et al.* Spontaneous activity of astrocytes is a stochastic functional signal for memory consolidation. *Proc. Natl. Acad. Sci. U. S. A.* **122**, e2500511122 (2025).

197. Vaidyanathan, T. V., Collard, M., Yokoyama, S., Reitman, M. E. & Poskanzer, K. E. Cortical astrocytes independently regulate sleep depth and duration via separate GPCR pathways. *eLife* **10**, e63329 (2021).

198. Choi, D. C., Gourley, S. L. & Ressler, K. J. Prelimbic BDNF and TrkB signaling regulates consolidation of both appetitive and aversive emotional learning. *Transl. Psychiatry* **2**, e205–e205 (2012).

199. Lu, Y. *et al.* TrkB as a potential synaptic and behavioral tag. *J. Neurosci. Off. J. Soc. Neurosci.* **31**, 11762–11771 (2011).

200. Maynard, K. R. *et al.* Bdnf mRNA splice variants differentially impact CA1 and CA3 dendrite complexity and spine morphology in the hippocampus. *Brain Struct. Funct.* **222**, 3295–3307 (2017).

201. Liu, I. Y. C., Lyons, W. E., Mamounas, L. A. & Thompson, R. F. Brain-derived neurotrophic factor plays a critical role in contextual fear conditioning. *J. Neurosci.* **24**, 7958–7963 (2004).

202. Hill, J. L. *et al.* Loss of promoter IV-driven BDNF expression impacts oscillatory activity during sleep, sensory information processing and fear regulation. *Transl. Psychiatry* **6**, e873–e873 (2016).

203. Ren, Q. *et al.* BDNF–TrkB signaling in the nucleus accumbens shell of mice has key role in methamphetamine withdrawal symptoms. *Transl. Psychiatry* **5**, e666–e666 (2015).

204. Chhatwal, J. P., Stanek-Rattiner, L., Davis, M. & Ressler, K. J. Amygdala BDNF signaling is required for consolidation but not encoding of extinction. *Nat. Neurosci.* **9**, 870–872 (2006).

205. Tischer, D. & Weiner, O. D. Illuminating cell signalling with optogenetic tools. *Nat. Rev. Mol. Cell Biol.* **15**, 551–558 (2014).

206. Hayashi-Takagi, A. *et al.* Labelling and optical erasure of synaptic memory traces in the motor cortex. *Nature* **525**, 333–338 (2015).

207. Letellier, M., Lagardère, M., Tessier, B., Janovjak, H. & Thoumine, O. Optogenetic control of excitatory post-synaptic differentiation through neuroligin-1 tyrosine phosphorylation. *eLife* **9**, e52027 (2020).

208. Sinnen, B. L. *et al.* Optogenetic Control of Synaptic Composition and Function. *Neuron* **93**, 646-660.e5 (2017).

209. Rost, B. R., Schneider-Warme, F., Schmitz, D. & Hegemann, P. Optogenetic Tools for Subcellular Applications in Neuroscience. *Neuron* **96**, 572–603 (2017).

210. Tischer, D. & Weiner, O. D. Illuminating cell signalling with optogenetic tools. *Nat. Rev. Mol. Cell Biol.* **15**, 551–558 (2014).

211. Huang, P. *et al.* Optical Activation of TrkB Signaling. *J. Mol. Biol.* **432**, 3761–3770 (2020).

212. Hong, J. & Heo, W. D. Optogenetic Modulation of TrkB Signaling in the Mouse Brain. *J. Mol. Biol.* **432**, 815–827 (2020).

213. Huang, E. J. & Reichardt, L. F. Trk receptors: roles in neuronal signal transduction. *Annu. Rev. Biochem.* **72**, 609–642 (2003).

214. Chang, K.-Y. *et al.* Light-inducible receptor tyrosine kinases that regulate neurotrophin signalling. *Nat. Commun.* **5**, 4057 (2014).

215. Lee, S. *et al.* Reversible protein inactivation by optogenetic trapping in cells. *Nat. Methods* **11**, 633–636 (2014).

216. Kim, N. *et al.* Spatiotemporal Control of Fibroblast Growth Factor Receptor Signals by Blue Light. *Chem. Biol.* **21**, 903–912 (2014).

217. Kyung, T. *et al.* Optogenetic control of endogenous Ca2+ channels in vivo. *Nat. Biotechnol.* **33**, 1092–1096 (2015).

218. Han, K. A. *et al.* Neurotrophin-3 regulates synapse development by modulating TrkC-PTPσ synaptic adhesion and intracellular signaling pathways. *J. Neurosci.* **36**, 4816–4831 (2016).

219. Liu, B., Liu, H., Zhong, D. & Lin, C. Searching for a photocycle of the cryptochrome photoreceptors. *Curr. Opin. Plant Biol.* **13**, 578–586 (2010).

220. Kim, S. *et al.* Non-invasive optical control of endogenous Ca2+ channels in awake mice. *Nat. Commun.* **11**, 210 (2020).

221. Lilja, A. *et al.* Optical Activation of TrkB (E281A) in Excitatory and Inhibitory Neurons of the Mouse Visual Cortex. *Int. J. Mol. Sci.* **23**, 10249 (2022).

222. Trifilieff, P., Calandreau, L., Herry, C., Mons, N. & Micheau, J. Biphasic ERK1/2 activation in both the hippocampus and amygdala may reveal a system consolidation of contextual fear memory. *Neurobiol. Learn. Mem.* **88**, 424–434 (2007).

223. Trifilieff, P. *et al.* Foreground contextual fear memory consolidation requires two independent phases of hippocampal ERK/CREB activation. *Learn. Mem.* **13**, 349–358 (2006).

224. Igaz, L. M., Bekinschtein, P., Izquierdo, I. & Medina, J. H. One-trial aversive learning induces late changes in hippocampal CaMKIIalpha, Homer 1a, Syntaxin 1a and ERK2 protein levels. *Brain Res. Mol. Brain Res.* **132**, 1–12 (2004).

225. Hu, B. *et al.* Changes in trkB-ERK1/2-CREB/Elk-1 pathways in hippocampal mossy fiber organization after traumatic brain injury. *J. Cereb. Blood Flow Metab. Off. J. Int. Soc. Cereb. Blood Flow Metab.* **24**, 934–943 (2004).

226. Davachi, L. Item, context and relational episodic encoding in humans. *Curr. Opin. Neurobiol.* **16**, 693–700 (2006).

227. Zola-Morgan, S., Squire, L. R., Amaral, D. G. & Suzuki, W. A. Lesions of perirhinal and parahippocampal cortex that spare the amygdala and hippocampal formation produce severe memory impairment. *J. Neurosci. Off. J. Soc. Neurosci.* **9**, 4355–4370 (1989).

228. Bonzanni, M., Rouleau, N., Levin, M. & Kaplan, D. L. On the Generalization of Habituation: How Discrete Biological Systems Respond to Repetitive Stimuli: A Novel Model of Habituation That Is Independent of Any Biological System. *BioEssays News Rev. Mol. Cell. Dev. Biol.* **41**, e1900028 (2019).

229. Dunuweera, A. N., Dunuweera, S. P. & Ranganathan, K. A Comprehensive Exploration of Bioluminescence Systems, Mechanisms, and Advanced Assays for Versatile Applications. *Biochem. Res. Int.* **2024**, 8273237 (2024).

230. Fenno, L., Yizhar, O. & Deisseroth, K. The Development and Application of Optogenetics. *Annu. Rev. Neurosci.* **34**, 389–412 (2011).

231. Prakash, M. *et al.* Selective control of synaptically-connected circuit elements by all-optical synapses. *Commun. Biol.* **5**, 33 (2022).

232. Welsh, J. P., Patel, K. G., Manthiram, K. & Swartz, J. R. Multiply mutated Gaussia luciferases provide prolonged and intense bioluminescence. *Biochem. Biophys. Res. Commun.* **389**, 563–568 (2009).

233. Wiles, S., Ferguson, K., Stefanidou, M., Young, D. B. & Robertson, B. D. Alternative Luciferase for Monitoring Bacterial Cells under Adverse Conditions. *Appl. Environ. Microbiol.* **71**, 3427–3432 (2005).

234. Verhaegent, M. & Christopoulos, T. K. Recombinant Gaussia luciferase. Overexpression, purification, and analytical application of a bioluminescent reporter for DNA hybridization. *Anal. Chem.* **74**, 4378–4385 (2002).

235. Pathe-Neuschäfer-Rube, A., Neuschäfer-Rube, F., Genz, L. & Püschel, G. P. Botulinum neurotoxin dose-dependently inhibits release of neurosecretory vesicle-targeted luciferase from neuronal cells. *ALTEX* **32**, 297–306 (2015).

236. Loh, Y. P., Maldonado, A., Zhang, C., Tam, W. H. & Cawley, N. Mechanism of sorting proopiomelanocortin and proenkephalin to the regulated secretory pathway of neuroendocrine cells. *Ann. N. Y. Acad. Sci.* **971**, 416–425 (2002).

237. Shimomura, O. *Bioluminescence: Chemical Principles And Methods*. (World Scientific, 2006).

238. Jiang, T., Song, J. & Zhang, Y. Coelenterazine-Type Bioluminescence-Induced Optical Probes for Sensing and Controlling Biological Processes. *Int. J. Mol. Sci.* **24**, 5074 (2023).

239. Macpherson, L. J. *et al.* Dynamic labelling of neural connections in multiple colours by trans-synaptic fluorescence complementation. *Nat. Commun.* **6**, 10024 (2015).

240. DeNardo, L. A. *et al.* Temporal Evolution of Cortical Ensembles Promoting Remote Memory Retrieval. *Nat. Neurosci.* **22**, 460–469 (2019).

241. Bramham, C. R. & Messaoudi, E. BDNF function in adult synaptic plasticity: The synaptic consolidation hypothesis. *Prog. Neurobiol.* **76**, 99–125 (2005).

242. Park, H. & Poo, M. Neurotrophin regulation of neural circuit development and function. *Nat. Rev. Neurosci.* **14**, 7–23 (2013).

243. Chang, K.-Y. *et al.* Light-inducible receptor tyrosine kinases that regulate neurotrophin signalling. *Nat. Commun.* **5**, 4057 (2014).

244. Seoane, A., Tinsley, C. J. & Brown, M. W. Interfering with perirhinal brain-derived neurotrophic factor expression impairs recognition memory in rats. *Hippocampus* **21**, 121–126 (2011).

245. Callaghan, C. K. & Kelly, Á. M. Differential BDNF signaling in dentate gyrus and perirhinal cortex during consolidation of recognition memory in the rat. *Hippocampus* **22**, 2127–2135 (2012).

246. Bekinschtein, P. *et al.* BDNF is essential to promote persistence of long-term memory storage. *Proc. Natl. Acad. Sci. U. S. A.* **105**, 2711–2716 (2008).

247. Mayes, A., Montaldi, D. & Migo, E. Associative memory and the medial temporal lobes. *Trends Cogn. Sci.* **11**, 126–135 (2007).

248. Aggleton, J. P., Brown, M. W. & Albasser, M. M. Contrasting brain activity patterns for item recognition memory and associative recognition memory: Insights from immediate-early gene functional imaging. *Neuropsychologia* **50**, 3141–3155 (2012).

249. Berry, A. *et al.* Social deprivation stress is a triggering factor for the emergence of anxiety- and depression-like behaviours and leads to reduced brain BDNF levels in C57BL/6J mice. *Psychoneuroendocrinology* **37**, 762–772 (2012).

250. Swiercz, A. P., Tsuda, M. C. & Cameron, H. A. The curious interpretation of novel object recognition tests. *Trends Neurosci.* **48**, 250–256 (2025).

251. Gouveia, K. & Hurst, J. L. Optimising reliability of mouse performance in behavioural testing: the major role of non-aversive handling. *Sci. Rep.* **7**, 44999 (2017).

252. Sierra, C., De Toma, I., Cascio, L. L., Vegas, E. & Dierssen, M. Social Factors Influence Behavior in the Novel Object Recognition Task in a Mouse Model of Down Syndrome. *Front. Behav. Neurosci.* **15**, 772734 (2021).

ACKNOWLEDGEMENTS

I would like to begin by expressing my appreciation to the members of the jury for reviewing this thesis and participating in the evaluation of my doctoral project.

I would like to thank my tutor, Prof. Marco Canossa, for welcoming me into his team and giving me the opportunity to work in a stimulating scientific environment and helping me develop my PhD research.

My research benefited greatly from the collaboration of several experts. I thank Prof. Michele Simonato and Beatrice Bettegazzi for their support regarding the production of OptoTrkB viral vectors. I am also grateful to Prof. Ute Hochgeschwender for sharing her expertise on the BL-OG system, adapting it to my needs, and providing the necessary constructs.

A special thanks goes to Beatrice Vignoli not only for her help during these three years but also for the constant support and fruitful discussion which helped me define my project. I would like to thank Clara Zaccaria for helping me with light stimulation setup, and providing the support I needed to create robust light stimulation protocols. I thank Asiye Malkoç, who helped me during the first year of my PhD by teaching me new protocols and techniques, and for setting an example that kept my motivation strong. Thanks to Yasaman Heydari for all the useful discussion, for always giving me confidence and for being a supportive friend.

I would like to thank Prof. Lorenzo Pavesi for giving me the chance to work alongside his team, and for providing me all the guidance and support for my doctoral project.

I wish to thank all the present and past team members that created a friendly working environment during the three years of my PhD.

Last but not least, I thank the animal facility staff of the University of Trento for their assistance and for the working environment from which my work benefited.

Some of the figures presented in this work were created with BioRender.com.